ASPECTS OF THE GEOLOGY OF THE MOUNTAIN ORE BODY, ROSH PINAH MINE, NAMIBIA.

by: P.R. SIEGFRIED
supervisor: Dr. J.M. MOORE

M.Sc. Thesis

UNIVERSITY OF CAPE TOWN
1990

ABSTRACT

The Rosh Pinah Zn-Pb-Cu sulphide deposit is located in the Gariep Group of southern Namibia. It is a stratiform sedimentary-exhalative deposit composed of mineralized dolomite and siliceous shales hosted within a uniform sequence of turbiditic feldspathic quartzites. Approximately 22 Mt of ore has been proved to date with an average grade of 6% Zn, 2% Pb, 0.25% Cu and 24 ppm Ag.

Directly underlying the ore bodies are zones of stockwork alteration as well as extensive brecciation. The aim of this thesis is to determine the cause of brecciation and its relationship to the ore body and mineralization. Methods of identification include field observations, transmitted and reflected light microscopy, staining and quantitative electron-microprobe analyses, carbonate isotope determination and an extensive literature survey.

The ore zone is contained within lower sediments of the clastic Rosh Pinah Formation, one of three facies types comprising the Kapok Subgroup. To the west of the Rosh Pinah Formation lies the predominantly felsic Spitzkop Formation. To the east occurs the structurally overlying, dolomitic Hilda Formation.

The ore horizon pinches and swells to form discrete ore bodies regarded as primary features reflecting palaeobasin control. Extensive structural control is also apparent. D1 produced layer-parallel foliation coupled with extensive stratigraphic duplication a result of south easterly directed thrusting. D2 produced tight, west-vergent folds; a result of backfolding associated with continued compression from the north west.

The ore horizon consists of black, banded, sulphidic cherts overlain by carbonaceous dolomites containing sphalerite, pyrite and galena. Areas are sporadically overlain by massive barite, sulphide or argillite. The underlying

breccias consist of angular, heterolithic quartzite blocks hosted in a barium carbonate-rich matrix.

Deposition of sulphide and sulphate material occurred as part of an active shallow water hydrothermal system. Mineralization is restricted to synsedimentary hydrothermal events such as silicification, brecciation and sulphidization. Initial mineralization consisted of extensive silicification and Cu introduction. Silica precipitation resulted in the formation of an impermeable self-sealed caprock trapping subsequent hydrothermal solutions. Pressure and temperature build-up resulted in a higher temperature system undergoing hydraulic fracture and brecciating the footwall. Stockwork filling precipitated consists of Mn-rich dolomite with sulphides. A later stage consisted of Ba-Cu-Ag enriched fluids producing rare crosscutting "flow-banded" and Ba-rich veins. Syngenetic Ba-rich ore was deposted over the dolomite ore at this stage. Economic sulphide deposition terminates with the resumption of clastic deposition.

Post-lithification reconstitution of ore zone sulphides began during D1. Thrusts developed in the footwall produced extensive structurally-controlled zones of brittle fracture. These zones are concentrated in areas of greatest silicification. Reprecipitation of sulphides, barytes and dolomite into the breccia matrix resulted in coarse veins of chalcopyrite and barite. D2 folding and metamorphism associated with CO_2-rich fluids produced pronounced open-system alteration with much of the barite being altered to barium-carbonates. The upper parts of some ore bodies were later affected by supergene alteration.

TABLE OF CONTENTS

1. INTRODUCTION

The Rosh Pinah Zn-Pb-Cu deposit (Page & Watson, 1976; van Vuuren, 1986) lies within thrusted metasediments of the Pan African Port Nolloth Assemblage (von Veh, 1988) of the Gariep Group (Kröner, 1974). It displays many of the general characteristics of a sediment-hosted exhalative (SEDEX) deposit (Large, 1983; Lydon, 1983). Structural deformation, specifically thrust as well as high-angle faulting, has severely complicated the morphology of the deposit (Page & Watson, 1976). However, the relative importance of structural control within the deposit remains poorly understood.

Sulphide minerals behave in a highly mobile fashion during deformation (Vokes, 1976; McClay,1983). This has resulted in many Zn-Pb-Cu massive sulphide deposits, including Rosh Pinah, being characterised by extensive alteration and reconstitution of the constituent minerals. The interpretation of the paragenesis and the metallogenic evolution of sulphide ore deposits within highly deformed terranes, is therefore a topic of extensive debate.

1.1 AIM

The aim of this project was to determine the genetic relationship between the ore bodies and the underlying "footwall breccias". These are zones of extensive silicification, veining and brecciation which are present below all the ore bodies of the deposit.

The common occurrence of alteration zones below volcanogenic deposits has often been documented (Franklin et al., 1981). Alteration below SEDEX deposits is, however, far less common but does occur (Gustafson & Williams, 1981; Large, 1981; Lydon, 1983). Comparable deposits such as Rammelsberg in Germany (Hannak, 1981), Sullivan in British Columbia (Hamilton, et al.., 1983) and Jason in the Yukon, Canada (Gardner & Hutcheon, 1985) display evidence of footwall alteration and in some cases brecciation. This has led to

the common assumption that the footwall breccia beneath the Rosh Pinah ore bodies has a hydrothermal origin.

Certain observations, such as the restriction of brecciation to certain beds, the occurrence of similar breccias in the hangingwall and the presence of unmineralized breccias elsewhere in the sequence, are together incompatible with the formation of a stockwork breccia through exhalative activity. The recognition of extensive thrust faulting in the surrounding area (Kindl, 1979) led to the suggestion by C. Hartnady (pers. comm.) that a relationship between the ore forming event and structural deformation could exist and that the ore is epigenetic in origin. Recent observations at Mount Isa in Queensland, Australia (Swager, 1985; Gulson et al., 1983) show the brecciated "silica-dolomite" of the copper-rich, lower ore zone, to be a result of D1 related faulting and not a syngenetic, hydrothermal stockwork breccia as previously accepted (Finlow-Bates, 1979). Previous studies of the Rosh Pinah deposit (Page & Watson, 1976; Watson, 1980), although recognizing extensive remobilization of the ore, interpreted the footwall breccia as hydrothermal.

Although the deposit is suggested in this study to be syngenetic, it is apparent that the breccias are intimately involved in the structural history of the area. This study, therefore, addresses the relationship between deformation, brecciation and ore paragenesis. A thorough understanding of these relationships will enable workers to identify other similar breccias in the sequence, and hopefully better constrain future exploration.

1.2 LOCATION

The Rosh Pinah Zn-Pb-Cu ore deposit is situated in the arid southern part of Namibia at 27° 31'E, 16° 48'S (Sperrgebiet). The village and mine are approximately 20 km north of the Orange River and 5 km east of Diamond Area No.1. The mine is situated at the southern extremity of the Kapok mountain range (Fig.1) with the village built in the valley floor. Mine development extends into the mountain by means of tunnels and level mining methods. The mine produces zinc and mixed lead-copper-silver concentrates which are transported 165 km north by truck to the Aus railhead.

The deposit was discovered in 1963 by M. D. McMillan during a regional mapping project for the Precambrian Research Unit of the University of Cape Town as part of his Ph.D dissertation. Mining began in 1969 and is run by Imkor Zinc (Pty) Ltd. a Namibian based subsidiary of the South African Iron and Steel Corporation (ISCOR).

The area is characterized by an exceedingly rugged landscape, resulting from the proximity to the major Orange River drainage system. Steep-sloped hills rise directly from the sand-covered valley floor. The sand cover has been proved by drilling to be in excess of 160 m and is the product of later infilling after incision of the steep sided valleys. The climate is arid (rainfall <70 mm p.a.) and has had a pronounced effect on the geomorphology of the area. Fairly extensive coverings of angular scree occur on the mountain slopes. Braided streams cover the valley floors and only flow episodically.

The vegetation types encountered are all adapted for desert survival and many rare and uncommon species occur. The mountains surrounding the mine are covered in kokerbome (*Aloe dichotoma*) and the halfmense (*Pachypodium namaquansis*). The valley floors are sparsely covered in boesmankerse

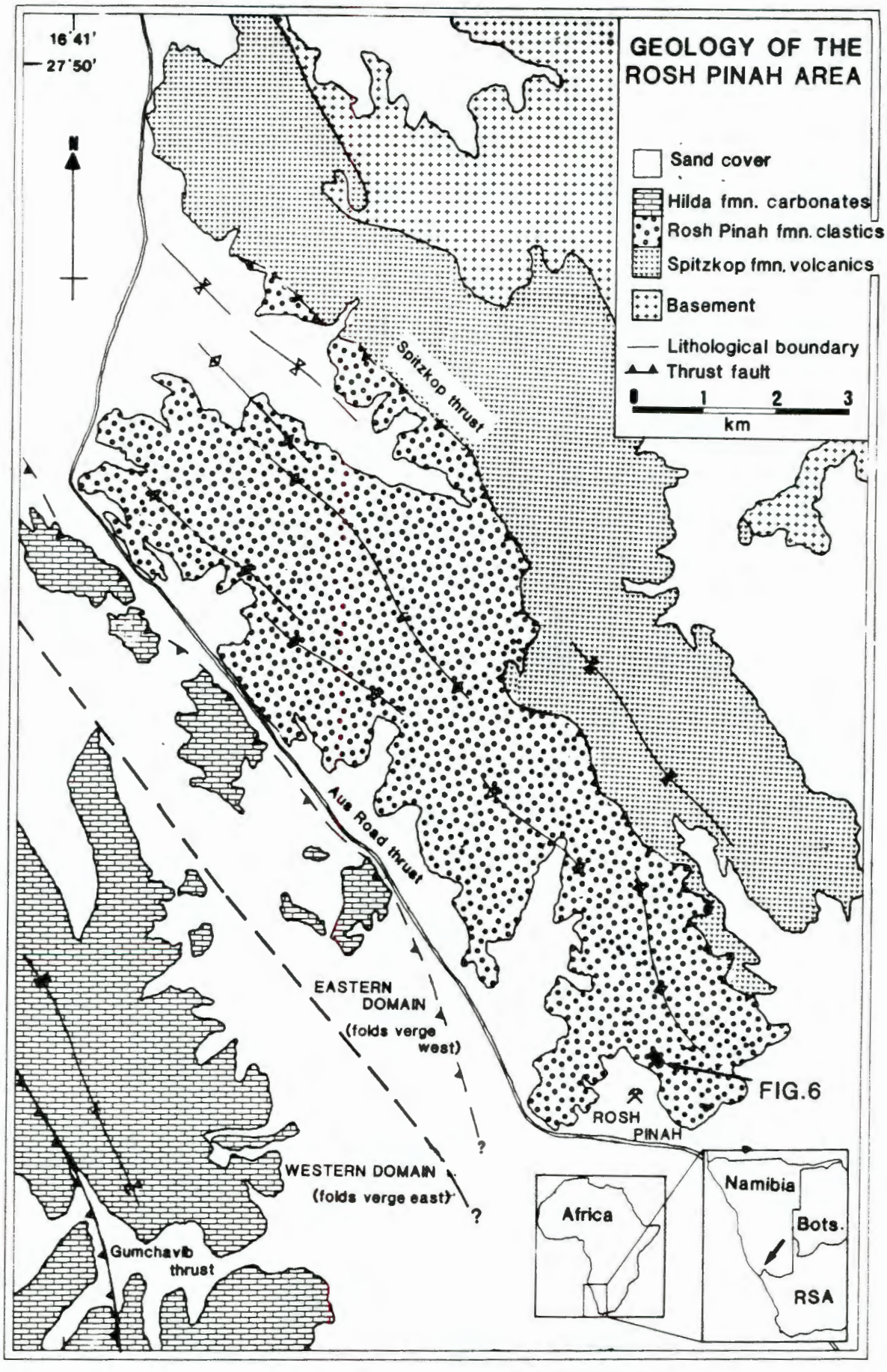

Figure 1: General geology of the Rosh Pinah area (after Kindl, 1979; van Vuuren, 1986).

(*Sarcocaulon spp.*) and melkbos (*Euphorbia spp.*). The euphorbia are important as drainage markers in the valleys. Large animals such as gemsbok (*Oryx gazella*), ostrich (*Struthio camelus*) and springbok (*Antidorcas marsupialis*) are found within the Sperrgebiet and often stray across to the mine area.

1.3 METHOD

Observations were recorded during routine underground mapping of the 490 level of the ore body (Fig.2) and supplemented by work on the 475 and 470 levels. The three dimensional perspective provided by tunnel exposure was complemented by intensive diamond drilling. Since the core was largely utilized for assay purposes, detailed logging and study was completed prior to sampling. Sections, displaying grade and geology at 10 m intervals, provided the best base on which structural as well as lithological interpretations could be made (Fig.5). Mapping of surface exposure was completed (Fig.6) in order to obtain an idea of the effects caused by weathering of fresh underground exposure. Petrographic samples were collected largely from borehole core, or where structural analysis was important, from orientated samples of the sidewalls.

Borehole core was sampled at 1.5 m intervals and analysed by atomic absorption spectrometry for Fe, Zn, Pb, Cu and Ag. Metal analyses were then used to establish the presence of metal zonation trends as discussed by Large (1980) and Lydon (1983). Owing to the pervasive affects of supergene alteration, effective usefulness of metal zonation diagrams was severely diminished. Certain broad generalization have, however, been made (Ch. 3.4).

The greatest problem encountered during petrographic study was the differentiation of the various carbonate minerals present. X-Ray diffraction, electron-microprobe and staining techniques were used to distinguish the minerals.

Staining, combined with quantitative microprobe data, provided a very good approximation of the carbonate composition (Warne, 1962). Staining techniques are invaluable as they are cheap, can be used on hand specimen scale and the samples are easy to prepare. Samples were etched for 3 min with 10 molal HCl and then reacted with Alazarine Red S for 5 min to distinguish between dolomite,

calcite and ankerite. Dolomite, Mn-dolomite and rhodochrosite are unaffected by the stain, whereas calcite and ankerite stain red and purple respectively. Samples were then re-etched and reacted with Rhodizonate to test for the presence of Ba, and hence the orthorhombic barium carbonates present.

Twelve samples of various carbonate minerals were analysed for their stable carbon and oxygen isotope compositions. Samples consisted of late-stage vein material because of their relatively sulphide-free and coarse-grained nature. Primary ore (both dolomitic as well as calcitic) is fine-grained and contains finely disseminated sulphides (<5 μm) and is therefore unsuitable for isotope analysis.

All samples were crushed, sieved and hand picked, the removal of sulphides or sulphide-bearing material being an important aspect of the process. Samples were then analysed using X-ray diffraction techniques. It was apparent that some samples of an homogeneous appearance consisted of two or three distinct carbonate minerals. Admixtures of calcite and norsethite, and baryto-calcite and calcite were separated using bromoform. Repeated X-ray diffraction analyses showed negligible mixing of these composite minerals after separation. Between 15 and 25 mg of separated sample (depending on the composition) were allowed to react overnight (12 hours) at 24.2°C with H_2PO_4 after evacuation and equilibration of the temperature of the reactants and the vessel. The resultant evolved CO_2 was collected and analysed on the VG602E double collection 2-ratio mass spectrometer of the Departament of Archeometry at the University of Cape Town. All samples were treated in duplicate and were within 0.8 permil (‰) agreement.

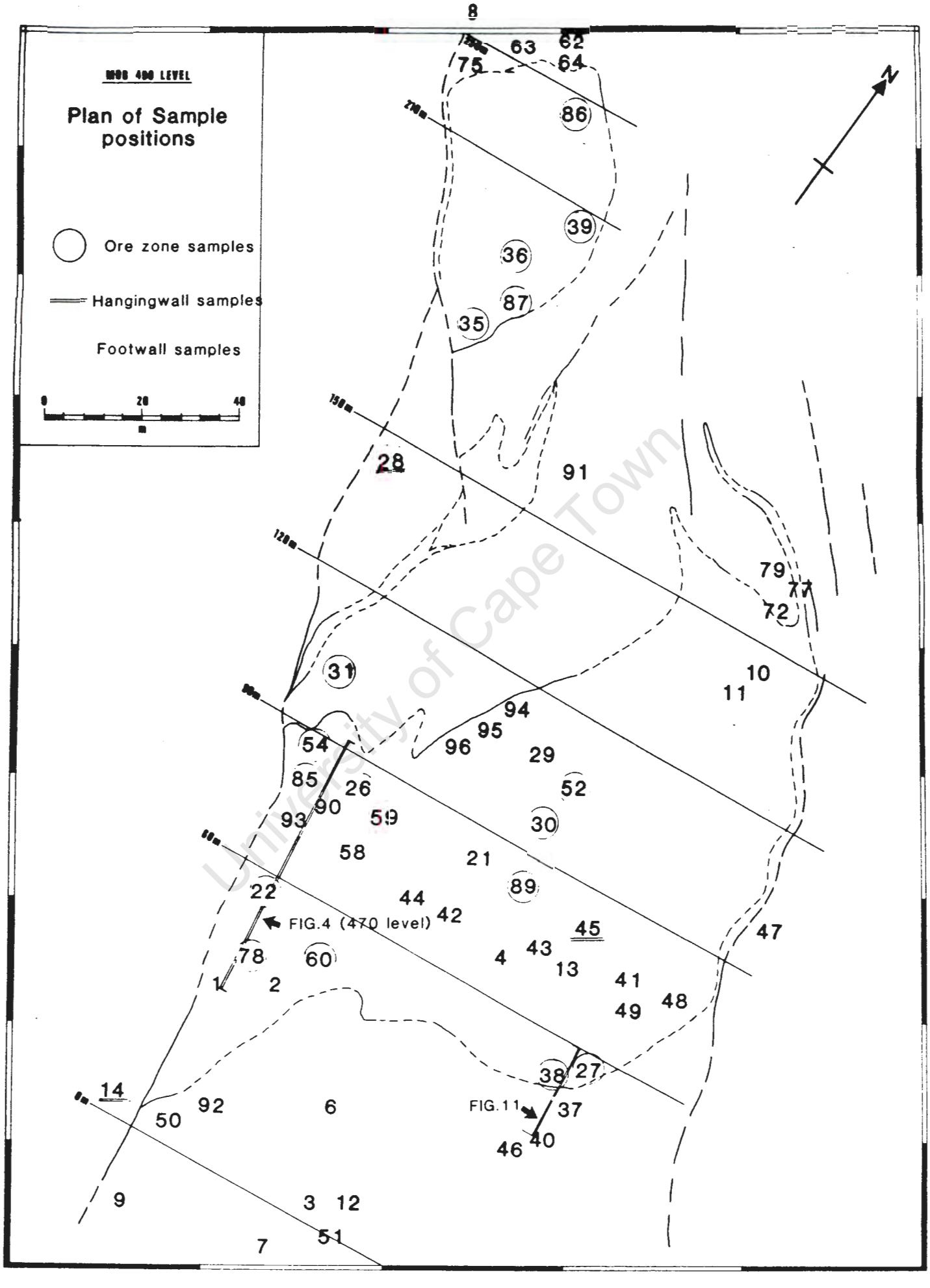

Figure 2: Sample positions in the Mountain Ore Body.

Most structural data were measured during routine underground mapping. Later observations were concentrated in problematic areas and field exposures. The various fabrics were differentiated using overprinting relationships as discussed by Williams (1984). Domains were initially separated on a basis of mine level and tunnel exposure. It was later found to be far more beneficial to treat the data set as one, on the grounds that no boundaries separating areas of changing fabric elements existed. Data was processed using G/ASTRA structural software package, adapted for the Precambrian Research Unit on the Department of Geochemistry Hewlett-Packard system. Extensive use of petrography, both transmitted and reflected light, elucidated many of the structural complexities. Three dimensional block diagrams have been used to represent important structural relationships. A comparative study with data already published for Rosh Pinah was also completed.

The following designations have been used to show positions where observations were made or samples collected. Reference to the mine level, i.e. 490, 475, 470 and the grid position on Map 1 are made as follows: [490 Bd]; while petrographic samples are prefixed PRS. Planar fabrics are described by strike and dip rather than dip direction.

2.1 INTRODUCTION

The Rosh Pinah sediment-hosted massive sulphide ore deposit, is contained within late Proterozoic sediments of the lower Gariep Group. The Group defines a structural arc along the north west coast of southern Africa from Kleinzee in South Africa to Luderitz in Namibia. The arc extends a maximum of 100 km inland. The Gariep Group is considered to comprise part of a sequence of geosynclinal provinces stretching from the Cape to northern Namibia (Martin & Porada, 1977). These predominantly sedimentary basins together comprised a major ocean system - the Adamastor Ocean (Hartnady et al., 1985). The Gariep Group appears to be coeval with the early deposition of the Damaran Province in central Namibia (Martin & Porada, 1977; Miller, 1983) and the Saldanian Province of the southern and southwestern Cape (Hartnady et al., 1974).

Clastic sediments dominate the eastern parts of the group while the western portion of the belt, however, is composed of basalts of ocean island affinity as well as associated deepwater sediments such as cherts and shales of the Oranjemund formation. The bimodal distribution of the lithologies was interpreted as a classic example of a geosynclinal basin by Kroner (1974). The eastern and western assemblages or terranes (Von Veh, 1988) are separated by a major dislocation - the Schakalsberg thrust fault. Estimates of throw using the bow and arrow method indicate up to 60 km of movement on this fault alone.

Table 1: Stratigraphy of the Gariep Group in the Rosh Pinah area as referred to in this study. (after Kindl, 1979; McMillan, 1969; von Veh, 1988; ISCOR reports).

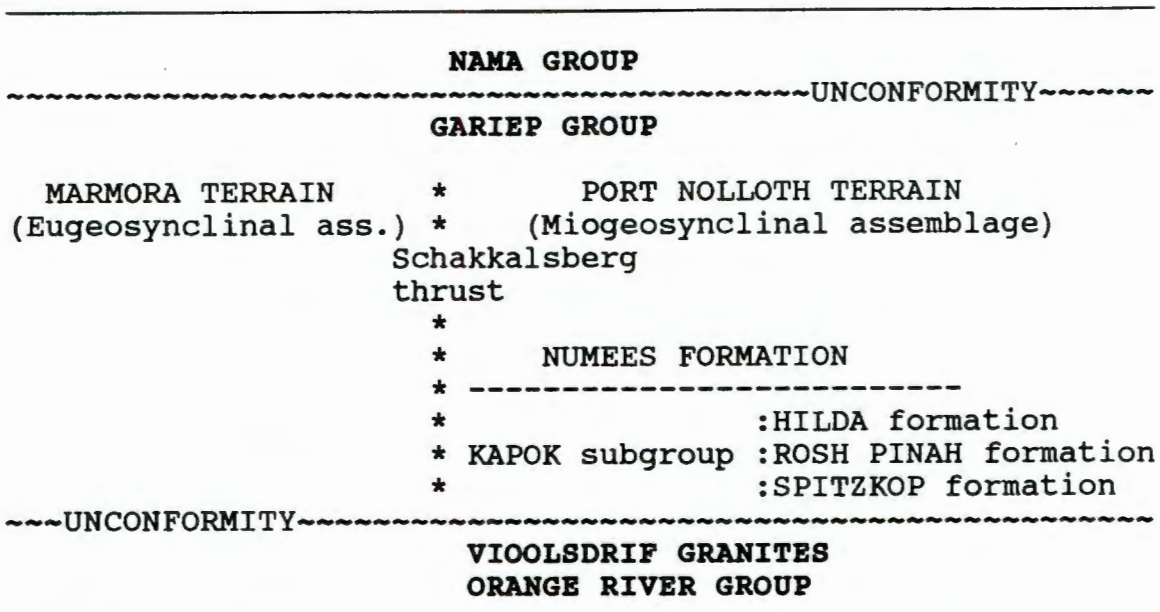

Any interpretation of the Group must take two important constraints into consideration. These are (i) the effect of thrust faulting and subsequent duplication of strata as well as extensive shortening of the basinal sediments, and (ii) the importance of extremely rapid facies changes in the area.

2.2 BASEMENT LITHOLOGIES

The Gariep cover sequences lie with a marked unconformity on the mainly granitic basement consisting of epizonal granites of the Vioolsdrif Intrusive Suite (Blignault, 1977). These granites are mainly granodioritic to tonalitic in composition and were intruded between 1900 and 1700 Ma (Reid, 1979a) into 2000 Ma, acid-dominant metavolcanics of the De Hoop Subgroup of the Orange River Group (Blignault, 1977; Ritter, 1976). A distinctive feature of the basement in this area is the numerous parallel, north-east to north-trending gabbroic dykes - the Gannakouriep dyke swarm (Reid, 1979b; Ransome, in prep.). These dykes have been interpreted as a tectono-magmatic response to the incipient rifting of the Adamastor Ocean (Hartnady et al., 1985). No reliable ages have been recorded, although all dykes

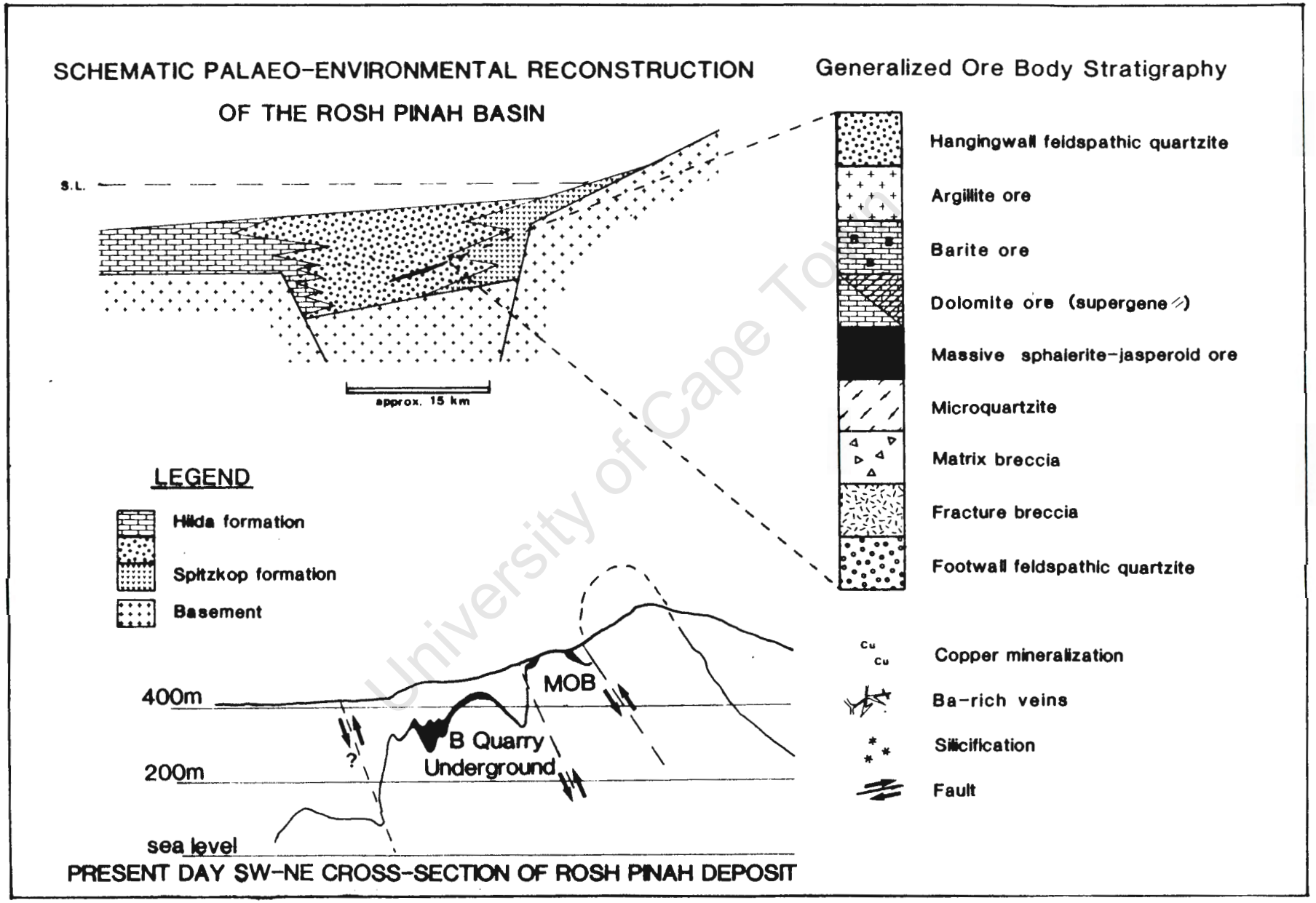

Figure 3: Schematic cross-section through the Rosh Pinah basin and present day structure of the deposit.

crosscut early intrusions of the Richtersveld Intrusive Complex. These granitic and leucogranitic rocks were sequentially intruded into the basement and yield a maximum age of 920 Ma (Allsopp et. al., 1979). Some of the later granites are as young as 700 Ma. One intrusion, Rooiberg II, contains xenoliths of Stinkfontein quartzite of the Gariep Group, which effectively constrains a minimum age of 780 ± 10 My. for the onset of Gariep deposition (Allsopp et. al., 1979).

2.3 GARIEP GROUP

The stratigraphy of the Gariep sediments has undergone extensive revision and renaming since the first attempt at classification in the early 1900's (Rogers, 1915). For a review one is referred to SACS (1980) or van Vuuren (1986). The detailed stratigraphy north of the Orange River, however, is still not well understood. This is, as stated, in large part due to the extensive thrust faulting superimposed upon lithologies which experienced extremely rapid facies changes.

Preliminary subdivision of these strata by SACS (1980) shows a two-fold division of the basal sequence, named the Kapok Formation, into a lower volcanic and upper clastic stage. This is overlain by a dominantly carbonate sequence, the Hilda Suite (SACS, 1980). A more recent stratigraphy (Davies & Coward, 1982) recognised the importance of thrust duplication and regarded the three assemblages as facies equivalents of each other. Their classification is the one which will be adopted in this study and a formational status will be assigned each of the facies types. These assemblages are as follows; the volcanic Spitzkop formation, clastic Rosh Pinah formation and carbonate dominated Hilda formation. It is suggested that the name Kapok Formation (SACS, 1980) be retained in preference to Rosh Pinah Formation (Davies & Coward, 1982) and be assigned a

"subgroup" status. The name Rosh Pinah, therefore being used to indicate the clastic facies (formation) and basin into which it was deposited.

2.3.1 SPITZKOP FORMATION

A detailed traverse across the basal unconformity to the north of the mine (Fig.1) shows the following sequence of lithologies. A foliation becomes apparent in the granite about 100 m from the contact and increases in intensity towards it. The unconformity itself is marked by a 3 m diamictite bed consisting of a micaceous matrix (sericite, chlorite, green biotite) hosting stretched, basement-derived clasts of granite, metaquartzite and diorite. This is capped by intensely foliated, blue-green schists crossed by numerous quartz veins.

These are followed by strongly altered chlorite-epidote rocks that represent metamorphosed intermediate volcanics. Numerous rotated shear pods of pure epidote are a feature of this lithology. This is followed by acid volcanic rocks consisting of ignimbrites, rhyolites and agglomerates. They are highly siliceous (Table 2) and have similar major element chemistries to volcanic rocks interbedded with the Stinkfontein quartzites (I.Ransome, pers comm.).

These lithologies are followed by volcaniclastics, the matrix composed of immature, basement-derived material supporting large rounded clasts of the underlying volcanic rocks. These sediments become progressively finer grained and take on the appearance of graded, feldspar-rich quartzite beds.

Table 2: Whole rock major element analyses of representative samples of Spitzkop formation volcanics, Kapok subgroup. na = not analysed. (Analyses carried out at ISCOR H.Q.)

SAMPLE	V0	V1	V2	V3	V4	V5	V6	V7
SiO2	72.5	72.4	69.8	70.7	82.1	71.5	72.6	75.5
Al2O3	9.6	12.0	13.2	12.6	10.4	12.7	11.9	10.9
Fe2O3	1.6	2.9	5.8	2.9	1.5	4.2	4.6	1.9
TiO2	0.01	0.15	0.23	0.15	0.09	0.60	0.14	0.01
P2O5	0.05	0.06	0.06	0.05	0.05	0.12	0.06	0.05
CaO	4.04	0.31	0.10	0.90	0.12	0.13	0.11	0.05
MgO	0.08	0.02	0.84	0.03	0.26	0.50	0.39	0.05
Na2O	0.26	0.40	0.20	0.20	0.20	0.20	0.30	2.01
K2O	10.2	10.1	6.3	10.2	3.5	7.0	6.9	9.1
Ba	na	0.04	0.04	0.17	0.01	0.06	0.18	na
SO3	0.2	0.3	0.4	0.3	0.3	0.3	0.3	0.9
MnO	0.05	0.03	0.04	0.09	0.02	0.02	0.02	0.05
CO2	0.35	0.51	0.15	0.55	0.26	0.18	0.15	0.01
LOI	0.6	0.6	2.3	1.0	2.1	2.0	2.0	0.4
F	1.91	na	na	na	na	na	na	0.5

A feature of the sequence in the Spitzkop area is the development of a particular unit, the VSMH or volcano-sedimentary marker horizon (Edwards, 1984). This consists of ripple-bedded tuffs, quartzites, limestones and iron formations that are enriched in Cu, Zn and Pb. Galena of a possible replacement origin occurs within dark brown carbonates. It has been postulated that this horizon is the stratigraphic equivalent of the Rosh Pinah ore zone but until the internal stratigraphy of the area is better understood continues to be speculative.

2.3.2 ROSH PINAH FORMATION

The area of the mine consists of a continuous sequence of feldspathic sandstones, the Rosh Pinah formation. These lithologies range from arkosic to quartzitic in composition

and are massively bedded. Bed thicknesses of up to 2.5 m were recorded. They possess few internal sedimentary structures other than upward-fining, graded bedding. Rare low-angle crossbedding has also been observed indicating high flow regime conditions. The quartzites are rusty red-brown weathering with a steel grey fresh surface. Coarse grains of white, potassium feldspar dot the rock. Some exposures are deeply weathered, a result of intense foliation and/or a large amount of carbonate material in the rock. Occasionally 5 to 10 cm of dark grey to black argillic material caps the bed. The argillite layers often exhibit fine laminations and more rarely flaser crossbedding. In areas the argillite layers thicken up to 20 m and form separate horizons. Flat-pebble conglomerates are occasionally interbedded with the feldspathic quartzites. Clasts consist of either argillic or carbonate material. The general absence of Bouma sequences in the quartzites as well as their massive and laterally continuous nature indicate that deposition occurred in the midfan area of a submarine fan (Walker, 1975,1976).

Carbonate material is common in the rocks and appears ubiquitous throughout the Gariep sediments to the north of the Orange River. Interbedded with these semimature clastic sediments are rare, basic, sill-like igneous layers. The presence of chilled and vesicular tops would, however, indicate synsedimentary eruption rather than later intrusion.

Intercalated with these coarse clastic sediments is a stratiform horizon of mineralized cherts and dolomites, the Rosh Pinah massive sulphide deposit. A generalised stratigraphy for the ore deposit is presented in Figure 3.

2.3.3 HILDA FORMATION

To the west of the area, shallow-water carbonate sediments and occasional clastic intercalations occur. The carbonates

are dominated by laminated dolomites with commonly developed graded beds. This would indicate periodic influxes of clastic material, and is supported by the occurrence of rare conglomerate lenses. It appears that these sediments were deposited as the distal equivalents of carbonate-rich turbidites in moderately shallow water. The presence of talc pseudomorphs after scapolite possibly indicates hypersaline even evaporitic conditions being attained at times (Swart, 1986).

2.3.4 NUMEES FORMATION

Capping the entire Kapok subgroup are glacially derived diamictites of the Numees Formation (Martin, 1965; Von Veh, 1988). The Numees itself consists of a thin, (1 - 2 m) iron-formation capped by tillite and in turn followed by varved shales and dolomites. Although a molasse-type origin has been discussed (Davies & Coward, 1982), the presence of dropstones and a largely basement-derived clast assemblage would argue against this. The Numees has been correlated with a Gondwanaland glaciation at the end of the Precambrian (Kröner and Rankama, 1972).

2.4 NAMA GROUP

The Nama is a predominantly carbonatic, shallow water sequence deposited over large parts of southern Namibia approximately 600 Ma ago (Tankard et al., 1982). The basal beds (Kuibis Subgroup) are quartzitic and are overlain by shales and dark grey dolomites of the Schwarzkalk formation. The Nama is exposed in the Rosh Pinah area as isolated cappings on the highest mountains. To the east and north it forms a continuous blanket lying with a marked unconformity on the basement. The Nama is folded in proximity to the Gariep and was involved in the later (D2(?), D3,) deformation events.

2.5 STRUCTURE AND METAMORPHISM

The three lithofacies comprising the Kapok Formation are separated by thrust faults (Fig.1) which vary in attitude from steeply dipping to almost horizontal. These faults formed during the initial compressive phase of deformation in the area (Davies & Coward, 1982) and are deformed by later events. Thrust faults of minor displacement are common within all the lithologies and are interpreted as being part of this D1 phase. Although many of these faults are deformed by later folding (Kindl, 1979; Davies & Coward, 1982; Siegfried, 1986), it seems probable that some continued to act as zones of movement during subsequent deformation as once formed, faults become inherent zones of weakness (Etheridge & Wilkie, 1979). Folds varying in intensity from open to isoclinal are widespread and can be differentiated into two domains. A narrow zone, unfortunately obscured by sand cover, separates these two areas (Fig.1).

The western area is characterized by eastward-verging folds while the eastern area, within which lies the Rosh Pinah deposit, is characterized by westward-verging folds. Associated with these folds is an intense lineation trending north-north-west, the plunge steepening towards the north.These folds are the result of D2 deformation (Davies & Coward, 1982; Von Veh, 1988). In the Rosh Pinah area they formed as backfolds along the lateral ramp of a major thrust package (Davies & Coward, 1982). The culmination of this deformation was the development of a series of parallel, east-dipping, reverse faults effectively imbricating parts of the deposit.

Plate 1: Recumbent D2 isoclinal fold (nappe) in Hilda formation carbonates. Fold vergence is to the east as opposed to the west-verging folds at Rosh Pinah. Locality 5 km west of Rosh Pinah.

Later cross-folding has resulted in doubly plunging anticlines and, in the case of the ore deposit, localized thickening of the ore zone.

Metamorphism is lower to middle greenschist facies as indicated by the common mineral assemblages of epidote + albite + quartz and chlorite + sericite + green biotite. Evidence of an earlier almandine-epidote peak metamorphism occurs in rocks towards the north west (AAC, 1983; Siegfried, 1986). Along the coast glaucophane (Greenman, 1966) and other high pressure minerals occur. Their presence is interpreted as indicating possible plate obduction during D1 deformation (Kroner, 1974; Hartnady et al, 1990).

2.6 MINERALIZATION

Base metal mineralization occurs associated with all three of the formations comprising the Kapok subgroup. Volcanogenic massive sulphide-type mineralization is present in the volcano-sedimentary marker horizon (VGMS) within the Spitzkop formation. Near the base of the Hilda formation, iron-formations display anomalous concentrations of Pb and Zn. The 80 Mt Zn-Pb Skorpion deposit occurs 35 km. to the north of Rosh Pinah and is regarded as a syngenetic massive sulphide deposit (AAC, 1983), although its heavily weathered nature obscures much of the detail. The Aus Road Thrust (Fig.1), which possibly crosses the Skorpion prospect, hosts minor mineralization along portions of its length. It is possible that sulphide-rich horizons acted as planes of structural weakness and along which D1 thrust faulting was initiated. Breccias, of many types, occur associated with all these areas.

3. THE GEOLOGY OF MOUNTAIN ORE BODY

3.1 INTRODUCTION

The Mountain Ore Body is one of 18 tabular ore bodies ranging in size from 0.8 Mt to 1.5 Mt which together make up the Rosh Pinah ore deposit. The ore bodies all occur along the same horizon but, due to structural complications, their attitude varies from horizontal to vertically dipping. The entire ore deposit has a strike length of approximately 1300m, although extension to the south seems probable. Total ore discovered to date is in the order of 22 Mt with an average grade of 6% Zn, 2% Pb, 0.25% Cu and 28 ppm Ag.

The ore zone is made up of discontinuous, interfingering lenses of chert, dolomite, massive sulphide, argillite and quartzite that are interbedded within a sequence of feldspathic quartzites. The footwall consists of locally silicified and brecciated quartzites while the hangingwall is largely unaltered. Such ore bodies as C-Mine, A-Mine and Southern Ore Field, all display a general ore-zone stratigraphy. The brecciated footwall quartzites are overlain by microquartzite, a mining term devised to describe the fine-grained, quartz-rich nature of this rock (Page & Watson, 1976). This is followed by grey mineralized dolomite which is capped by massive sulphide, argillite or barytes rock. Sugary quartz, another mine term (Page & Watson, 1976), is a medium-grained transgressive chert that occurs within carbonate and microquartzite ore. It appears to have a replacement origin. The contact with the hangingwall feldspathic quartzites is usually sharp with rip-up clasts of ore zone lithologies commonly present in the coarse grained, basal portions of these beds. The Mountain Ore Body lies to the northern side of the Rosh Pinah deposit and is far less deformed than the bodies which lie to the south. The Mountain Ore Body itself is roughly

horizontal with a tonnage of approximately 0.9 Mt (Fig.5). It stretches 240 m in length and is 30 to 100 m wide. The maximum thickness of the sulphide horizon is 45 m. The Mountain Ore Body is bounded by high-angle reverse faults to the east and west, whereas it outcrops as a truncated anticline to the south (Fig.6). The average grade for the ore body is 8% Zn, 4% Pb, 0.5% Cu and 44 ppm Ag. The ore body displays most of the mineralogical and lithological characteristics of the other ore bodies, although it also possesses certain properties which make it unique within the deposit. The most important of these is the extensive alteration which has occurred to the ore-zone lithologies due to supergene processes (Ch. 3.2.6).

3.2 PETROGRAPHY

The Mountain Ore Body consists dominantly of three ore zone rock types: a carbon-rich, bedded chert (microquartzite); a fine-grained, sulphide-rich dolomite; and, a massive, coarse-grained barytes rock. Barytes as a lithotype is absent in most of the other ore bodies which are predominantly composed of carbonate material.

The various ore-zone lithologies described below are from observations made in the Mountain Ore Body. They can, however, be considered to be descriptive of the ore deposit as a whole.

3.2.1 FOOTWALL QUARTZITE

The footwall lithologies are almost exclusively feldspathic quartzites which have been affected in the vicinity of the ore body by silicification and subsequent brecciation (Ch. 4). The most intense alteration occurs beneath the thickest parts of the ore bodies and decreases away from these centres. Quartzites unaffected by alteration and

brecciation are texturally and mineralogically identical to those of the hangingwall.

Table 3: Modal analyses of representative Rosh Pinah footwall and hangingwall feldspathic quartzites. Each sample represents 600 counts. * Vein material

	FOOTWALL			: HANGINGWALL		
MINERALS	PRS102	PRS5	PRS11	: PRS100	PRS14	RP5
quartz	82.6	75.1	85.3	70.5	60.2	74.0
K-feldspar	9.8	5.2	12.1	7.1	4.8	4.3
plagioclase	-	-	-	1.3	-	1.5
carbonate	5.6	14.3*	1.0	-	5.2	-
sericite	0.1	0.3	0.5	17.8	25.8	15.5
opaques	1.6	5.1	0.8	3.1	3.7	4.5
zircon	-	-	0.1	-	0.3	-

To the east of the Mountain Ore Body anticline (Fig.6) the quartzite is particularly muscovite rich, the flakes 3 to 5 mm in length and of possible detrital origin

Plate 2: Hydrothermal matrix breccia with evidence of early incomplete silicification as well as heterolithic clast assemblage. Locality MOB surface exposure.

3.2.2. MICROQUARTZITE

Microquartzite occurs as two main lenses in the lower part of the Mountain Ore Body. Minor lenses occur within the footwall lithologies as well as towards the north where they grade into massive argillite.

Microquartzite is an informal mine term suggesting its siliceous nature. The rock is very fine-grained and usually black, the colour being caused by organic carbon (C_{org} = 1 - 2%). In the footwall contact zone [470 Bg], interbedded light grey and black layers occur. Microquartzite associated with the massive barytes is also light grey and appears to be of a chemical origin. In thin section (PRS 51), the quartz and sulphides are observed to have crystallized simultaneously. A few poorly rounded quartz clasts of detrital origin are also present. Microquartzite commonly contains laminations of sulphides, chiefly pyrite and yellow sphalerite. Fining upwards sequences are sometimes observable and microfolding of the laminated beds is vividly developed. Massive microquartzite also occurs and is usually poorly mineralized, the sulphides being present as disseminated specks. The microquartzite in the Mountain Ore Body is very often brecciated by transgressive, light grey carbonate veins identical to those of the footwall.

3.2.3 CARBONATE ORE

The carbonate lithologies within the ore body consist predominantly of dolomite with minor amounts of limestone. A rare suite of barium-bearing carbonates is present and occasionally, as in the A-Mine (Page & Watson, 1976), constitutes a lithology of its own.
The carbonate ore overlies the microquartzite and footwall quartzite lithologies. The contact is sharp, although usually characterized by cross-cutting carbonate veins and brecciation. The upper contact of the carbonate lithologies

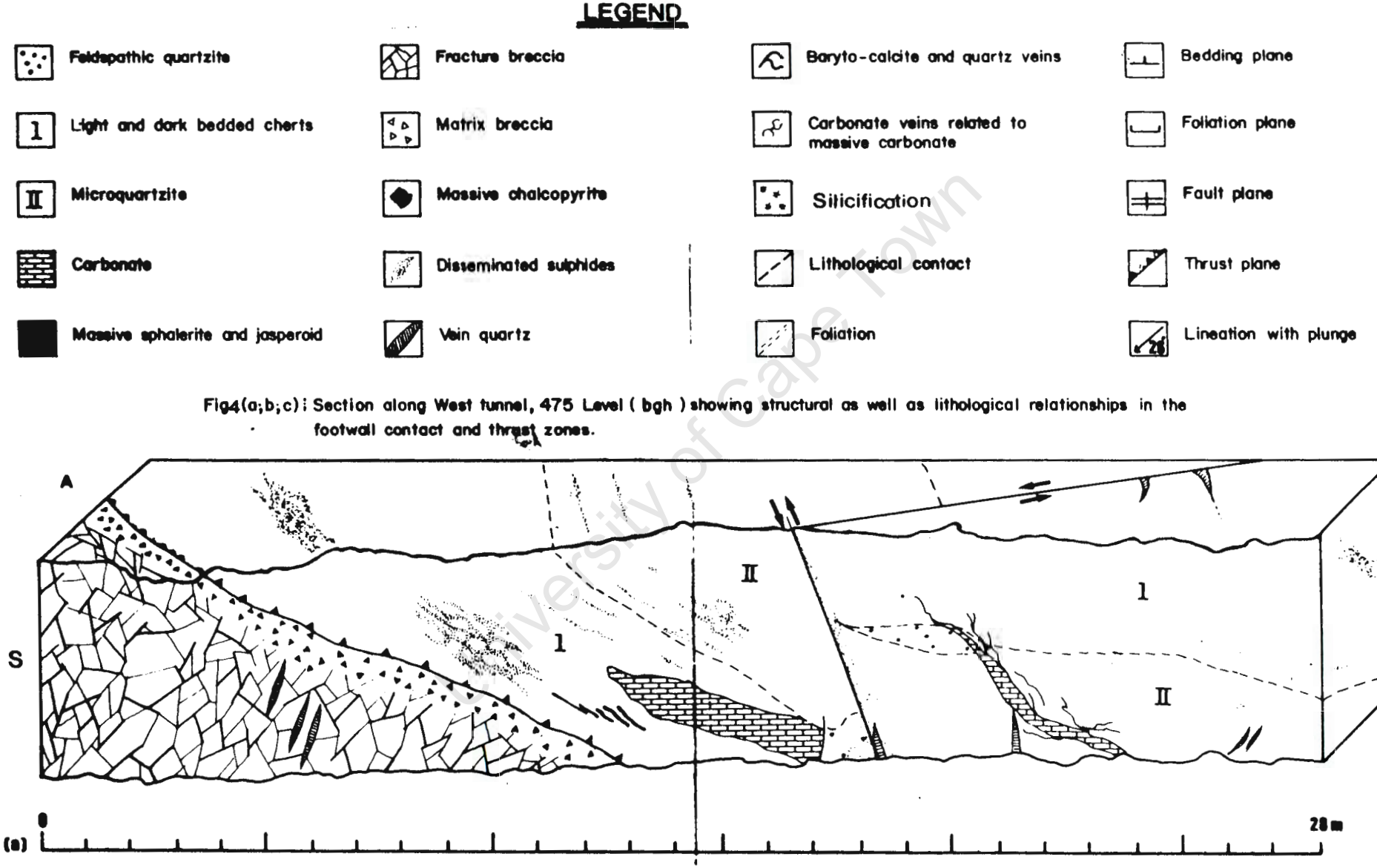

Fig4(a;b;c): Section along West tunnel, 475 Level (bgh) showing structural as well as lithological relationships in the footwall contact and thrust zones.

Fig4(a;b;c): Section along West tunnel, 475 Level (bgh) showing structural as well as lithological relationships in the footwall contact and thrust zones.

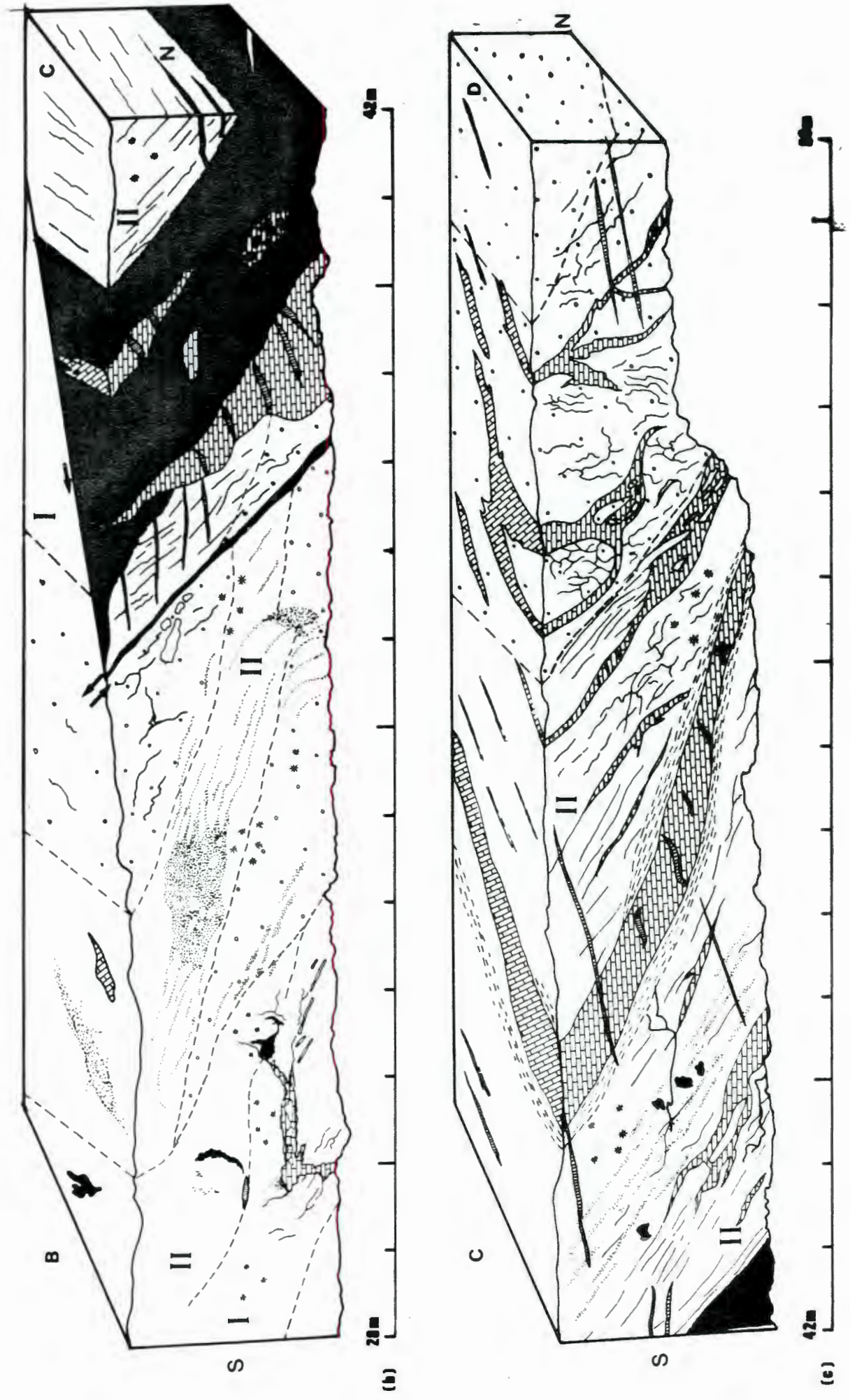
C
N
II
I
II
B
I
II
S
28m
(b)
N
D
II
C
II
S
42m
(c)

is usually marked by the development of a thin lens of massive sulphide, microquartzite or argillite. As a result of supergene alteration, the upper contacts of the bulk of the Mountain Ore Body could not be sampled. In the northern areas of the ore body, the carbonate ore grades into massive barytic rock.

The carbonate rock weathers deep tan with encrustations of varied, darker brown secondary minerals coating the surface. Underground exposure shows the rock to be typically a homogeneous, medium to dark, blue-grey crystalline carbonate usually containing spots, clots and veins of white, generally coarsely grained carbonate material. Occasionally faint banding is present, the bands being laterally discontinuous and due to deformation. Localized areas of silicification imparting a hard, sacharroidal texture to the rock are also present.

Coarse-grained pyrite and sphalerite veins crosscut the rock. Irregular segregations (< 1.0 cm) of pyrite, sphalerite, chalcopyrite and galena (py > sph > cpy > gal) occur. Disseminated grains of these sulphides are also found distributed throughout the ore.

The white carbonate spots are commonly subhedral to euhedral, 0.2 to 1.5 cm in size and have a lathlike habit. These laths also occur in the microquartzite and have been termed "hensfoot" structures (Page & Watson, 1976; van Vuuren, 1988). They occur in locally orientated aggregates less than 20 cm in size often parallel to the foliation (Plate 4).

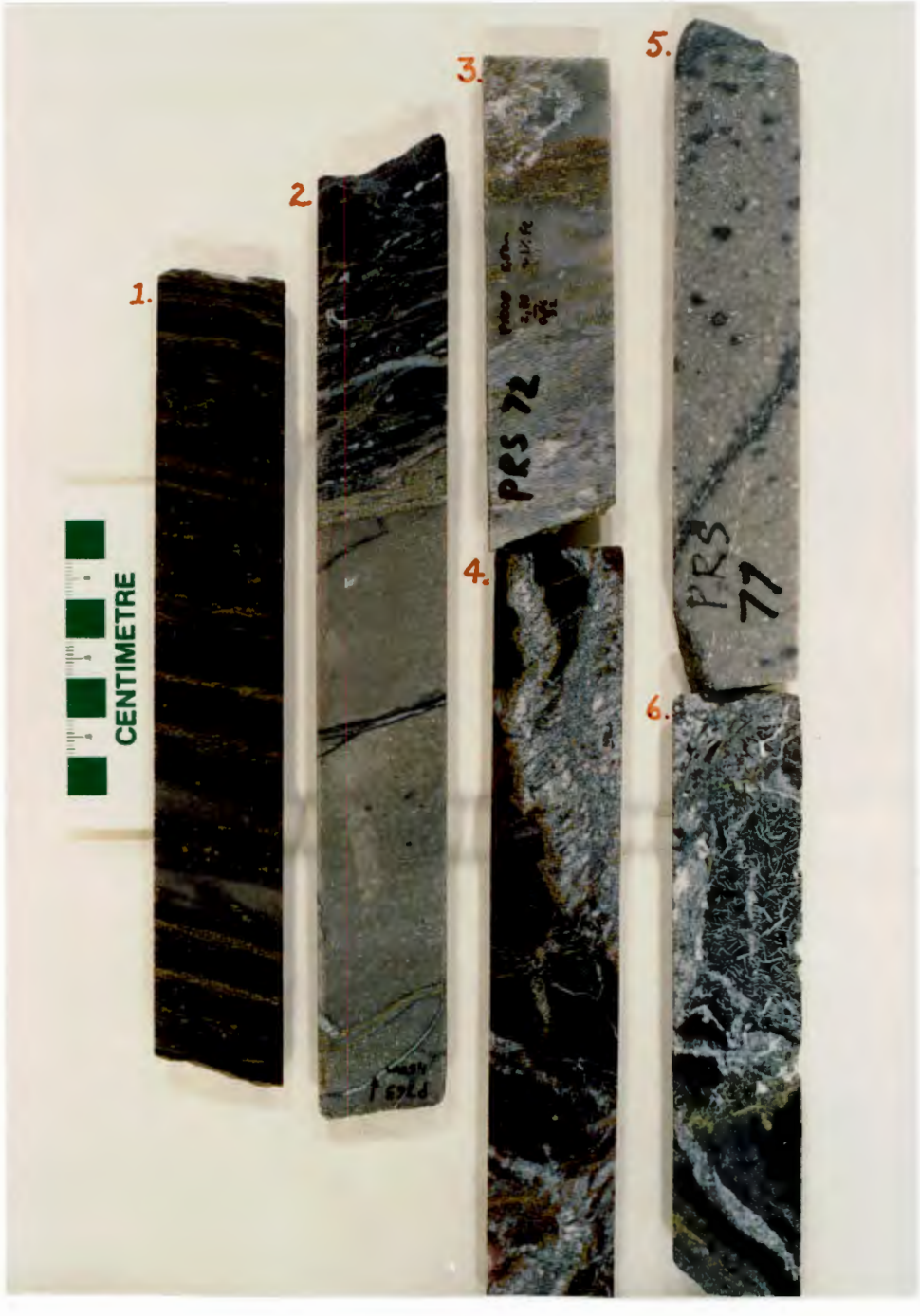

Plate 3: Silicic footwall rocks of Mountain Ore Body. (1) microquartzite with lamellae of sphalerite and diagenetic barite laths. (2) Brecciated footwall quartzite and microquartzite. Note increase in breccia intensity with decrease in grain size. (3) Footwall quartzite replaced by sugary quartz. (4) replacement veins. Note concretionary growth of matrix dolomite around clasts. (5) Incipient carbonate alteration of footwall quartzite. (6) Replaced barite veins which parallel bedding.

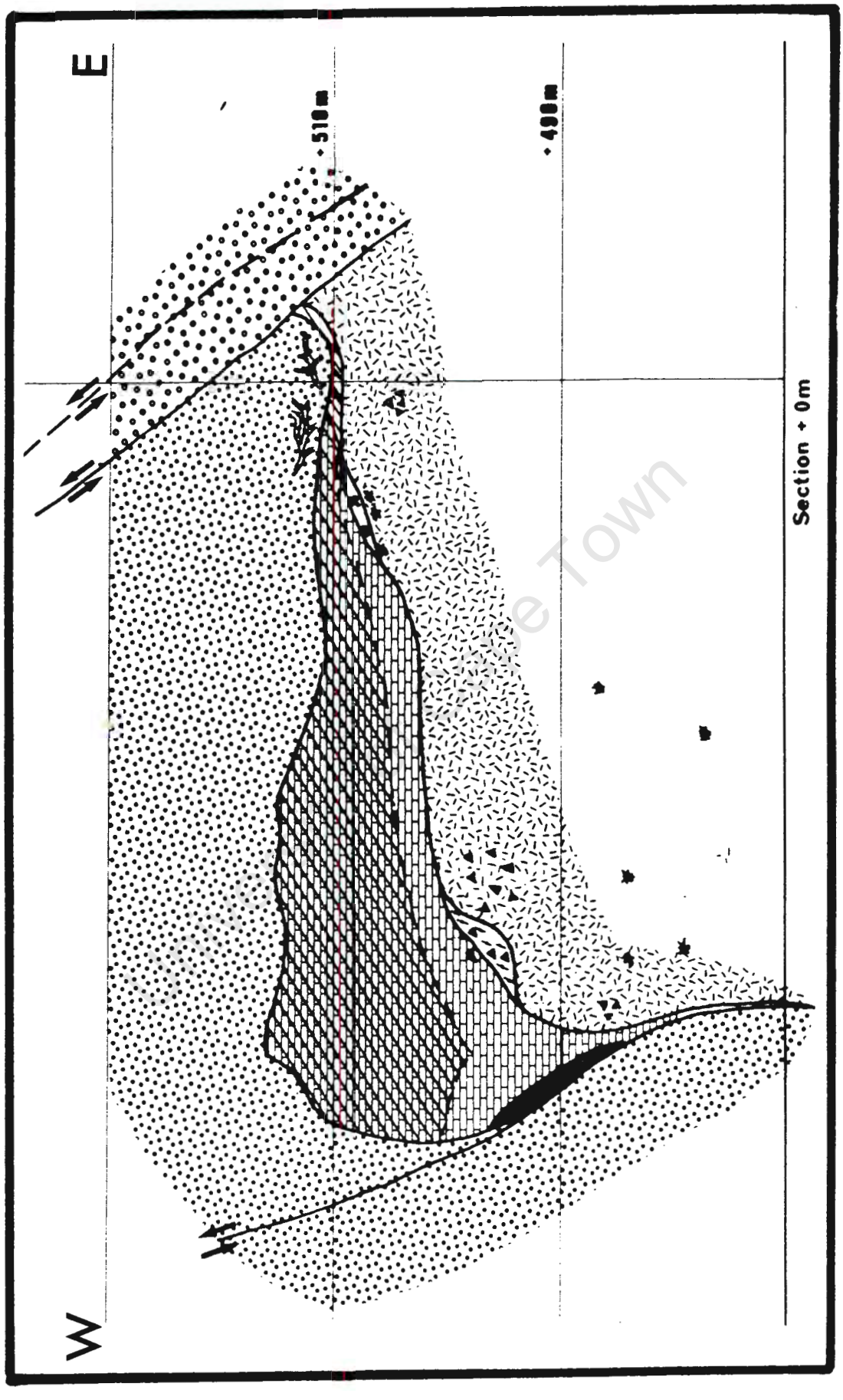

Figure 5: East/West cross-sections through the Mountain Ore Body. Refer to Map 1 for orientation and Fig. 3 for legend.

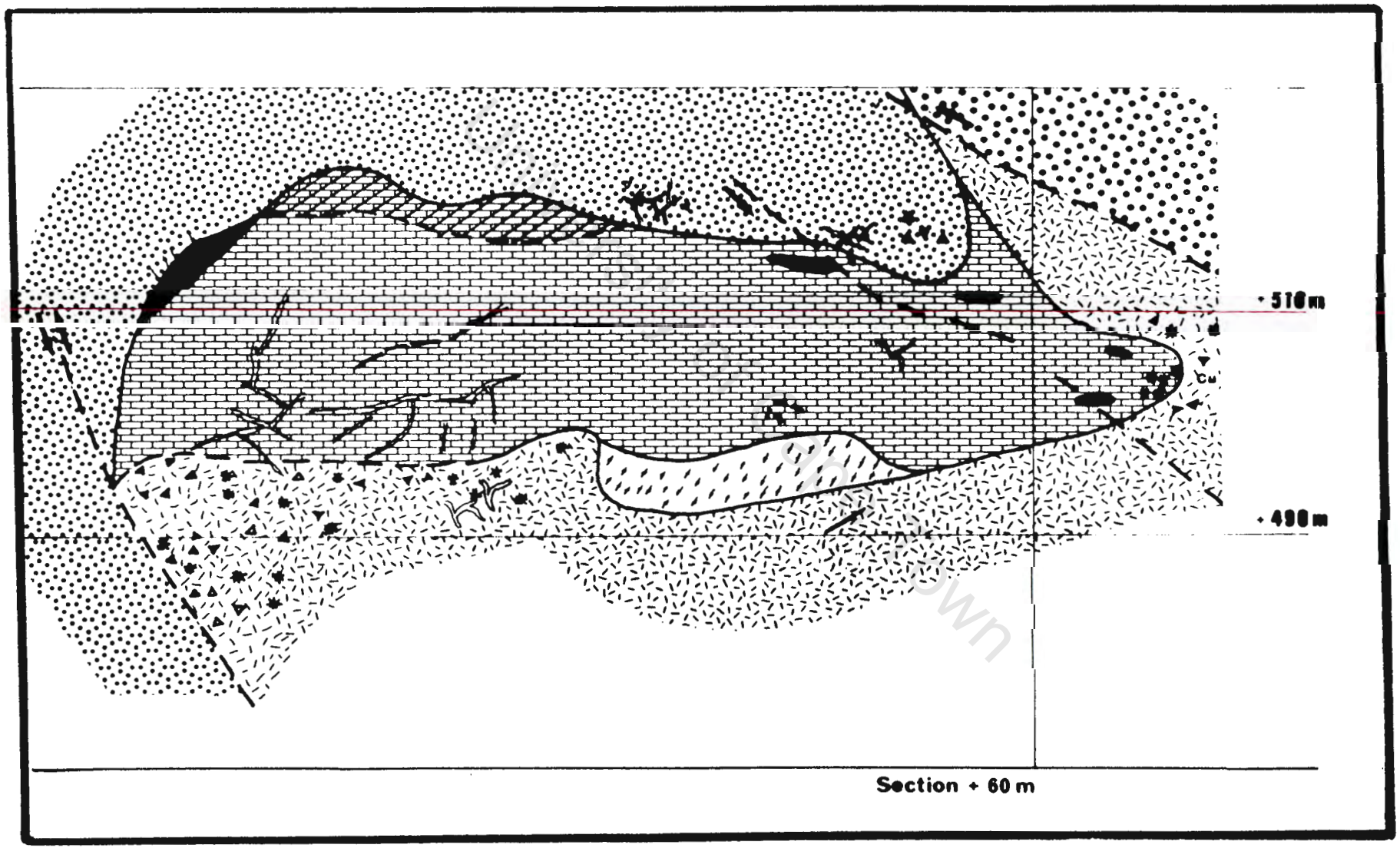
+ 516 m
+ 498 m
Section + 60 m

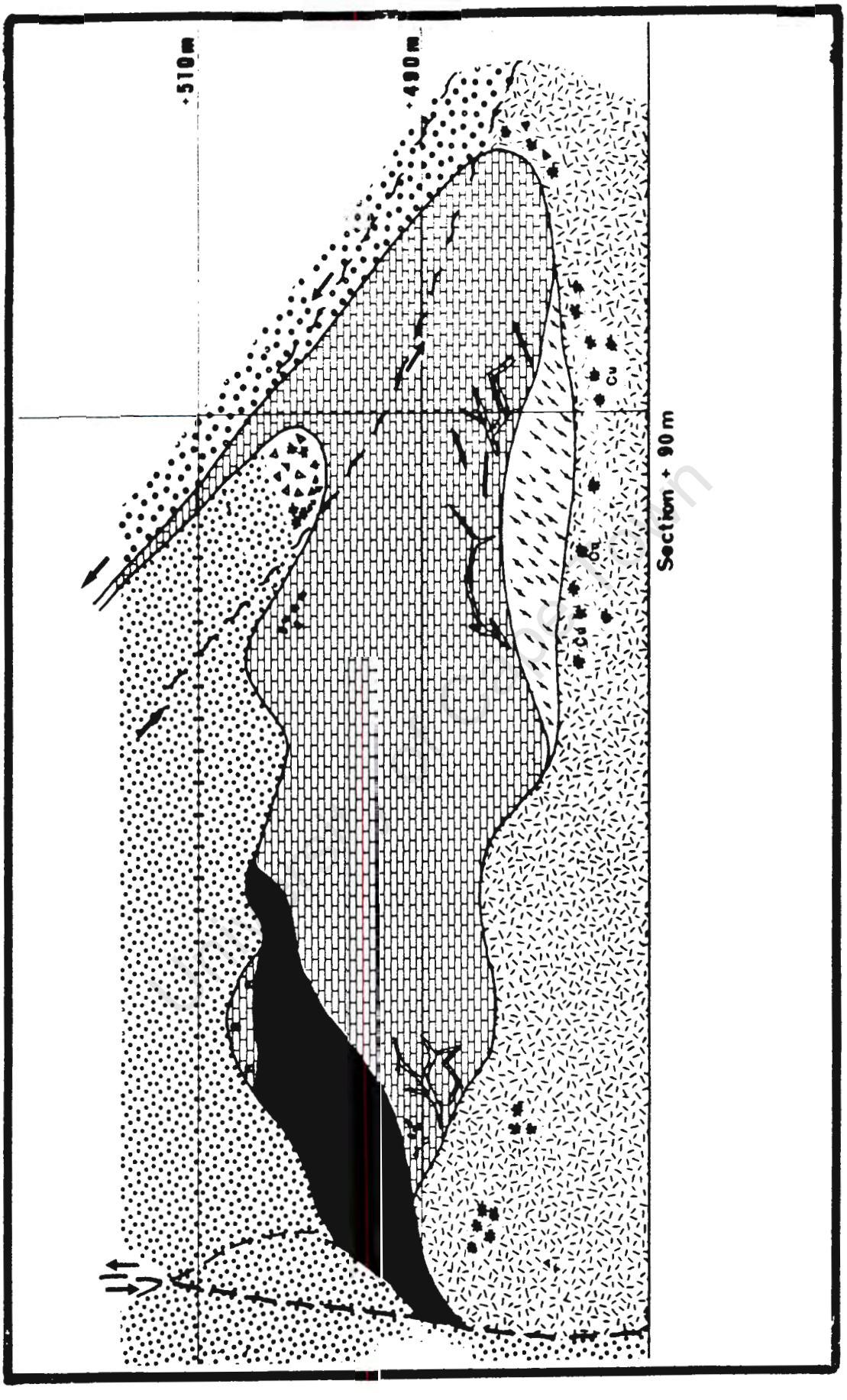
+510 m
+490 m
Cu
Cu
Cu
Section + 90 m

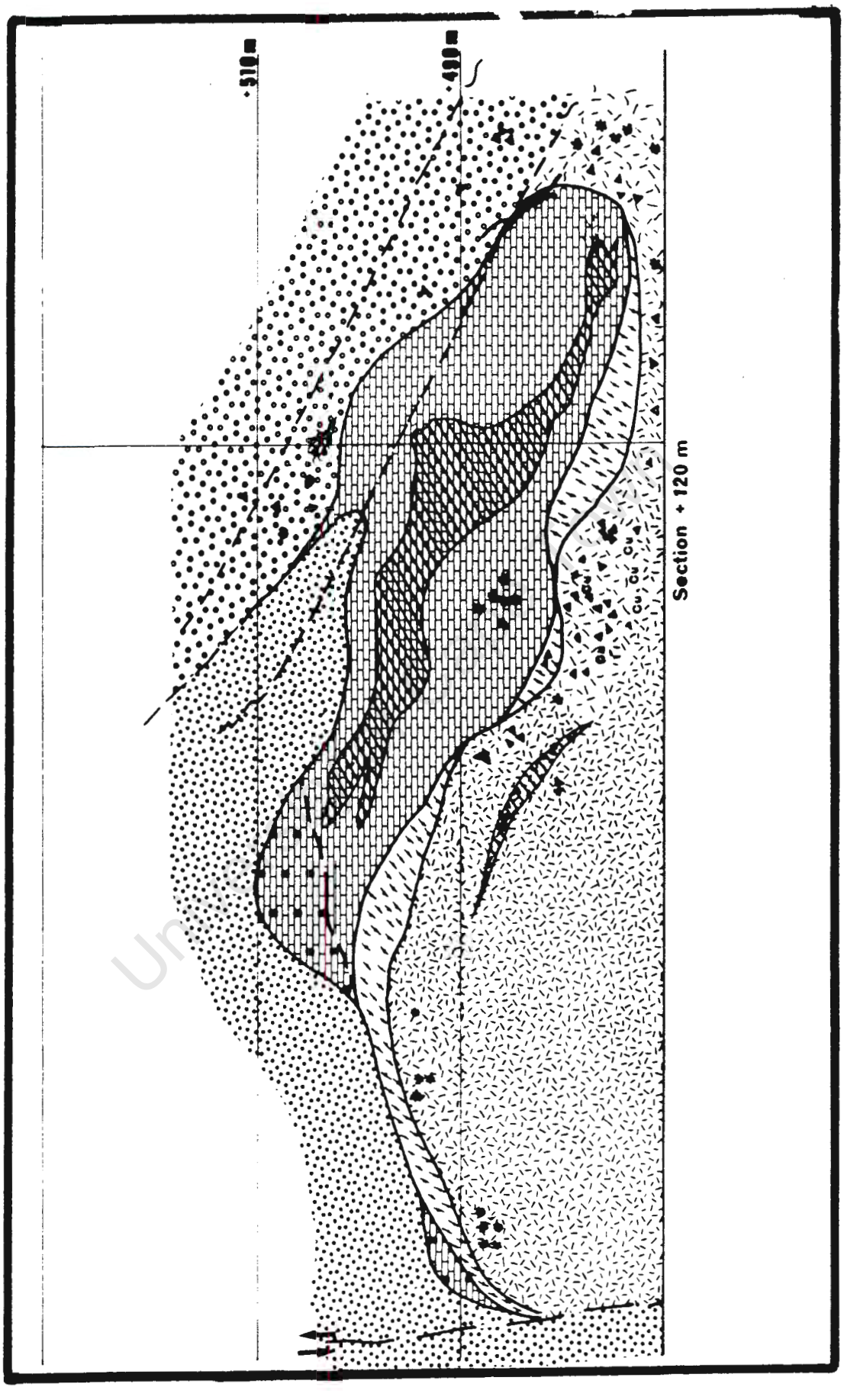
510
490
Section + 120 m
Cu
Cu
Cu
Cu

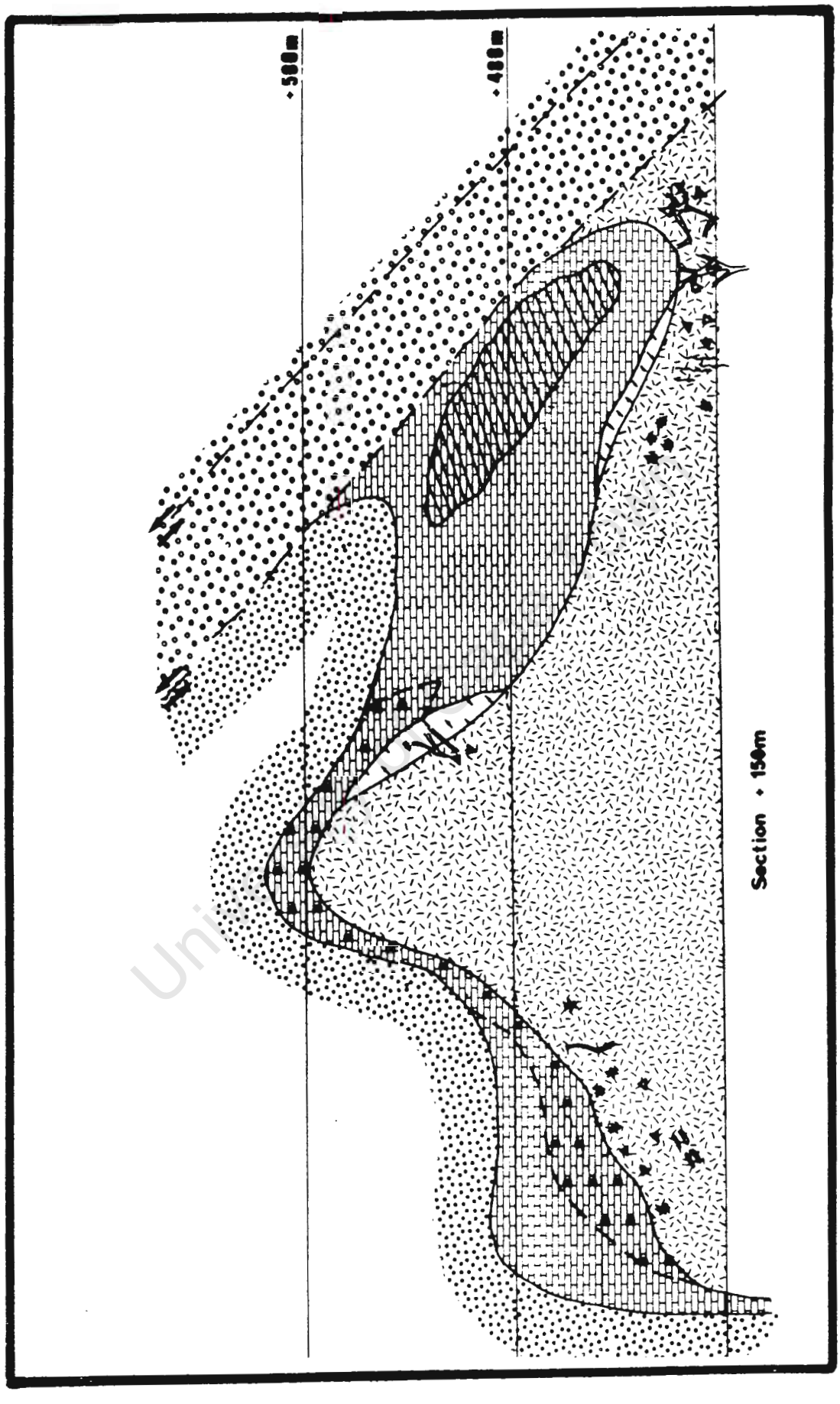
+500m
+400m
Section + 150m

Plate 4: Textures of ore zone lithologies. (1,2) Massive sulphide ore. (3) Laths of barium carbonate are hosted by dolomite. (4) Soft sediment deformation in mixed sulphide-argillite layers. (5) Density bedded silica-barite rock with evidence of flame structures and density contrasts. (6) Typical dolomite ore with blebs and laths of barium carbonate .

Very fine-grained pyrite is commonly found surrounding these laths, while coarser grained sulphides, especially amber-coloured sphalerite and euhedral pyrite, is found surrounding these areas as recrystallized grains.

Two main types of carbonate are distinguishable. The typical blue-grey dolomitic carbonate makes up the bulk of the ore body while a much lighter, cream-coloured carbonate is transgressive into the dolomitic carbonate.

The dolomitic carbonates are carbon-rich (0.5 - 2.0% C_{org}) and contain very fine-grained disseminated pyrite (Table 4). The presence of these two constituents causes the dark grey colour. The dolomite is Mn-rich and generally finer-grained than the barytic carbonates. Some samples are heterolithic with clasts and stringers of more argillic-rich material. These clasts appear to be soft-sediment deformed. Other samples contain evidence of brecciation with both carbonate types being present. Later concretionary growth around some clasts appears to have taken place with some of the laminae showing irregular almost stylolitic contacts. The rounded white carbonate segregations described are commonly tectonized with evidence of rotation as well as simple shear having occurred.

The baritic carbonate occurs in the footwall and lower ore zone lithologies as matrix to the breccia or as bedding parallel veins. It also occurs as spotty veins and segregations with gradational contacts within dolomitic carbonate host rock. Coarsely recrystallized and mineralized baryitic carbonates were noted comprising the ore zone in the severely stretched and deformed parts of the

Table 4: Whole rock analyses of dolomitic ore and hangingwall carbonate rock (data from de Kock, 1988). na = not analysed.

	DOLOMITIC ORE		HANGINGWALL DOLOMITE	
		(%)		
SiO_2	0.68	1.02	10.20	3.10
TiO_2	-	0.15	0.05	0.07
Al_2O_3	0.14	0.90	1.40	0.09
Fe_2O_3	9.74	9.80	1.20	1.51
MnO	2.80	0.43	0.32	0.20
MgO	11.33	13.94	16.44	19.03
CaO	17.56	20.98	27.43	30.03
Na_2O	1.94	0.01	0.80	0.03
K_2O	-	0.03	0.58	0.14
P_2O_5	-	-	0.03	-
CO_2	na	33.60	na	na
C_{org}	na	1.83	na	2.18
S	na	11.08	na	0.18
		(ppm)		
Zn	124000	64000	570	90
Pb	39000	18000	140	60
Cu	500	1200	20	6
Ag	80	na	4	na
Ba	na	5000	na	22
Cd	290	160	6	5
Sr	563	15	302	2100
Rb	34	16	28	5
Co	4	na	4	na
Ni	164	na	5	6
Zr	103	na	29	na

ore body such as [470 Ba]. These carbonates are also recognised by the absence of particularly fine-grained sulphides such as pyrite as well as the relative enrichment of Cu in the form of chalcopyrite.

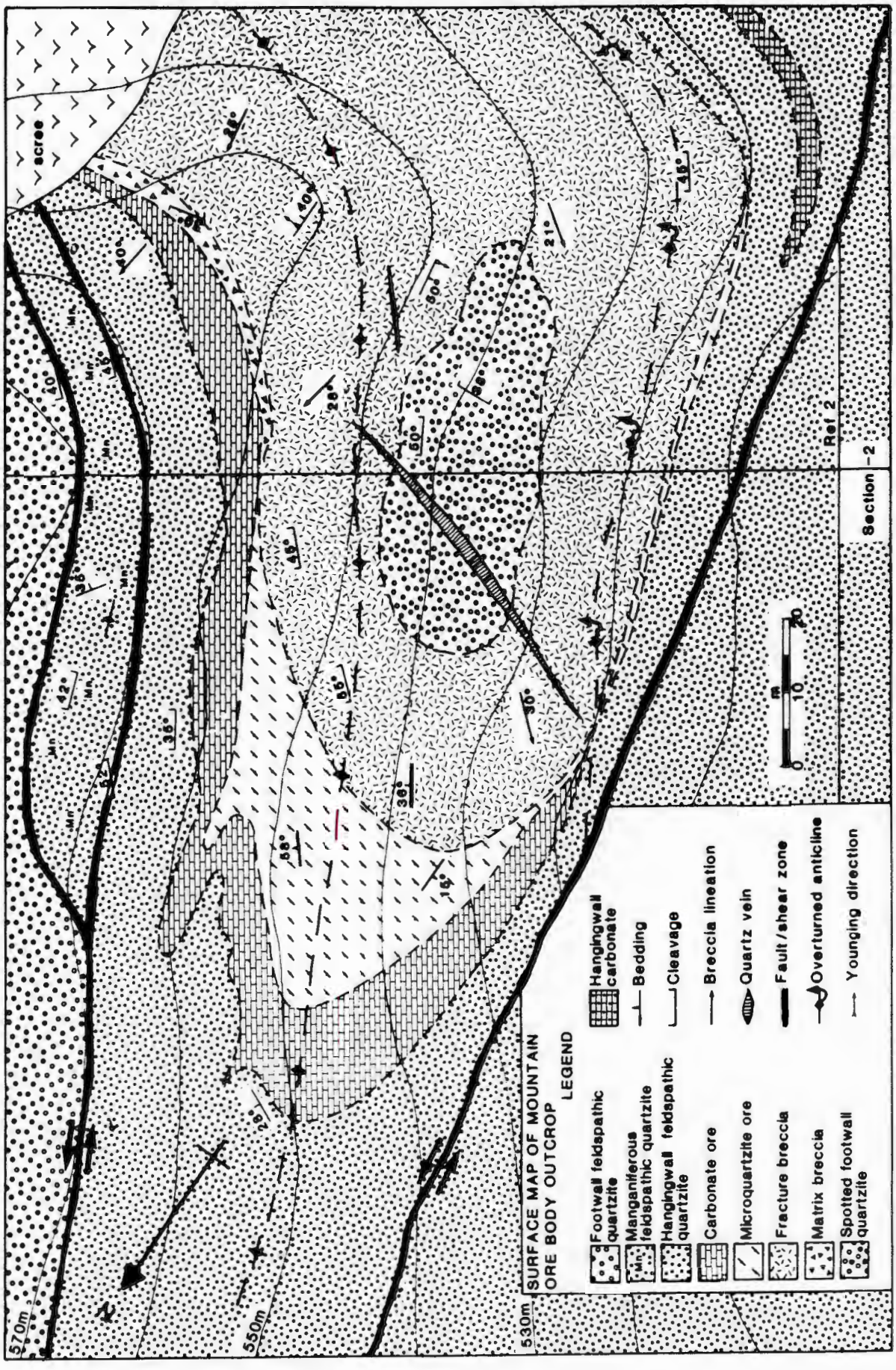

Figure 6: Surface exposure of the Mountain Ore Body.

3.2.4 BARITE ORE

The northern extension of the ore body [490 Cc-490 Ca] consists almost exclusively of massive barite. Barite ore also occurs as a capping to the massive sulphide and carbonate lithologies on the eastern side of the ore body [490 Ef]. Here barite extends down into the footwall where it occurs as veins and as secondary encrustations and joint fillings. In places [490 De] barite forms the matrix to the massive ore. It is possible that this is due to later remobilization.

Plate 5: Pod of rhodochrosite with intergrown barite laths. Host rock is massive barite ore. MOB [490Cb].

The barite ore is generally a heterogeneous, light grey, medium-grained, sugary-textured rock containing glassy "porphyroblasts" of barite up to 2 cm in size. Colour variations are common, (from yellow, orange, red and green to purple and brown) and primarily a result of disseminated sphalerite. In many areas carbonate, consisting primarily of dolomite, is present in the rock and ranges from trace amounts to 35%. The carbonate occurs either as discordant

dolomite-rich veins or as discrete grains of barium carbonate.

Stringers and irregular elongate patches of alabandite [MnS] as well as rhodochrosite occur in the northern portions of the Mountain Ore Body. Some segregations of rhodochrosite have radiating, euhedral laths of barite approximately 1.0 cm in length (Plate 5) associated with them. The barite ore is also more enriched with respect to lead (Fig. 7a) and depleted with respect to iron (Fe = 0.72%), compared to the other ore types.

Laminated chert and barite (plate 4) horizons occur in the northern portion of the ore body. Geopetal structures such as rip-up clasts and slumps were observed. These features arise as a result of the density contrast between the layers of denser barite and less dense siliceous ooze present during deposition. Way-up is indicated by "balling" of the barite into the chert layers and is supported by graded bedding nearby in the sequence.

3.2.5 SUGARY QUARTZ

Sugary quartz itself is a light grey to black, granular, medium grained, cherty rock. Yellow, brown and orange colouration of this rock type is due to sphalerite. It appears to be a replacement chert similar to the Mount Isa "silica dolomite" (Swager, 1985). It therefore should correctly be known as a "jasperoid" (Lovering, 1972).

Sugary quartz occurs mainly at the footwall contact with the ore zone where it is richly mineralized with brown sphalerite. It has also been observed in the footwall quartzites 6 m below the ore zone contact (PRS 72). Sugary quartz occurs in irregular areas within the silicified quartzite and microquartzite layers. In the C-Mine sugary quartz occurs as irregular masses within the carbonate portion of the ore body.

3.2.6 SUPERGENE ALTERATION ZONES

The Mountain Ore Body is the topographically highest lying of all the ore bodies at Rosh Pinah. The morphology of the ore body, i.e., a shallow plunging anticline which outcrops to the southeast, compounded by the presence of two faults bordering the ore body, has resulted in the interaction of meteoric (surface) water with the ore. Leaching and remobilization of the sulphides and carbonate gangue has occurred, and evidence of alteration under both oxidizing as well as reducing conditions is present.

The most oxidized ore lies in the southwestern area of the ore body and extends as a capping and intermixed with the unaltered ore from section 0 m to section 150 m (Fig.5). The oxidized ore consists essentially of iron oxides and hydroxides and secondary Zn, Pb and Cu-bearing minerals. It has the appearance of a cellular, brick-coloured boxwork. The contact between oxidized and underlying leached ore is normally sharp (<1 m) and it would appear that much of the ore was leached of carbonate material prior to the onset of oxidation.

The leached zones extend over the entire ore body and are controlled by areas of pre-existing structural weakness. The carbonate ore alters to a dirty cream-coloured, Pb-enriched, Zn-depleted friable rock. Cubic galena has been observed to form ribbon-like encrustations or draperies over areas of this rock. Marcasite has also precipitated as thick botryoidal layers and is often associated with barite. The barite appears always to be post marcasite formation and occurs both as euhedral, honey-coloured, tabular and flattened octahedral crystals as well as earthy concretions.

3.2.7 HANGINGWALL LITHOLOGIES

The rocks overlying the ore body are essentially unaltered feldspathic quartzites, although minor carbonate and argillite lenses occur. The rock is dark, blue-grey and spotted with white clasts of feldspar approximately 4.0 mm in diamter. The majority of feldspars are microcline with subordinate orthoclase and rare, sodic plagioclase. Large, (0.5 - 1.0 cm) detrital quartz grains are commonly subrounded and transparent. Some quartz clasts contain rutile needles as well as zircon inclusions. A characteristic of these rocks is the presence of opalescent blue quartz clasts.

The quartzites that compose the hangingwall are generally more carbonate-rich and micaceous than those in the footwall (Table 3) although this is due in part to the silicification of the footwall lithologies. Carbonate occurs as intergranular filling showing no alteration of feldspar grains as opposed to the crosscutting veins of the footwall. The hangingwall carbonate analysed is exclusively dolomitic in composition.

Carbonate lenses occur sporadically throughout the hangingwall succession as well as in a discontinuous horizon 5 to 20 m above the orezone contact. They have a marked similarity to beds described within the Hilda facies (Kindl,1979; Siegfried, 1986). Sedimentary structures such as graded bedding and rip-up clasts consisting of gritty carbonate are present in these lenses. The carbonate rock itself is fine-grained and rich in organic carbon (2.2%). In the vicinity of these lenses, the quartzite is far more carbonate-rich and in fact grades into the carbonate rock. Carbonate debris flows occur to the east of the mine and consist of light grey and red-brown weathering clasts up to 50 cm in diameter hosted in blue-grey dolomite. Similar but finer grained sedimentary breccias occur above the 490 adit to Mountain Ore Body.

In some borehole intersections to the north of the Mountain Ore Body, felsic agglomerates were encountered. These rocks consist of light green, sericite-rich clasts 2 to 3 cm in

diameter hosted by a grey, fine-grained quartz-feldspar matrix. Pyrrhotite is a notable component commonly forming up to 2% of these rocks. No outcrop of these agglomerates was found. However, exposure of similar volcanics has been noted to the south-east in the vicinity of Southern Ore Field. A volcaniclastic horizon has been described in the vicinity of A-Mine (Watson, 1980).

3.3 MINERALOGY

The sulphide species occurring at the mine consist essentially of a simple suite of metal sulphide complexes (ZnS, PbS, FeS_2, $CuFeS_4$) which are a characteristic of most SEDEX type deposits (Large, 1983). Although dominated by pyrite, sphalerite, galena and chalcopyrite, trace amounts of other sulphide minerals do occur (Table 5). The sulphides at Rosh Pinah have undergone changes in original mineralogy as a result of deformation and metamorphic reconstitution. The formation of sulphides associated with syngenetically deposited ore deposits is still a controversial subject and theories range from diagenetic and epigenetic replacement of carbonates (Kucha, 1988), sulphates (Lange et. al., 1985) and ferromagnesian silicates (Mallio & Gheith, 1972) to direct precipitation from the hydrothermal vent (Lydon, 1983).

3.3.1 PYRITE

The iron is almost completely bound up in pyrite (FeS_2). Three distinct generations of pyrite were identified occurring in the ore zone, although remobilisation during deformation has obliterated many of the original primary textures such as colloform banding and framboidal habits.

The two textures which are the most prevalent are the first generation pyrites which are fine-grained (<50 um), subrounded to irregular grains that sometimes occur as framboids and more rarely as small cubes. These grains occur in stringlike aggregates, trails and irregular clusters. These aggregates occur parallel to bedding in the microquartzite lithologies, while in the carbonate lithologies they surround the laths.

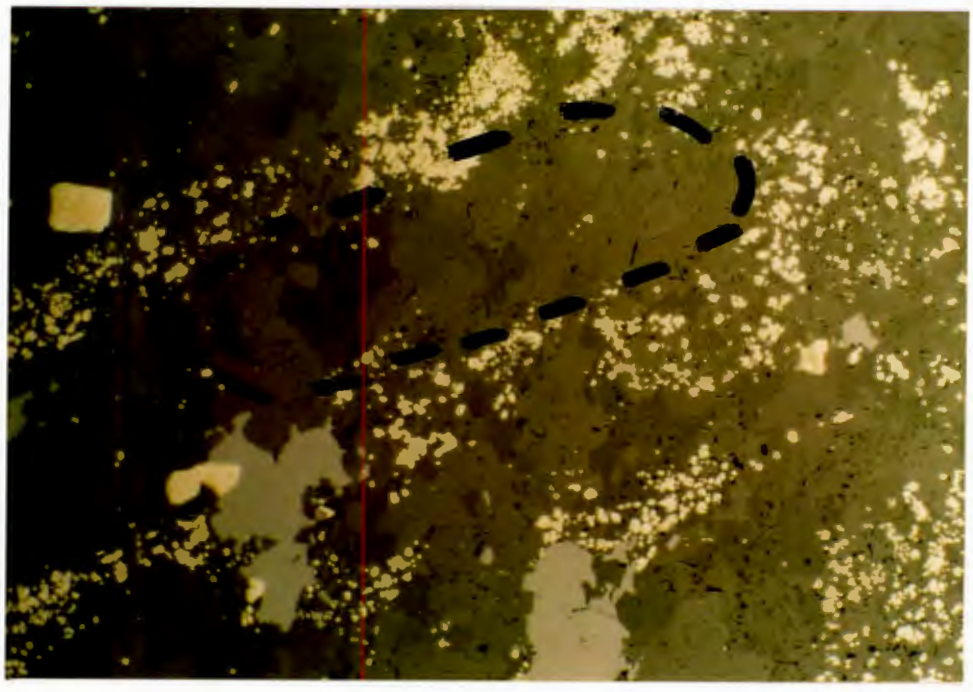

Plate 6: Fine-grained, first generation pyrite surrounds a large laths of barium carbonate grains (dotted). Sphalerite (light grey) is reconstituted during metamorphism. PRS 26, X.10

Second generation pyrites are much coarser-grained (approximately 200 um), subhedral to euhedral but generally rounded. These pyrites occur in all lithologies and are commonly surrounded by sphalerite or chalcopyrite. They appear to be the result of metamorphic reconstitution of the first generation pyrites (Chauhan, 1984) as can be seen by the complete gradation from loose aggregates of fine-grained pyrite through to euhedral "porphyroblasts". Regrowth on porous second generation pyrites, noticed in some of the later, pyrite-rich crackle breccias, is considered to represent a third period of pyrite growth. Many of the euhedral pyrites occuring in sheared lithologies such as microquartzite display cataclastic fractures (Ramdohr, 1969), most of which have been annealed by chalcopyrite (Plate 8). In some of the later deformation-related, type 3 sulphide veins (Ch. 4.3.3.3), pyrite grains with angular habit similar to that of arsenopyrite, occur (Plate 7). Of note in these veins is the cruciform replacement of pyrite

by chalcopyrite. Similar replacement textures have been described for sphalerite replacing galena (Watson, 1980).

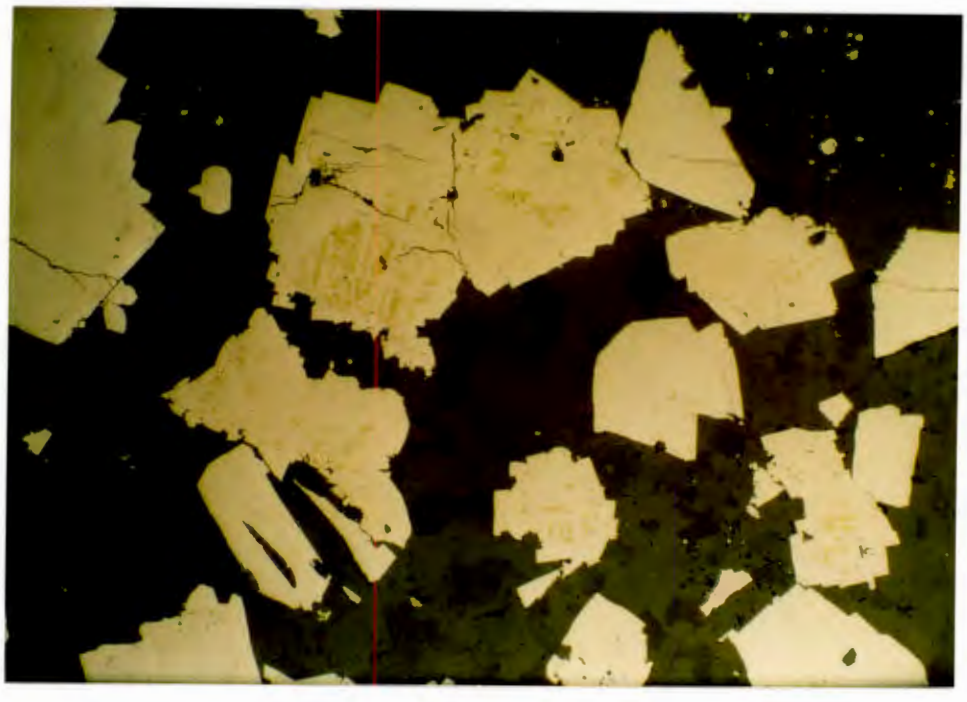

Plate 7: Angular pyrite present in type 3 sulphide veins. Cruciform chalcopyrite replacement can be noticed. PRS 95, X.40

3.3.2 SPHALERITE

Two generations of sphalerite can be identified on grounds of textural as well as compositional criteria. Early sphalerite occurs as fine to medium-grained (<0.5 mm), disseminated grains generally concentrated along the edges of carbonate laths. The bulk of the sphalerite, however, consists of medium to large grains approximately 2.0 mm in size. These grains appear to be the result of metamorphic recrystallization of the early fine grained sphalerite and are usually irregular and flamelike in appearance. They are predominantly associated with second generation pyrite, are inclusion free and are more iron-rich (Table 6).

A characteristic of the sphalerite present within Mountain Ore Body is the variety of colours which it can possess.

Specimens ranging from blood red to honey yellow, light cream to black as well as various shades of brown have been noted. The main reason for colouration is ascribed to traces of Fe, Cd or Mn substituting for Zn in the sphalerite lattice (Watson, 1980).

Amber- and honey-coloured varieties in Mountain Ore Body were found to contain 0.9% Fe on average with lesser Mn. Dark brown to black, massive, coarse-grained (>1 cm) sphalerite occurs as remobilised veins and patches commonly in proximity to the footwall contact zone. It was found to be particularly Fe-rich (4 - 6 wt% Fe) as well as containing much disseminated chalcopyrite or chalcopyrite disease. Of note was a bright orange sphalerite of supergene origin which contained 7.2 wt% Mn with little to no Fe.

The assemblage pyrite-sphalerite-pyrrhotite is an important geothermometer (Scott & Barnes, 1971) the amount of iron occurring within the sphalerite being indicative of the temperature at which the sphalerite crystallised. Although pyrrhotite occurs within the hangingwall lithologies, it is an uncommon sulphide mineral within the deposit. A sample of argillite (PRS 81) was found to contain granular vein calcite with dark brown sphalerite, subhedral to euhedral pyrite and irregular masses of pyrrhotite. The veins are parallel to S0 and deformed by S1 and S2 foliations. Unfortunately the sphalerite proved to contain insufficient amounts of iron (< 10% Fe) so that pressure and temperature estimates could not be obtained.

Table 6: Microprobe analyses of (a), fine-grained, first generation sphalerite and (b), coarse-grained, second generation (metamorphic) sphalerite. Low totals in (a) are ascribed to presence of Cd which was not analysed.

	Fe	Zn	Mn	S	TOTAL
a	0.89	65.19	0.52	32.53	99.13
	0.70	65.45	0.48	32.71	99.34
	0.75	65.33	0.57	32.52	99.17
	0.87	65.43	0.45	32.71	99.46
	0.68	65.54	0.54	32.61	99.37
	0.80	65.27	0.49	32.41	98.97
	0.70	65.92	0.54	32.31	99.47
	0.59	65.23	0.46	32.47	98.75
	0.80	65.20	0.52	32.49	99.01
b	1.19	64.85	0.73	32.66	99.43
	1.13	65.05	0.78	33.09	100.05
	1.25	64.53	0.75	32.59	99.12
	1.34	65.14	0.80	32.75	100.03
	1.28	65.66	0.78	32.70	100.42
	1.28	64.56	0.97	32.88	99.69
	1.20	64.97	0.75	32.67	99.59
	1.21	65.04	0.77	32.71	99.73
	1.27	65.31	0.78	32.68	100.04

3.3.3 GALENA

The majority of the galena occurs in the upper portions of the ore body, the absence of Pb mineralisation often being used to delineate the hangingwall contact (van Vuuren, 1986). All galena is remobilized and segregations of galena, sequentially rimmed by sphalerite and pyrite, are common in the carbonate ore. Framboids of galena (approx. 5 μm) have been described occurring in microquartzite ore (P. Munk, pers. comm.) but could be pseudomorphs after pyrite. Galena is most enriched in the baritic lithologies and also occurs as a major sulphide mineral in the supergene alteration zone.

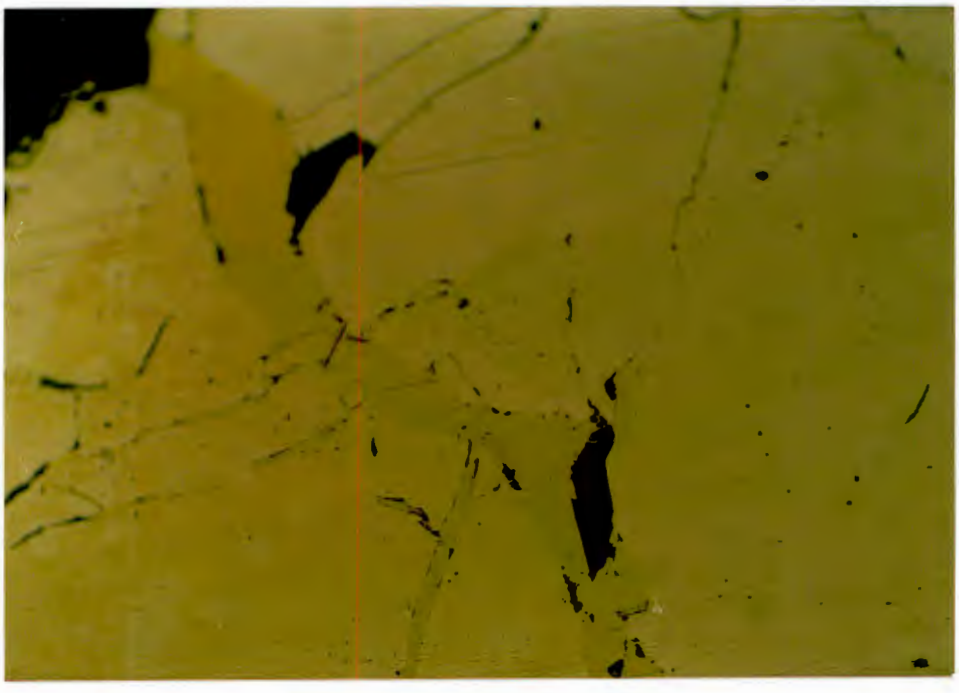

Plate 8: Fractures in cataclastically deformed pyrite being filled with chalcopyrite. PRS 29, X.100

3.3.4 CHALCOPYRITE

Chalcopyrite is the dominant Cu-bearing mineral in the ore body. It occurs as large clots preferentially in the footwall regions were it is associated with silica. Much of the chalcopyrite is remobilized and is found as late stage veins, fissure-fillings and replacement textures (Plates 7,8,28).

3.3.5 ALABANDITE

Alabandite occurs in the northern, rich portion of Mountain Ore Body in association with rounded grains of pyrite and unidentified, weathered carbonate laths. The areas of alabandite enrichment are marked by dark brown, elongate lenses and stringers conformable to bedding. The mineral is easily recognised as it oxidises after only a few days exposure to air and becomes coated with a soft, dark brown

rust-like alteration product. Alabandite was documented in B-Mine (Watson, 1980) in association with kutnahorite [$Ca(Mn,Mg)(CO_3)_2$] and Mn-bearing dolomite.

3.3.6 OTHER SULPHIDES

Although many sulphide species have been identified at Rosh Pinah (Table 5) only members of the Cu-bearing or Ag-bearing minerals are common in trace amounts.

The most numerous of these is tennantite, the As-rich end member of the tennantite-tetrahedrite sulpho-salt series. It is associated with late stage veins of norsethite and baryto-calcite, bornite-rich areas of sugary quartz and with massive clots of chalcopyrite in the footwall. In the A-Mine tennantite was associated with the norsethite-rich core zone (Watson, 1980).

In the Mountain Ore Body bornite is present in well-mineralized areas of the baritic ore as well as associated with sugary quartz. It is also observed in a zone of massive ore crosscut by the Western Boundary Fault [490 Aj]. In all cases the bornite appears to be a breakdown product of chalcopyrite (PRS 121), and contains scattered inclusions of chalcopyrite and Ag-bearing sulphides.

The Ag-bearing minerals, which are economically important, are associated with tennantite, chalcopyrite and bornite. Although the baritic ore is Ag-rich as well as Pb-rich the majority of the silver minerals are associated with chalcopyrite. The minerals commonly present are stromeyerite [$(Ag,Cu)S_2$], Mckinstryite [$(Ag,Cu_{1.2-X})S_2$] and acanthite [AgS_2]. They are present as scattered, emulsoid-like grains less than 15 µm in size, alteration rims to tennantite and late crosscutting veins.

3.3.7 BARIUM CARBONATES

This rare suite of carbonate minerals is a volumetrically minor but genetically important component of the ore deposit. The carbonates identified are norsethite [$BaMg(CO_3)_2$], baryto-calcite [$BaCa(CO_3)_2$], alstonite [$Ba(Ca,Sr)(CO_3)_2$], witherite [$BaCO_3$] and benstonite [$MgCa_6Ba_6(CO_3)_{13}$]. All these minerals are orthorhombic carbonates in the same class as aragonite (Speer, 1983). Other members of this class, namely cerussite [$PbCO_3$] and strontianite [$SrCO_3$], almost certainly occur in the ore zone but were not identified during this study.

The barium carbonate minerals occur as the main component of the baritic carbonate, make up the laths and segregations in the dolomitic carbonate or are present as late-stage veins and cavity fillings (Ch. 4.3.2). The laths and less distinct spots in the dolomitic ore were found to consist of medium grained, granular aggregates generally composed of norsethite. The aggregates consist of irregular rounded grains with seriate grain edges that are surrounded by fine-grained dolomite. The grain contacts of the barium carbonates show no relationship to the outlines of the laths. It appears therefore that the barium carbonates have replaced some pre-existing mineral.

Barium carbonate grains also occasionally show evidence of being replaced by dolomite (PRS 74). The replacement occurs preferentially along grain contacts. Although baryto-calcite and witherite have been recorded as high temperature (>550^{o} C) alteration products of benstonite in a carbonatite occurring in the USSR (Vorob'yev, et al, 1985), the majority of occurrences appear to have formed under low temperature, late-stage, commonly diagenetic, conditions (Mrose et al., 1961). At Langban, a sedimentary-exhalative, Ba-Mn deposit, carbonates, including baryto-calcite, witherite and rhodochrosite, form open-space fillings in cavities related to deformation (Sundias, 1966). In the Jason and nearby Tom deposits of the Selwyn basin in Canada, norsethite, benstonite, witherite and baryto-calcite occur in the barite-rich parts of the ore bodies (Gardner & Hutcheon,

1985). These barium carbonates are associated with celsian and kaolinite and are secondary, having formed during early diagenetic conditions. Norsethite, baryto-calcite and witherite have also been recorded forming within dolomitic oil shales underlying the trona deposits of the Green River Formation, Wyoming, USA (Mrose, et al., 1961) and are associated with other authigenic minerals such as shortite, searlesite and labuntsovite.

Another common occurrence of baryto-calcite and witherite is as a replacement of barite or anhydrite (Speer, 1983). They documented examples of barite deposits in the central United States which were substantially altered to barium carbonate as a result of the through-flushing of CO_2-rich fluids during deformation. It is possible that at Rosh Pinah a similar process could explain the presence of barium carbonates.

Rhodochrosite, although not a barium-bearing carbonate, occurs in association with barite ore as lenticular or irregular pods (Plate 5). Some pods appear to have been incorporated in the barite ore while partially solidified. The association of the two minerals (barite and rhodochrosite) is interesting as rhodochrosite has a restricted paragenesis. Lenses of rhodochrosite were noted at Roseberry in Tasmania (Braithwaite, 1974) as well as at Meggen in Germany (Hannak, 1981) and in both cases indicate the more distal regions of ore deposition.

3.3.8 FLUID INCLUSIONS

Barite laths originating from the bedded chert and barite ore (PRS 86) contain numerous fluid inclusions. Although no experimental work was carried out, a few generalisations regarding these inclusions can be made (Evans, 1987; Roedder, 1984). Two, and possibly three generations of fluid inclusions can be recognised. The inclusions form slightly sinuous, parallel trails, presumably controlled by

3.4 BASE METAL DISTRIBUTION

Metal zonation, both vertical as well as lateral, has been documented many times in exhalative deposits (Large, 1983; Gustafson & Williams, 1981; Plimer, 1988). This zonation is a result of the deposition of base metals at a specific time or distance from the hydrothermal source. The primary controls of this deposition are pH, Eh, fO_2, fS_2, temperature and availability of ions (Lydon, 1982), of which the most important appears to be temperature (Sato, 1972). This means elements soluble at high temperatures, such as Cu, will be deposited in the vicinity of the vent (McKay & Hazeldene, 1987), while lower temperature elements, such as Mn, will be deposited towards the periphery or distal areas of the deposit. This principle has been effective in the delineation of ore-bodies (Jambohr, 1979) as well as exploration strategies (Smee & Bailes, 1986). Most mining operations posses a vast data bank of analyzed metal values and it is these values, and ratios, of Zn, Cu, Pb, Fe and Ag which have been utilized with varied success in the definition of metallogenic zones.

A distinct metallostratigraphy has been recorded within the Rosh Pinah ore bodies (van Vuuren, 1986) and is well known to workers on the mine. The footwall of each ore body is copper-rich while lead only occurs in appreciable amounts near the hangingwall contact. The geochemical work of De Kock (1987) found the same metallostratigraphy to exist.

A study (Siegfried & Tilbrook, 1985), showed distinct zonation between ore bodies. A high copper area was found to surround the central area of the ore deposit in the vicinity of B-Mine. When structural complications were restored by "unrolling" the folded ore zone, Pb/Zn, Ag/Cu and Ag/Pb zonation was found to describe a predominantly linear feature with statistical correlations of up to 0.98 ($n = 7$). This was interpreted to be a result of primary depositional control along a palaeo-fault, each ore body

representing a single, evolved feeder zone along this postulated fault.

Within Mountain Ore Body itself distinct lateral as well as vertical zonation occurs. The most striking example is the occurrence of the baritic facies in the upper zones as well as towards the northern edge (periphery) of the ore body. This is identical to the baritic facies described at Meggen (Krebbs, 1981) as well as many Kuroko deposits (Sato, 1977). Associated with the barite ore are appreciable amounts of manganese, that occur as discrete Mn-bearing minerals such as alabandite and rhodochrosite. A similar association was noted at Roseberry (Braithwaite, 1974; Green, et al., 1981).

A manganese halo is recorded at Silvermines in Ireland, stretching up to 5 km from the deposit (Taylor & Andrew, 1978). Similar Mn-enrichment occurs at Rosh Pinah with a dark, rust weathering feldspathic quartzite occurring in the immediate hangingwall of the ore body (Fig.6). Manganese enrichment of up to 4% was recorded albeit enriched due to secondary weathering processes (Rosh Pinah chemical analysis). Analyses of hydrothermal dolomites in the footwall as well as the ore zone show manganese to make up an important constituent of the hydrothermal fluids. Manganese-rich sediments associated with exhalative activity are found along spreading ridges. These are, however, regarded as a result of low temperature (<200 ^{o}C) deposition of manganese originating through shallow leaching of the ridge basalts (Fehn, 1986).

It has often been suggested that the metal zonation recorded in the ore bodies is a feature of host rock composition implying the mineralization and gangue minerals are genetically related. To test this, rock types were discriminated and plotted with various weightings. The best discrimination was achieved on Zn-Cu-Ag and Zn-Pb-Ag ternary diagrams.

Little discrimination between footwall quartzites and microquartzites (Fig. 7c) could be seen suggesting that

mineralization of the two rock types is related. This would agree with the interpretation that the microquartzite was silicified by the same or similar solutions which produced the footwall silicification. The Ba-rich, type 3 carbonate veins of the footwall, and the baritic facies of the ore zone, plotted into two distinct populations indicating that the footwall veins are unrelated to the formation of the baritic facies (Fig. 7a, b). The barite ore is characterised by high Pb values while the veins are Cu-rich as well as showing Ag-enrichment. This relationship suggests that the bulk of the thicker footwall veins are not the feeders to the baritic and carbonate ores as has been suggested in the past (Page & Watson, 1976) but are of another origin. The dolomite ore samples can be shown to represent a progression from Zn-rich to Pb-rich composition. This possibly reflects a gradual cooling down of the hydrothermal system before the deposition of the baritic facies.

Ternary diagrams have also been used to differentiate SEDEX deposits from volcanogenic massive sulphides (Large, 1983). A similar plot of Zn:Pb:Cu was constructed to see if the metal contents of various Mountain Ore Body samples could be used to determine a source of mineralization (Fig. 7d). Although it was found that the bulk of the Mountain Ore Body samples plot in the common area there is a trend to plot within the volcanogenic field implying the source of the metals may not be sedimentary but of a more direct magmatic origin.

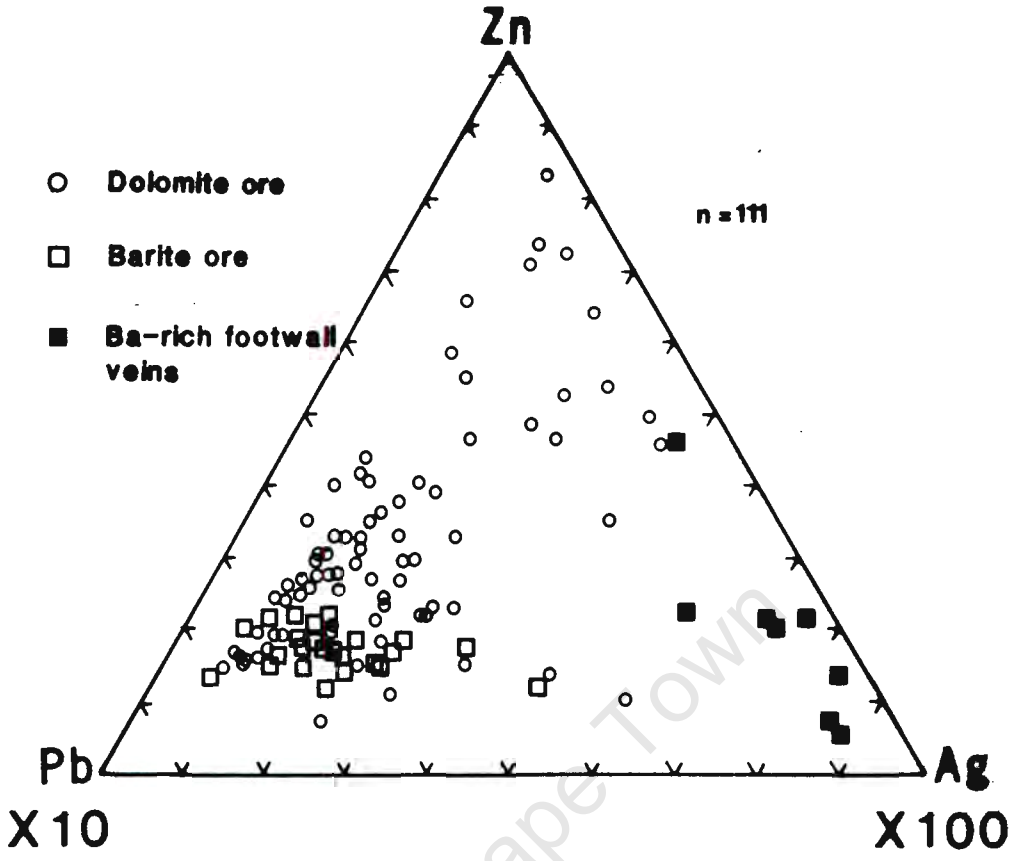

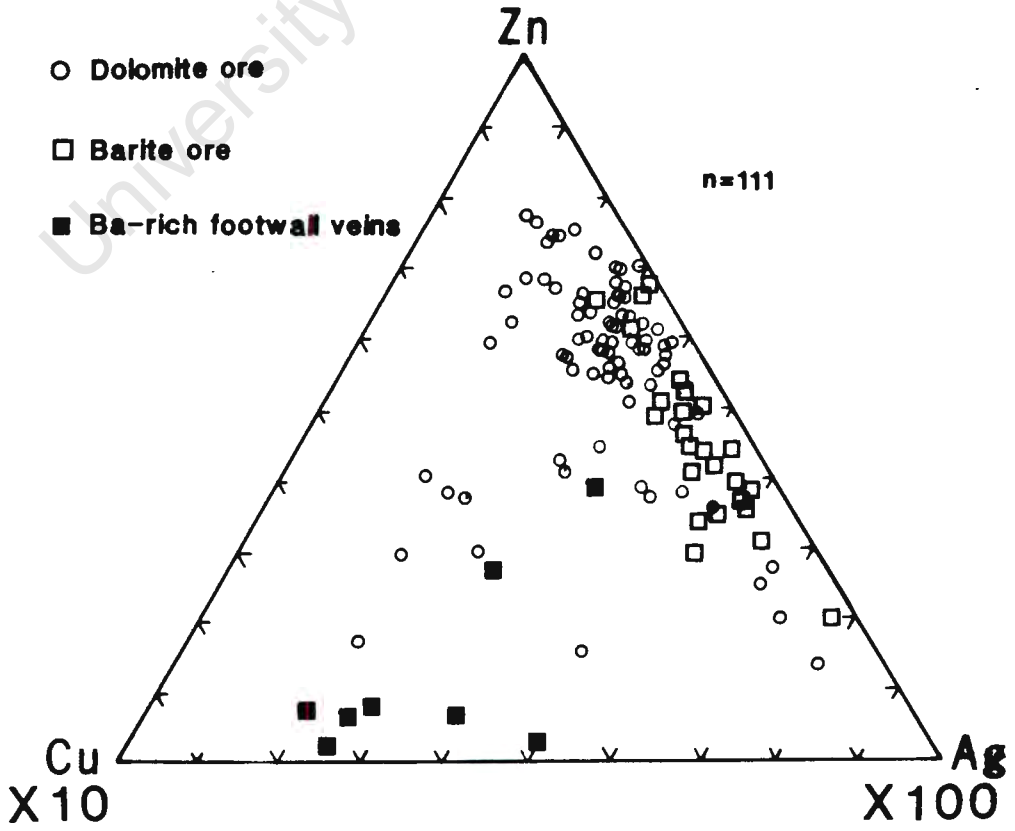

Figure 7a: Ternary diagram of base metal distribution in carbonate lithologies.

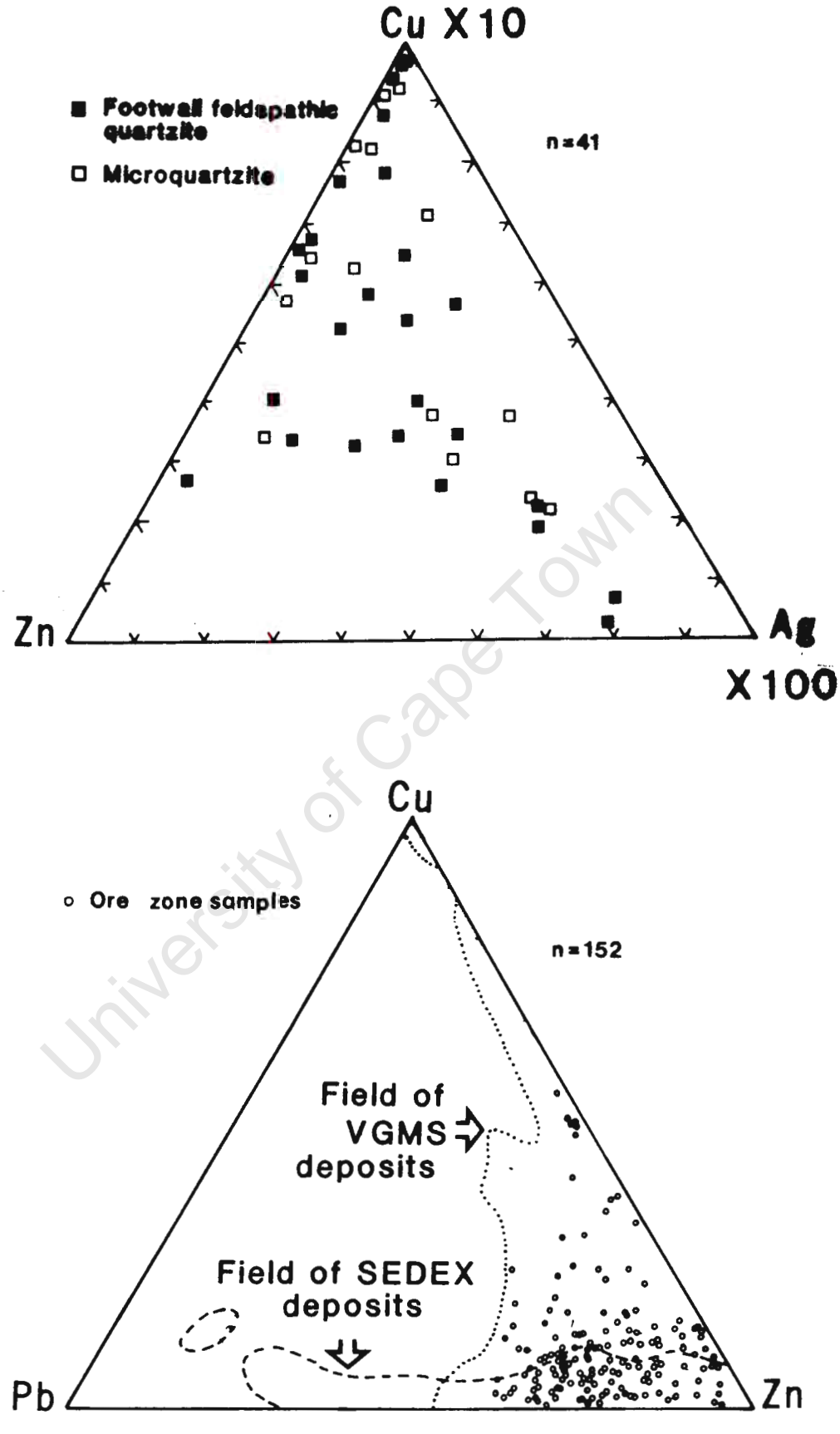

Figure 7b: Ternary diagrams of silicic lithologies and distribution of all base metal samples.

3.5 STABLE ISOTOPES (CARBON AND OXYGEN)

3.5.1 INTRODUCTION

Stable isotope geochemistry has been utilised as an important tool in the understanding of ore genesis (Hoefs, 1980). A good indication of the source, as well as the temperature of the hydrothermal fluids involved in the formation of the minerals of an ore deposit, can be achieved by analyzing the isotope composition of the constituent elements involved. To this end, oxygen and hydrogen, sulphur, carbon and lead have been utilised with great success (Rye & Ohmoto, 1974). It was decided to analyze only certain carbonate samples for their oxygen and carbon isotope signatures as the process is reasonably cheap and simple and full facilities exist at the University of Cape Town.

Carbonates characterized by isotopically light values (less than -25‰) of ^{13}C, are interpreted as being the result of biogenic reduction while carbonates of a marine origin (Hoefs, 1980) have a mean ^{13}C of 0‰. Marine carbonates are also characterized by enriched ^{18}O values while only meteoric water is composed of very light oxygen usually less than -10‰.

In the majority of analysed hydrothermal carbonate deposits, (Rye & Ohmoto, 1974) there is a general increase in the ^{13}C isotope composition from early carbonate generations to late - i.e. the early generations of carbonate minerals are more depleted than the later. The carbonate minerals of these deposits are therefore interpreted as originally formed while interacting with magmatic waters (-4 to -8‰ ^{13}C) which have become progressively enriched with cooling and/or time.

Many deposits show that the carbonate solutions postdate the sulphidic solutions (Rye & Ohmoto, 1974) and that they are generally unrelated. However, the presence of carbonate

associated with the introduction of sulphides at Rosh Pinah, as well as evidence from the Irish deposits (Kucha & Wieczorek, 1974) showing that the metals were deposited as carbonate complexes and were later sulphidised below the sediment interface, implies that this is certainly not always the case and that carbonate is at times an important constituent of the mineralizing fluids.

The reconstitution of the carbonate material of a carbonate hostrock into coarse-grained veins, commonly results in a depletion of the heavy ^{13}C isotope of the mineral in the vein, compared to that of the wallrock (Schidlowski et al., 1975). Mississippi Valley Type deposits reveal zones of veining, silicification and recrystallization. Isotope analyses of these zones shows that the mineralizing fluids caused a depletion in both ^{18}O and ^{13}C with a drop of up to 5‰ in ^{13}C (Pinckney & Rye, 1972), indicating that these areas were channels for isotope exchange with the wallrock (Heyl, 1974). This depletion is due to partial exchange between the host rocks and mineralizing fluids with the fluids having a depleted, possibly organic ^{13}C composition.

The affect of equilibration with super-depleted organic material can be ignored as reaction between $^{13}C_{cc}$ and $^{13}C_{org}$ only occurs at high temperatures (Valley & O'Neill, 1984), and has a maximum effect of approximately 3‰ at greenschist to lower amphibolite facies conditions. If the carbonates which have been analysed represent the segregation of carbonates of marine origin (approx. 1‰ ^{13}C), a depletion of no more than approximately 3‰ will be recorded.

3.5.2 RESULTS

The ore zone carbonate samples analysed represent late-stage precipitation of carbonate material or the replacement of pre-existing minerals. The presence of the distinctive, Ba-bearing, orthorhombic carbonates is, as discussed, indicative of low temperature deposition and hence puts an

important constraint on the interpretation of the isotope values obtained.

Two samples of supposed marine carbonates were analysed in conjunction to determine if their isotope composition departed significantly from normal marine carbonates. Sample PRS 32 originates from a clean limestone horizon in the Hilda formation while PRS 23 consists of dolomite from the hangingwall carbonate horizon.

PRS 35 and 88 represent barite that has been altered to baryto-calcite. Both exhibit extremely depleted ^{13}C values(-16.6‰ and -10.8‰ respectively). An organic source is implied in order to achieve such depleted values.

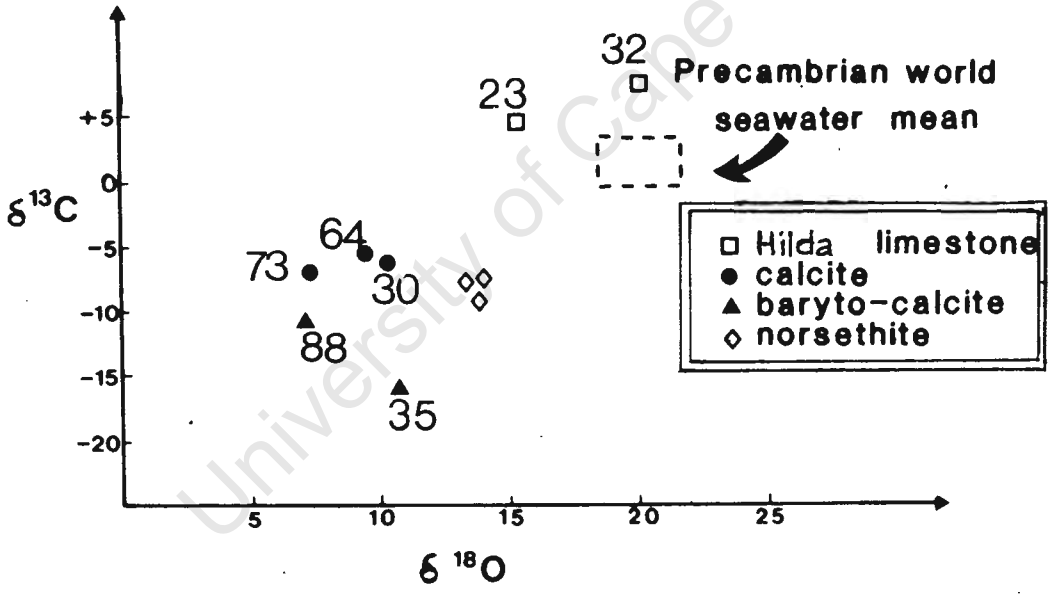

Figure 8: Plot of $\delta^{18}O$ against $\delta^{13}C$ for select Rosh Pinah carbonate samples.

Replacement of barite laths is represented by the norsethite samples. As the precursor sulphate contains no CO_2, the ^{13}C of the norsethite should reflect the carbon isotopic composition of the introduced fluids.

The oxygen isotopic signature of Rosh Pinah barite is at present unknown as no samples have been analyzed. Almost

all sulphate material analysed to date (Hoefs, 1980) indicates a heavy, enriched, seawater source for the sulphate and a similar origin is therefore assumed at Rosh Pinah. The depleted ^{18}O values of all ore zone carbonate samples analysed, are explained as a result of the interaction of depleted CO_2-rich fluids with ^{18}O enriched sulphate material. These fluids were possibly introduced during late D2 faulting and so could have a depleted, organic-rich sedimentary source.

Table 7: Isotope and mineral compositions of analysed carbonate minerals. $\delta^{18}O$ is relative to SMOW, $\delta^{13}C$ is relative to PDB.

SAMPLE	COMPOSITION	^{18}O	^{13}C
PRS 32	CaCO3	19.9	7.7
PRS 23	CaMg(CO3)2	15.2	4.2
PRS 30	CaCO3	13.1	-7.0
PRS 64	CaCO3	11.9	-6.7
PRS 73	CaCO3	9.3	-5.5
PRS 88	BaCa(CO3)2	7.7	-10.8
PRS 35	BaCa(CO3)2	10.8	-16.6
PRS 30	BaMg(CO3)2	13.1	-7.0
PRS 105	BaMg(CO3)2	13.8	-8.8
PRS 106	BaMg(CO3)2	13.4	-7.5

The two marine carbonate samples analysed possess anomalous ^{13}C values. Both are extremely heavy (+4.2‰ and +7.7‰) compared to standard Precambrian seawater (+1.0‰). Occurrences are known where heavy C-isotopes occur such as the Lomagundi Group and Karelian limestones (Schidlowski et al., 1975). These values are explained as reflecting an increased C_{org}/C_{carb} ratio in the total carbon flux entering the sedimentary reservoir. The large amount of light ^{13}C being organically fixed will result in a relative enrichment of heavy, ^{13}C in the seawater and therefore available for precipitation as limestone or dolomite. In the order of 50% C_{org} would have to be present as opposed to the usual 20% C_{org} present. The organic-rich nature of almost all the

sediments in the Rosh Pinah area indicates that the seawater carbonate was possibly enriched with respect to ^{13}C and that heavy carbonates were formed during Gariep deposition.

The ^{18}O agrees with those of normal marine carbonates although PRS 23 is slightly depleted with respect to ^{18}O. As this sample originates from the hangingwall carbonate horizon it could indicate the continuation of very minor exhalative activity and interaction of the dolomite with continued magmatic fluids. This would decrease the heavy, dominantly seawater ^{18}O composition of the rock.

3.6 STRUCTURE

The footwall breccia has been suggested to be of a tectonic origin, and therefore, to have a structural relationship to the ore body. In order to fully understand this association, if any, a good understanding of the structural evolution of the area is needed. Few previous studies have, however, concentrated on the regional structure of the Rosh Pinah area, owing to the inaccessibility and harshness of the terrane. This, compounded with complex structural overprinting relationships, has meant that varied structural interpretations have been suggested. Much of the understanding of the deformational history of the area has also been extrapolated across the Orange River from observations regarding the structure of the Gariep Group observed in the Richtersveld (Kröner, 1974; Von Veh, 1988). It is apparent that the terrain surrounding Rosh Pinah displays some unique aspects of Gariepian orogenesis and that a thorough structural study of the Mountain Ore Body would solve many of these complexities.

3.6.1 FAULTS

3.6.1.1 D1 Thrust faults

The earliest observable faults are S0-parallel thrusts which show early, mid and late D1 movements. They are usually developed in the thicker quartzitic layers where extensive shearing occurs along bedding partings. Intensely cleaved rocks in the parting zones consist of fine-grained, carbonate-rich material with a micaceous schistosity. Associated ramp structures and imbricate zones that are characteristic of thrust-faulted terrains (Boyer & Elliot, 1982; Butler, 1982), are observed.

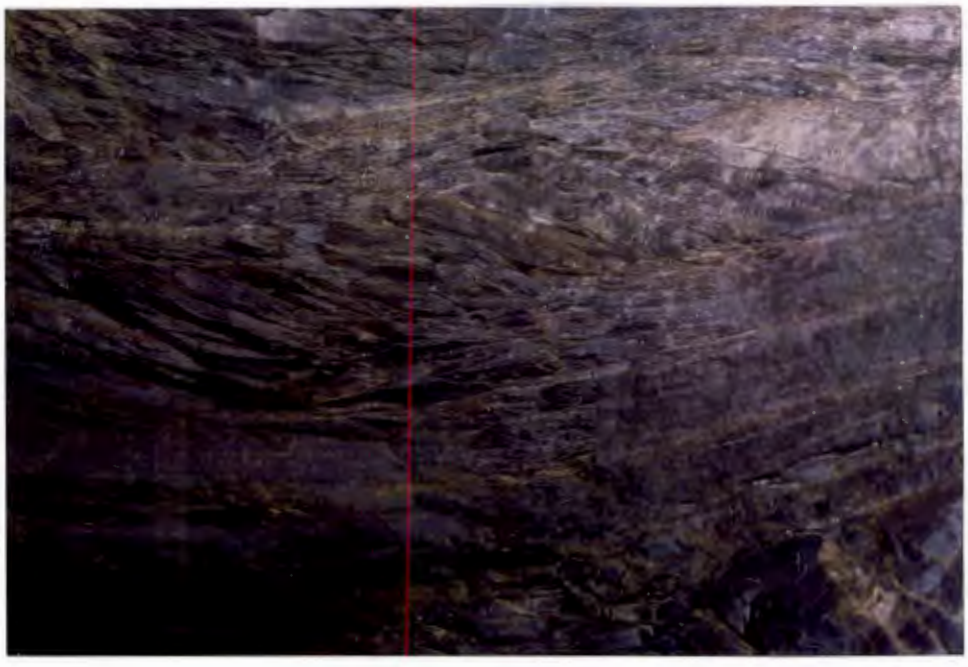

Plate 9: Imbrication of footwall feldspathic quartzites produced during D1. Dislocation occurs in finer-grained, laminated quartzite. Locality MOB [475 Ae]

Imbrication can be noted occurring along the 475 level (Fig.4) and here approximately 75% shortening occurs within 3,6 m. The thrusting direction is oriented towards the south-south-east. Mylonite is not observed although at [490 Aj] approximately 2 m long chloritised stringers, parallel to the regional fabric (Fig.10c) can be observed. Truncation of calcite and quartz veins at locality [470 Dg] indicates that precipitation of vein material was followed by episodic movement.

3.6.1.2 Eastern Boundary Fault

This fault is a 2 to 5 m thick shear zone trending roughly 330/50 with an internal fabric of 315/45. The shear zone is parallel to the regional fabric with no sharp discontinuity between foliated and non-foliated rock. It is concordant with the regional foliation and has a reverse sense of throw. The shear zone appears to have followed the axis of a pre-existing syncline to the immediate east of the

Mountain Ore Body structure. Complex areas of interleaved hangingwall and footwall lithologies occur with associated sulphides as well as brecciation in the vicinity of the ore body. The sulphides occur as remobilised veins, breccia-matrix filling and disseminated grains. The proportion of galena to sphalerite increases markedly in some mineralized areas of this zone indicating preferential remobilization of galena.

3.6.1.3 Western Boundary Fault

Although subparallel to the regional fabric, this fault experienced more recent movement than the previous fault as it truncates breccia zones and D2 structures. It trends 340/60 and consists of a discrete, undulatory fault plane with numerous anastomosing conjugate faults that strike parallel to the major dislocation surface. Intense rodding occurs in the downthrown hanging wall rocks with associated pyrite crackle breccias. Oxidation is observed to at least 120 m below surface.

3.6.1.4 Minor faults and shear zones

Various shear zones with minor displacement occur within the ore-zone and footwall rocks. Most of these are parallel to the local foliation (Fig.9) and occur in groups with similar trends. In areas of complex deformation [490 Dc,Dd], they are crosscutting and appear unrelated to any major structures. Mean orientations of the various fault sets are as follows; 320/65, 340/75 (E-downthrow), 120/72, 045/62. Reverse faults along the footwall contact zone (Fig.10f) show minor displacement parallel to the early D1 faults but crosscut the S1 foliation developed.

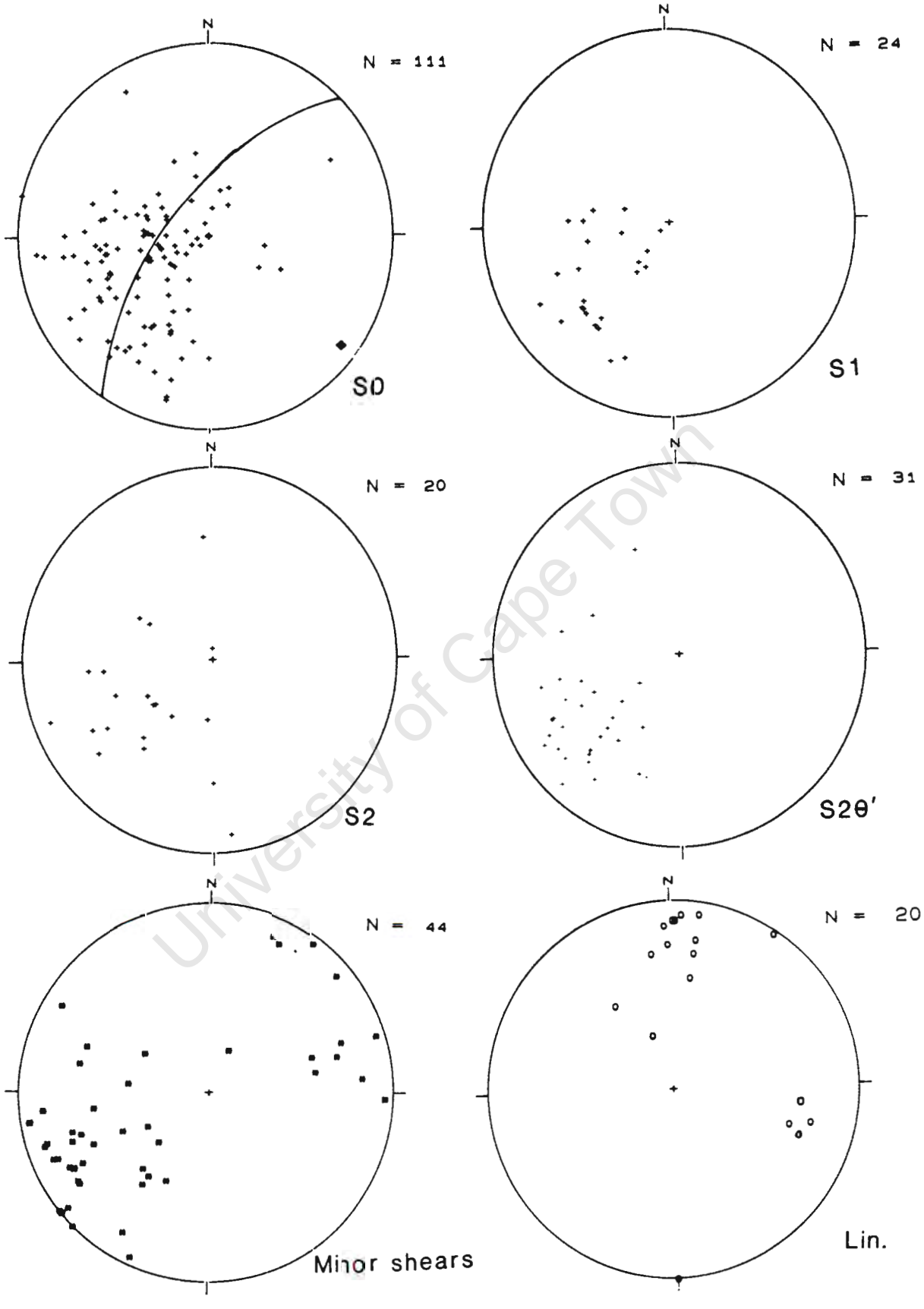

Figure 9: Stereonet plots of fabrics observed in the Mountain Ore Body.

3.6.2 FOLD STRUCTURES

3.6.2.1 D2 Regional folds

The earliest fold structures identified are the regional, west-vergent, similar folds oriented at 340 (Fig.5). They are non-cylindrical, open to isoclinal and usually overturned to the west. In the Mountain Ore Body two major anticlinal structures exist, the westernmost being truncated by the Western Boundary Fault (Fig.6). The intensity of folding increases towards the north (Fig.5e) where thinning of the ore-zone has attenuated the effect of folding. An associated transverse, axial-planar, sigmoidal cleavage (S2) was developed during the formation of these folds.

Piercement and cusp structures (Maiden et al., 1986) have been observed (Fig.10bd) and are related to this event. Observations made in the C-Mine by T. Blaauw (pers. comm.) show extensive piercement structures developed parallel to the regional axial plane orientation and which deform an earlier (S1) schistosity (Fig.10i).

3.6.2.2 D3 Regional folds

These minor folds are parallel to D2 folds but possess a weakly developed cleavage, overprinting the axial planar cleavage developed during D2. In the area of the mine grant they are observed as small-scale, minor folds coaxial to the D2 folds. Carbonate lithologies of the upper Numees Formation as well as Nama Group sediments east of the field area show this deformation more distinctly where the sigmoidal cleavage of D2 is absent.

3.6.2.3 D4 Crossfolds

These folds are rarely observed and it is rather the undulatory nature of the D2 folds which suggests their existence. Associated with these folds is a local weakly developed fracture cleavage.

3.6.3 CLEAVAGES

3.6.3.1 S1 Foliation

The S1 foliation developed, is parallel to S0. It is marked by intense preferred mineral orientation, the development of graphite within argillic units, recrystallization of sulphide minerals (such as pyrite 1 to pyrite 2) within the ore-zone lithologies and zones of intense shear occurring along the bedding partings of the quartzites.

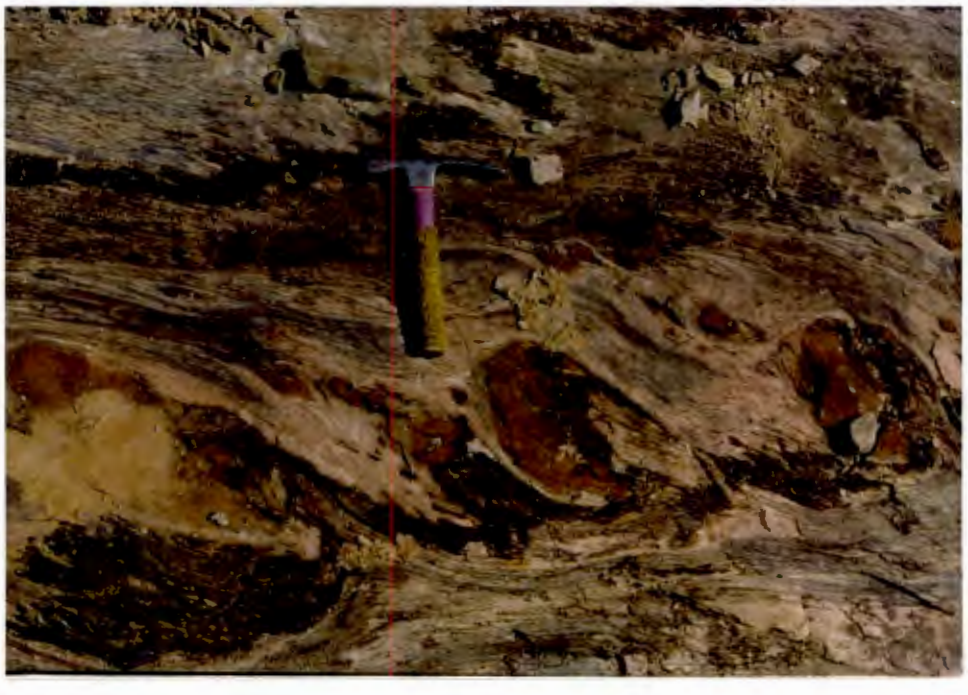

Plate 10: Imbrication of marble band produced during D1. Extreme rotation of blocks can be noticed. Locality 7.2 km north-east of mine grant.

In massive, bedded sphalerite-pyrite ore [490 Bf] there are two foliations. The earlier S1 is defined by recrystallized pyrite cubes rotated parallel to the bedding. The later crosscutting cleavage is axial planar to microfolds within the ore.

In the carbonate lithologies, however, the effects of deformation are not as obvious. This is due to the homogeneous nature of fresh, underground exposure of the ore-bearing carbonates. Dolomite structure can best be observed when weathering produces the subtle textural and colour differences in which bedding, cleavage, etc. can be observed. In areas of carbonate lath development the laths are oriented parallel to the local foliation. On the 490 level [490 Bg], a S0-parallel shear within quartzite lithologies trends 300/28 while segregations in the adjacent carbonate ore zone are oriented at 310/15 and 305/28 respectively. This implies growth of the segregations prior to the initial D1 deformation event. A related feature observed in the northern baritic portion of the ore body [490 Cb] is the rotation of diagenetic "porphyroblasts" of barite. The sense of shear, parallel to the hangingwall contact, is sinistral (looking east).

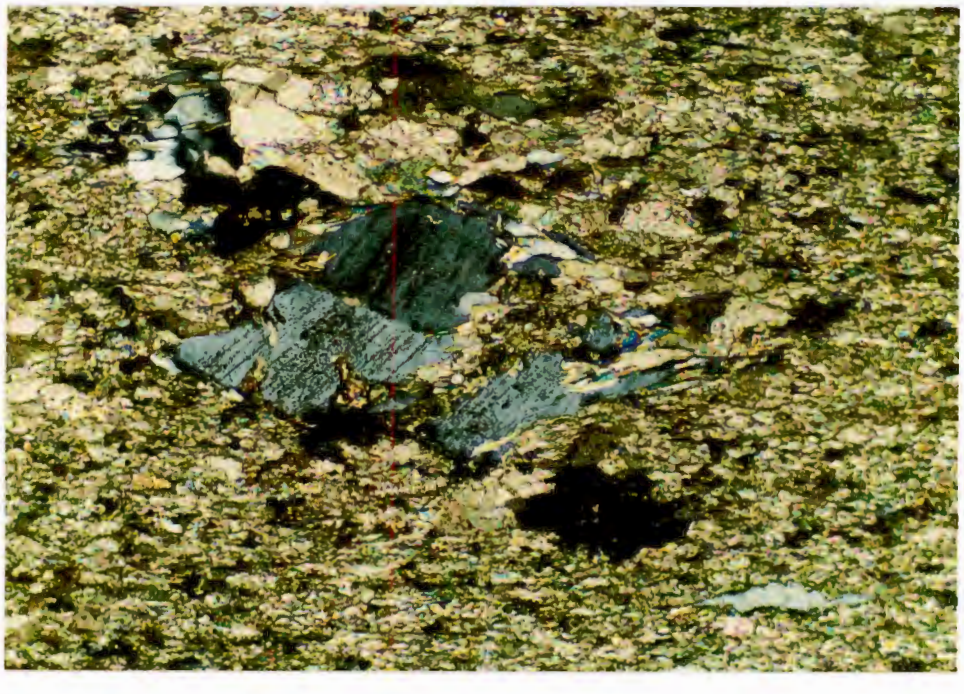

Plate 11: Highly sheared footwall quartzite. Sample originates from D1-related dolomite-rich shear zone and fabric is bedding parallel. Autoclasis of detrital feldspar can be seen. PRS 97, X.100

In the matrix breccias of the footwall lithologies the carbonate matrix is observed to be preferentially deformed. Elongate grains of carbonate (length:breadth = 6:1) are associated with recrystallized as well as shardlike quartz and feldspar grains which result in areas of pressure shadow. Many of these feldspars (Plate 11) display evidence of cataclasis (Engelder, 1974). The sample displaying the most intense stretching (length:breadth = 10:1) is also the most pervasively recrystalized (PRS 12). Many of the quartz clasts are subangular with long axes parallel to the foliation running through the carbonate. In some instances fine-grained, rounded pyrite grains form trails parallel to the foliation.

Distinct zones of cataclastic deformation, macroscopically resembling slaty intercalations, were noted in samples of Southern Ore Field carbonate ore (ISCOR internal report, 1983) in which feldspar grains were completely crushed. Free carbon was also found to compose up to 3% of these layers as opposed to 1.7% in country rock analyses.

Partings between the massive quartzitic beds consist of approximately 60% carbonate material, 30% white mica and 3% graphite. The micas often occur as fine S1 parallel trains of only two or three grains thickness. These deformation related "veins" are continuous through the rock. The carbonate grains are fine-grained and polygonally recrystallized.

McMillan (1968) observes a (tectonic?) raft of felsite contained within folded limestone lithologies in the vicinity of Namuskluft. A well developed cleavage dipping 45^{o} to the northwest is present in the limestone host rock which he interprets as the result of an unspecified thrusting event. The contact observed between the Rosh Pinah quartzites, and the tuffs and agglomerates east of the mine (Spitzkop formation) suggests that the quartzites overlie the tuffs on a thrust faulted contact. Within the tuffs, an early cleavage strikes at 234/16 and is crosscut by the penetrative regional cleavage of 014/45 and

associated lineation of 015/28. This is one of many localities in the area where thrust faults appear to separate major lithological changes.

Plate 12: Characteristic S2 sigmoidal cleavage developed in 40 cm thick beds of footwall quartzite. Locality MOB [490 De].

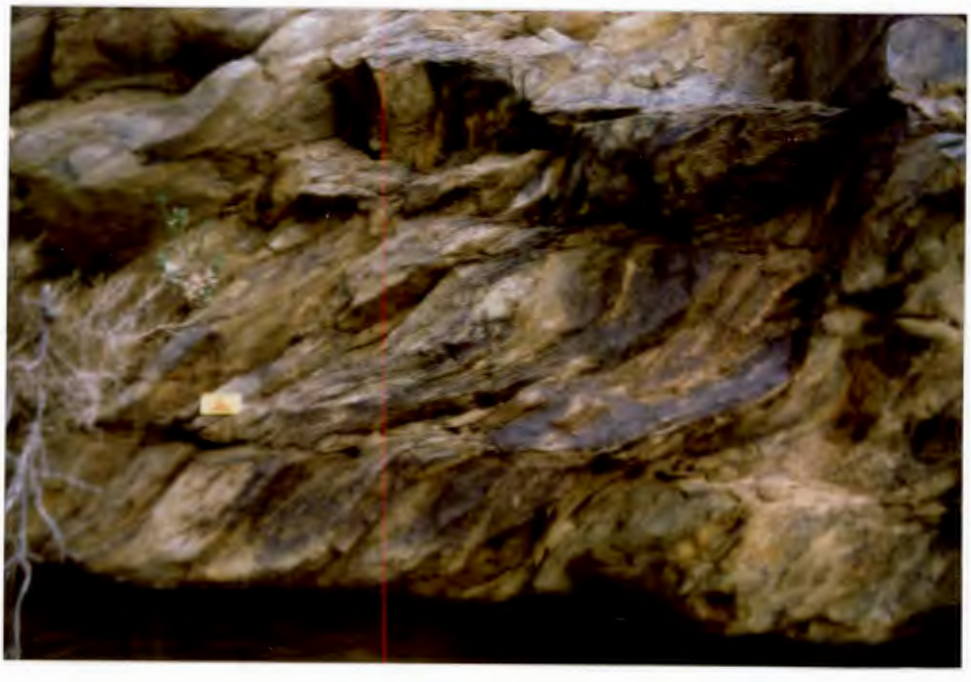

Plate 13: S2 sigmoidal cleavage present in carbonate-rich feldspathic quartzites of the hangingwall succession. Locality approximately 1 km north of mine grant.

3.6.3.2 S2 Foliation

The dominant foliation observed underground is best developed in the quartzitic lithologies (Plates 12,13). This is the characteristic S2 sigmoidal, climbing cleavage. It strikes 338\59 and is axial planar to the regional fold structures.

The pre-existing, bedding-plane-parallel foliation is intimately involved in the formation of this cleavage which was produced during D2 deformation. This fabric will be

referred to as 0′ or the shear fabric (Ramsay, 1980) and is the product of compressive shearing. The foliation planes are usually marked by the development of preferred

orientation in muscovite and a north plunging stretching lineation. The mutual intersection of the S1 and 0' cleavage planes has produced elongate pods of rock which are most visible in the quartzitic units. As these structures are bounded by highly sheared movement planes they can be referred to as horses (Boyer & Elliott, 1982). Figure 10 f,h shows the development of these structures. It can be noticed that these cleavages crosscut areas of brecciation.

Examination of the stereonets (Fig.9) show that S1 and S2 fabrics are coaxial with S2 (0') distinguishable in having a steeper dip. This is an indication that formation of the S2 fabric was largely controlled by the pre-existence of the S1 foliation planes.

3.6.3.3 S3 Foliation

This cleavage was rarely observed and could only be constrained in areas where the S2 sigmoidal cleavage was overprinted (Fig.10h). It appears to be axial planar to the D3 folds but does not show evidence of associated movement along the bedding planes.

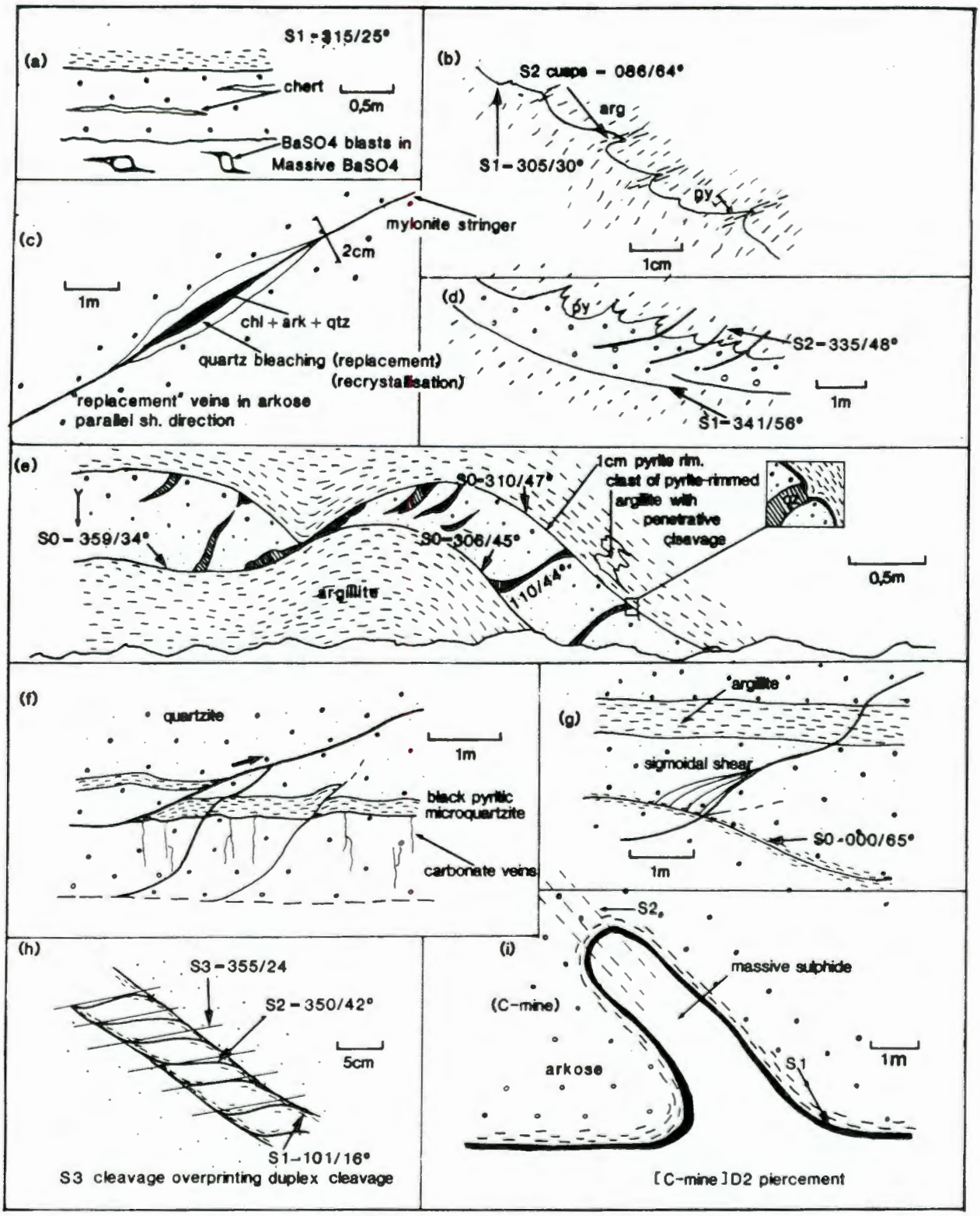

Figure 10: Field sketches of various fabric elements and structures observed underground Co-ordinates are as follows, (a)490Cb, (b)470Cd, (c)490Aj, (d)490Cd, (e)490Ea, (f)490Ce, (g)490De, (h)470Cd, (i)C-Mine

Plate 14: Photomicrograph of S2 sigmoidal shear in footwall quartzite. Shear is predominantly composed of muscovite. Fine grain size near upper contact indicates bulk of movement occurred here. PRS 47, X.20

4. FOOTWALL BRECCIA OF THE MOUNTAIN ORE BODY

The footwall feldspathic quartzites are mineralogically and texturally identical to other feldspathic quartzites in the Rosh Pinah formation.

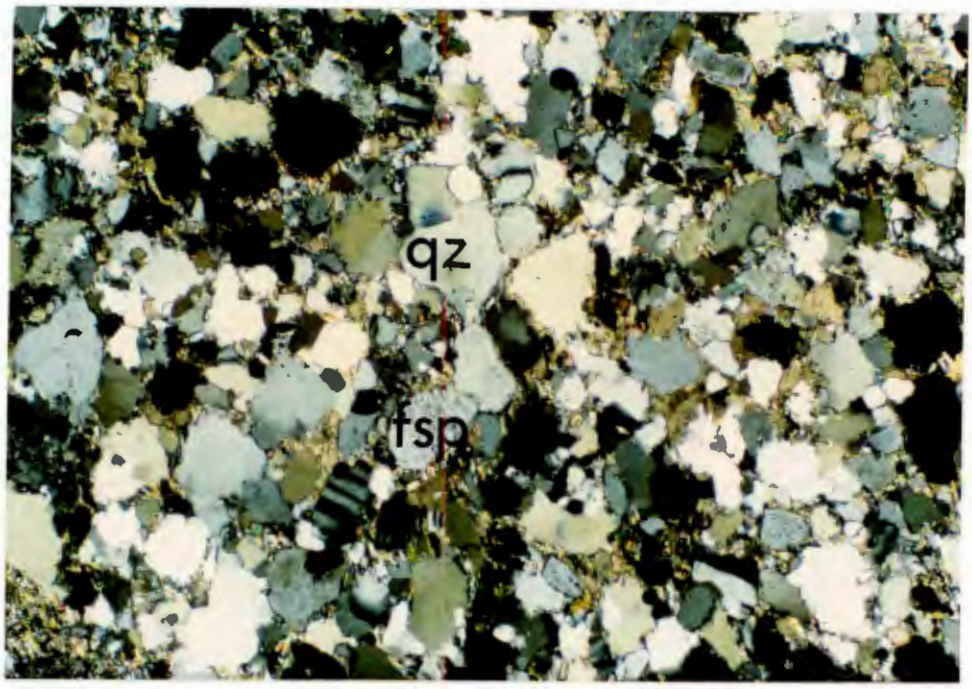

Plate 15: Typical Rosh Pinah formation feldspathic quartzite. Quartz grains (qz) appear more angular than feldspars (fsp) and are often recrystallized. Matrix composed of dolomite and sericite. PRS 76, X.40

However, in the immediate vicinity of, and underlying the ore bodies it appears as bleached, brecciated and silicified zones. These zones are brecciated as well as crosscut by numerous veins of differing age and composition. The various alteration assemblages identified are listed below.

4.1 ALTERATION

4.1.1 SILICIFICATION

The marked silicification of the footwall lithologies is a typical feature of the Rosh Pinah deposit (Page & Watson, 1976). Silicification is a characteristic alteration associated with many hydrothermal deposits, although most descriptions of syngenetic silicification are, however, predominantly associated with volcanogenic deposits or lithologies. Footwall silicification is described associated with Kuroko-type deposits (Sato, 1977) as well as many of the Cu-Fe deposits of the Iberian belt (S.J. Sawkins pers comm.). One example of a SEDEX deposit possessing a siliceous footwall similar to that of Rosh Pinah, is Rammelsberg in the Harzberge of Germany (Hannak, 1976). The ore-body is underlain by a Cu-rich, silicified pipe-like zone known as the "kniest" which is brecciated and interpreted as the feeder for the synsedimentary sulphide lenses. Silicification occurs associated with the copper-rich mineralization present at Mount Isa where it forms extensive brecciated areas of replaced dolomite (Mathias & Clark, 1975) associated with copper mineralization, however, post dates the Pb-Zn minaralization (which formed by exhalative activity) by as much as 200 million years.

Many Archaean mafic and ultramafic lithologies show metasomatic silicification which occurred shortly after crystallization (Duchac & Hanor, 1987), the silica being introduced isovolumetrically. Cherts have been described that are regarded as being the products of hydrothermal activity (Paris, et al., 1985) but no evidence of silicification in the underlying "feeder" areas was noted.

The replacement of the quartz-rich sediments of the footwall by silica, predominantly affected the matrix of the sediments.

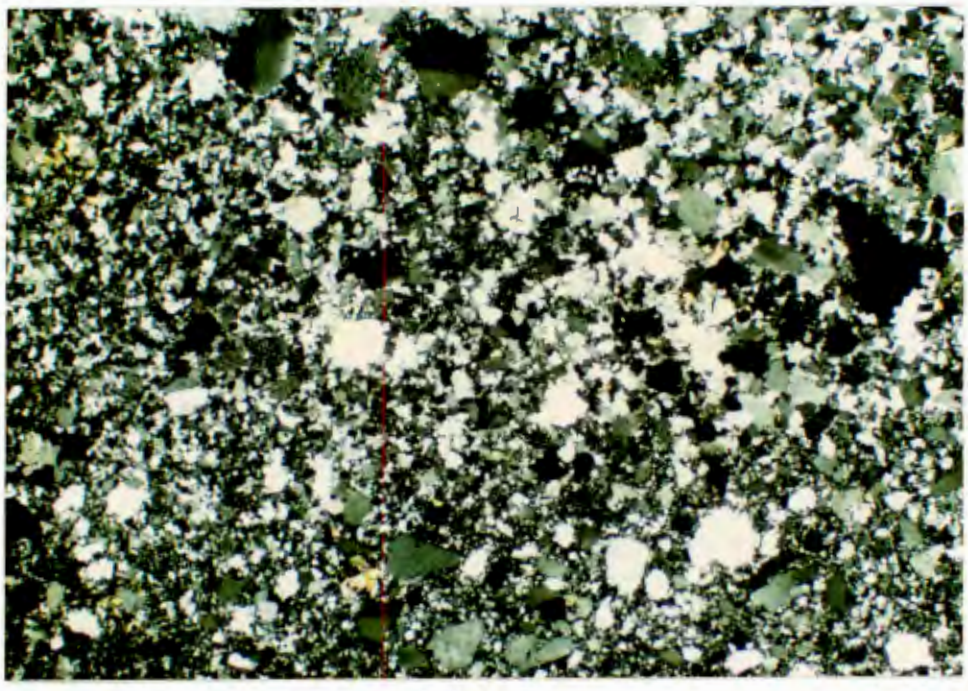

Plate 16: Silicified footwall quartzite. Removal of all components other than silica can be noticed with the matrix being replaced by fine-grained to cryptocrystalline silica. PRS 46, X.20

The large detrital feldspar grains were seemingly unaffected. The introduction of silica with the concomitant removal of micaceous, carbonate and clay minerals is supported by modal (Table 3), as well as chemical analyses (De Kock, 1987). "Bleaching" of the feldspathic quartzites has often been cited as signifying silicification but rather appears to be a result of negligible free carbon included within the matrix of the rock type. Sample PRS 76 originated from a particularly bleached-appearing hangingwall quartzite which under microscopic examination revealed no evidence of silicification.

The footwall silicification is far more widespread than the localized areas of sugary quartz development or silicification associated with later faulting. The replacement of carbonate rock by silica, as has occurred during the formation of sugary quartz, is pervasive as opposed to the silicification observed in the footwall

quartzites which preferentially affects the fine-grained matrix.

Affects of intense silicification are illustrated by the replacement of detrital feldspars. Mortar textures are developed around ragged-edged feldspars as well as around quartz clasts. The feldspars show invasion by quartz along fractures parallel to their cleavage planes. These fractures also provide locci for the invasion of later carbonate solutions. Carious embayments involving the replacement of K-feldspar by quartz were also noted. Quartz overgrowths with seriate grain boundaries occur around the larger detrital quartz grains. The most widespread indication of silicification is the presence of tiny (5 - 20 μm) rounded inclusions of quartz in the center of the feldspar grains. Complete gradation from inclusion-spotted grains to total replacement occurs. The matrix of the footwall quartzite is composed of fine to medium-grained recrystallised quartz (Plate 16) which is crosscut by later carbonate breccia veins.

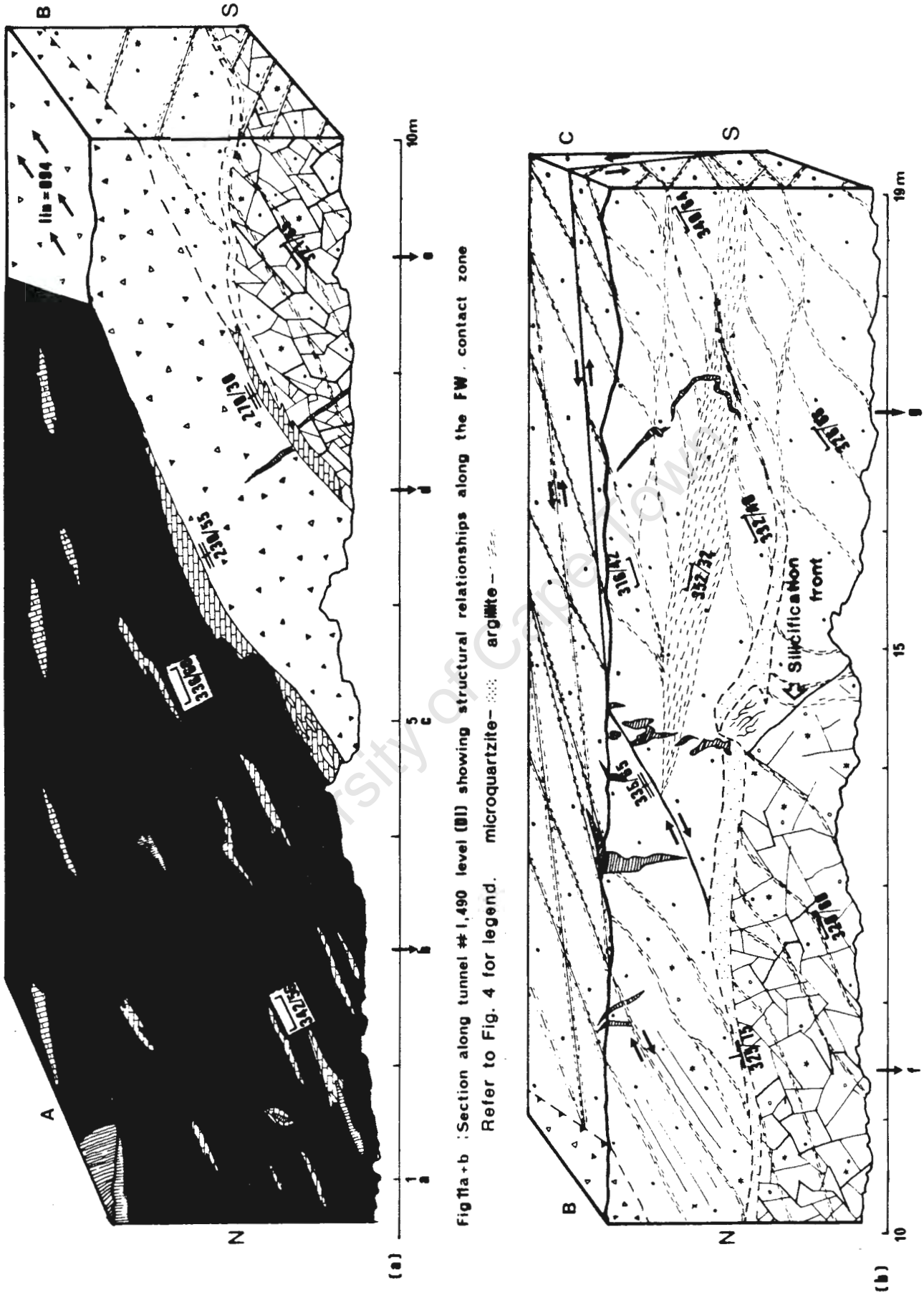

Fig 11a+b :Section along tunnel #1,490 level (Bl) showing structural relationships along the FW. contact zone
Refer to Fig. 4 for legend. microquartzite- argillite-

Figure 11: Mapped section along footwall contact zone, Mountain Ore Body 490 level.

Table 8: Base metal content of footwall contact zone of Mountain Ore Body, 490 level. Refer to Fig.11 for sample positions. (Analyst: B. Strauss).

SAMPLE	Fe%	Zn%	Pb%	Cu%	Ag ppm.
a	1.23	12.85	0.09	-	5
b	1.40	13.30	0.07	-	5
c	1.78	10.85	0.11	0.05	11
d	1.52	7.00	0.13	0.04	10
e	1.03	0.45	0.01	0.16	-
f	0.93	0.29	0.04	0.05	-
g	1.04	0.08	0.01	0.01	-

Extensive Cu was deposited during silicification as indicated by mine assay values (Table 8) as well as underground exposure (Plate 17). The silicification occurred prior to brecciation and probably shortly after the deposition of the lower ore zone lithologies.

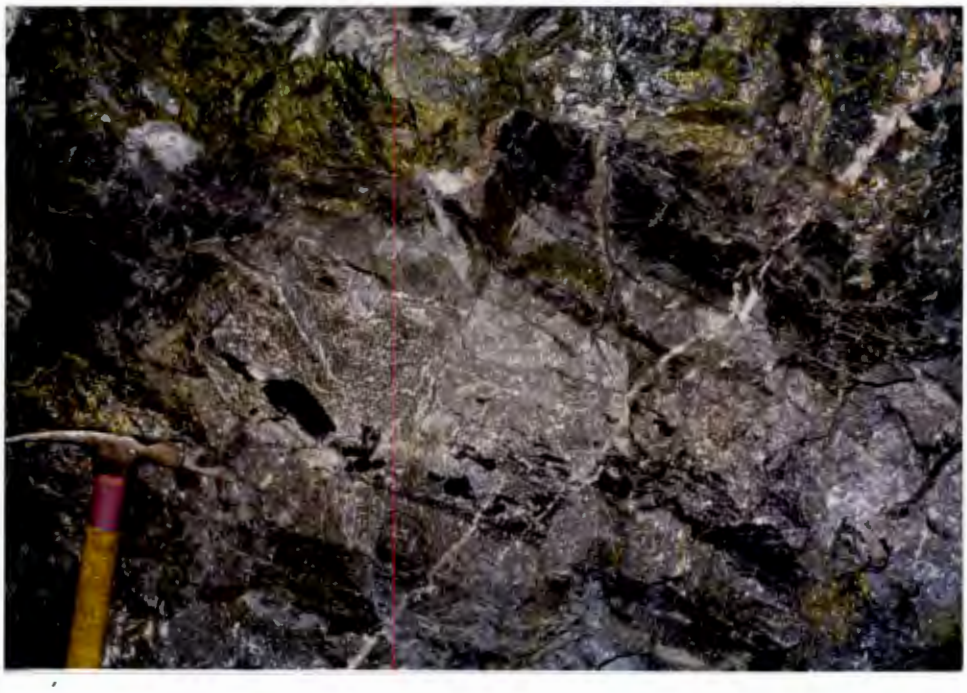

Plate 17: Intense silicification of footwall feldspathic quartzite. Rounded rip-up clasts of argillite (now microquartzite) occur near the base of the bed. Clots of chalcopyrite can be noticed.

4.1.2 OTHER ALTERATION

Wallrock alteration other than silicification is not common at Rosh Pinah although varying degrees of carbonatization have been noted (De Kock, 1987). The quartz grains, however, show little effect of carbonate alteration. Some feldspars show carbonate replacement with a texture similar to that exhibited by siliceous replacement. In the lower footwall the light grey, silicic quartzites are spotted with dark patches 1 cm in size (Plate 3). These spots were previously interpreted as the result of sericitisation (De Kock, 1987) but have been identified as irregular aggregates of carbon-rich dolomite.

In some portions of the central zone of Mountain Ore Body [470 Df,Ef], the quartzites appear friable and have a very high carbonate content. This alteration is a result of secondary supergene processes (Ch. 3.2.6) rather than carbonatization associated with the carbonate breccia-forming period.

A rare example of potassic metasomatism was recorded from the Southern Ore Field region of the deposit (De Kock, 1987). Chloritization accompanied by the development of phlogopite and orthoclase is recorded. Pyrrhotite occurs as an accessory mineral. The extent of this alteration appears to be localized but does indicate that potassium metasomatism occurred during the formation of the ore. Potassium metasomatism is usually recorded in epithermal, felsic igneous-related deposits (Barnes, 1979) and its localized restriction at Rosh Pinah is not clear.

In the hangingwall of the Mountain Ore Body, potassium feldspars have been enriched with barium. Secondary overgrowths of hyalophane around microcline as well as orthoclase are observed. Barium enrichment decreases exponentially away from the hangingwall-ore zone contact (from data of De Kock, 1987). This feature has been recorded at the Jason prospect in western Canada (Smee & Bailes, 1986) as well as at Moyvoughly in Ireland (Kucha,

1988), where secondary growth of hyalophane surrounds detrital feldspar clasts.

4.2 BRECCIATION

4.2.1 INTRODUCTION TO PROCESSES OF BRECCIATION

Many varied processes can result in brecciation and breccias of different origin often appear identical in appearance. A profusion of nonspecific descriptive terms in the literature has resulted in most schemes for the classification of breccias being very confusing. The best classification is that of Sillitoe (1985), although most examples cited were restricted to phreatomagmatic breccias composed of acid volcanic rocks.

The environment in which a breccia forms, is as important as the formative process in determining the breccias textural characteristics. After much study it became apparent that breccias can best be classified on a broad genetic framework. The classification scheme arrived at (Table 9) defines four groups of breccia formation. These groups are: depositional or sedimentary breccias, chemical breccias, hydrothermal breccias and tectonic breccias.

4.2.1.1 Depositional Breccias

These are breccias which form due to synsedimentary instabilities in recently as well as semi-lithified sediment. They are usually present at the shelf or reef edge, as well as in rift environments of deposition. They are characterized by medium to poor sorting and some rounding of the clasts.

Depositional breccias are particularly common in carbonate reef environments (Blount & Moore, 1969) where megabreccias and olistrosomes can form. Clasts of up to 100 m have been recorded. The brecciation of fine-grained laminated lithologies can result in the formation of a specific imbricated breccia known as a shingle breccia (Krause & Oldershaw, 1979) possessing a planar-clast fabric (Lash, 1984) which is indicative of a debris flow mechanism. Sedimentary breccias can be composed of volcanic material and are common in marine volcanic environments (Sillitoe, 1985). The steep-sided topography results in rapid, chaotic deposition of volcanoclastic material with the crystalline volcanic rocks rarely becoming rounded.

On the island of Hydra, sedimentary breccias ranging from mass flow breccias to internal breccias, which involve no relative movement of the clasts, are recorded (Fuchtbauer & Richter, 1981). Light grey, micritic limestones make up the host rock while in zones of brecciation the limestone clasts are hosted by red shale. As the clasts of these breccias sometimes have a very high degree of fit, the matrix shale can only enter during a state of dilation. It is envisaged that this process happened along the shelf-slope break during active extensional tectonism. Earthquakes, associated with these areas, act as the trigger mechanism for the initiation of the flow breccias.

Diamictites composed of glacial talus could perhaps be confused with mass flow breccias but the recognition of polished and striated clasts as well as dropstones in the associated rocks is indicative of a glacial origin.

Depositional breccias can be recognised by their restriction to a certain bed or horizon and bedding parallel nature as well as the absence of associated veining. They are also the best sorted of all breccia types and utilizing this feature can be recognised by measuring the grain size frequency distribution. The applicability of this concept to breccias still needs revision but its use in clastic

sediments has been well illustrated (Tucker, 1981; Harrel, 1984).

4.2.1.2 Chemical Breccias

Chemical breccias can be divided into two main types according to the process which forms them. These types are either solution-collapse or replacement breccias.Brecciation, caused by the dissolution of material such as carbonate, with subsequent collapse of rock into the resulting cavities, has long been recorded in areas of karst topography. The great majority of Mississippi Valley Type deposits form in solution-collapse cavities that are commonly unconformity related (Ohle, 1985). Later infilling, by mineralized fluids formed the ore. The matrix consists essentially therefore of carbonate, silica and sulphides as well as fluorite and/or barite. Concretionary infilling of the cavities is often vividly developed and is a good argument in favour of open space filling of the cavities produced during the collapse event. Breccias involving the replacement of the country rock by dolomite do occur. They have the appearance of breccia-filled veins without any appreciable dilation recognizable in the rock. The pseudobreccias and replacement breccias of the copper-rich zone of the Mount Isa ore deposit are of this type (Perkins, 1984).

Some highly siliceous breccias observed in Mississippi Valley Type deposits possess a very high degree of fit. An expansive brecciation mechanism, known as cement-aggregate or alkali-reactivity reaction (Sawkins, 1969) appears to be the cause. It is the result of the reaction of alkalis with fine-grained dolomite or silica. Expansive forces of over 14 kbar have been measured in dolomite immersed in 1M NaOH (Hadley, 1961 in Sawkins, 1969). Angular breccia fragments form with very little rotation of clasts. These breccias have been known as "jigsaw" or "mosaic" breccias.

Silicified volcanic vent breccias occurring in rhyolites at the McLaughlin Au-deposit, California (Nelson & Giles, 1985), show a similar progressive replacement of the clasts. In this case sulphidic, Au-bearing microcrystalline silica forms the matrix material. The resultant mosaic textured breccias are absent in unsilicified vent breccias.

Chemical breccias of the replacement type can therefore be recognised by the absence of rotation between the clasts, as well as the presence of jigsaw or mosaic textures. Features such as bedding and early veining are not displaced by later veins. A progressive digestion of clasts can commonly be observed. The breccia veins are rarely straight-edged and regular and become more irregular with an increase in thickness. Breccias of a solution-collapse origin can be recognised by a sometimes chaotically oriented breccia with concretionary growth textures observable within the matrix.

4.2.1.3 Hydrothermal Breccias

A hydrothermal fluid is one defined as a hot, aqueous solution (Barnes, 1979). If these fluids are hot enough so that boiling, due either directly to heating or depressurization, takes place, the contained fluid can become overpressured (White, 1981; Nelson & Giles,1985). In other words the fluid pressure becomes greater than the sum of the lithostatic load and the rock tensile strength. Nearby intrusion of magma or localized seismic activity can also cause a rapid influx of volatiles and hence result in an overpressured fluid. Self-sealing of hydrothermal conduits and formation of a "cap rock" in a caldera situation commonly results in overpressurization. Fracturing commences with pore fluid expansion and fracture propagation at depth. As the fluids rise they rapidly devolatilize and the fracture density and intensity increases. Stockwork breccias, pebble dykes, deep fractures, etc., form in this way. If the fluid is contained beneath a caprock and is CO_2-rich as well as vapour-dominated, it is quite conceivable to obtain an

effective overpressure of 1 kbar (Nelson & Giles, 1985). Explosive boiling will therefore occur once fracture initiation takes place. The shock of propagation can result in stylolitic-appearing fracture breccias. These are sometimes referred to as "crackle" breccias and are often associated with acid volcanism (Sillitoe, 1985).

Although these breccias are commonly associated with volcanic areas such as the Kuroko deposits they can quite conceivably arise in sediments within a zone of hydrothermal activity, especially if developed beneath an impermeable layer such as a shale or chert layer.

Hydrothermal breccias are best identified in the context of the alteration of the associated sediments as well as the lithologies involved. As discussed by Sillitoe (1985) there are no acid volcanic piles which do not possess some form of brecciation. This is primarily a result of the extensive H_2O interaction during acid igneous activity, be it caldera or porphyry intrusion related. The presence of heterolithic breccias, flow-banding and clast rotation as well as the occurrence of pseudostylolite breccias is diagnostic.

4.2.1.4 Tectonic Breccias

Breccias of a tectonic origin are almost exclusively fault related. Brecciation caused by folding of lithologies of contrasting competency does occur (Thorman & Nahass, 1979) but is of localized importance.

The majority of tectonic breccias involve the mechanical breakdown of the wall rock by frictional abrasion. The ultra fine-grained matrix can be compositionally proved to consist of finely comminuted particles of the wallrock. Depending on the rock types involved in the fault process, various lithologies can be represented within the matrix material. The sole thrust in the Naukluft Nappe Complex consists of an approximately 1 m thick recrystallized dolomite layer, hosting clasts of many varied lithologies (Hartnady, 1978).

Fault rocks can be divided into three types on textural grounds (White et al., 1986). Incohesive fault gouges occur at shallow depth where temperatures are not high enough for sufficient clay mineral growth or precipitation of secondary minerals to bind the rock (Engelder, 1974). At greater depths, cataclasites and mylonites form (Obee & White, 1985; Hodgson, 1989). The distinction of the two is that cataclasites do not possess a banding or foliation whereas mylonites do. Mylonites as a whole represent deep zones of deformation where shearing takes place under ductile conditions (Etheridge & Wilkie, 1979)

A second mechanism of brecciation which is associated with tectonism is the process of hydraulic fracture. Fluids contained within the zone of movement become overpressured and brecciation ensues to dissipate the high fluid pressure. In a dilatent jog associated with faulting, an implosion breccia can result. In a thrust environment, episodic slip and stick will produce extensive overprinting by later brecciation events. Hydraulic fracture can also operate during dewatering. In the Natal Group (Matthews, 1988), zones of breccia occur consisting of angular quartzite fragments set in a red shale matrix. These zones are parallel to bedding and are interpreted as occurring during dewatering. Hydraulic fracturing, as described under hydrothermal breccias, occurs under conditions of high pore-fluid pressure as opposed to high confining stress. In tectonic-related, carbonate breccias, hydraulic fracture can be recognized by the presence of new vein growth. The presence of comminuted grains would however indicate high confining pressures (Robertson & Woodcock, 1986).

Tectonic breccias can usually be recognised by a homolithic clast assemblage, although as stated, in some fault zones as well as mylonites, heterolithic breccias are present. Clasts are often oriented parallel to the fabric as well as being slightly rounded on the microscale. The matrix consists of finely comminuted wallrock or "rock flour". There is often little mixing across lithologic boundaries.

Metamorphic assemblages are lower grade than the surrounding rocks and specific associations such as phyllonites can form.

	TYPE OF BRECCIA			
	DEPOSITIONAL	CHEMICAL	HYDROTHERMAL	TECTONIC
CLAST SHAPE	Irregular to symmetrically angular	Irregular to very angular	Usually angular, rounding can take place by reaction with hot fluids	Angular to rounded, often in pods parallel to fabric
CLAST COMPOSITION	Heterolithic to homolithic, often has exotic clasts	Homolithic, wall rock derived	Heterolithic to homolithic	Usually homolithic, clasts same composition as immediate wall rock. Some heterolithic examples
MATRIX COMPOSITION	Fine-grained carbonate, tuffaceous or lithic sediment	carbonate (cc, ank, dol), barite, fluorite, quartz (microcrystalline) and sulphides	carbonate (Fe-cc, ank, dol) sulphides, silica, tourmaline, oxides, mgt	Comminuted wall rock and carb, quartz cement
CLAST TO CLAST RELATIONSHIP	Well-sorted	Irregular	Irregular to none	None
DISLOCATION	Low (internal), complete (mass flow)	Low to medium	High, low in crackle breccias	Very high
VEINING	Post-lithification, post-breccia	Post-lithification, pre-breccia, post-breccia	Post-lithification; pre, syn and post-breccia	Pre, syn and post-breccia

	TYPE OF BRECCIA (continued)			
	DEPOSITIONAL	CHEMICAL	HYDROTHERMAL	TECTONIC
RELATIONSHIP TO STRATIGRAPHY	Stratabound, laterally continuous to discontinuous	Often stratiform but can be pipelike, linear or irregular	Often pipelike or irregular with intense brecciation towards centre. Breccia intensity increases up-stratigraphy	Poorly stratafied unless associated with thrusting
FORMATIVE PROCESS	Slumping, glacial deposition	solution collapse, cement aggregate reaction	Boiling fluids, overpressurization	Frictional abrasion, hydraulic fracture

Table 9: Classification of breccia types with respect to formative mechanism. (See text for sources).

4.2.2 ROSH PINAH FOOTWALL BRECCIA

Brecciation in the footwall lithologies is manifested as closely to widely spaced, angular, polygonal fractures, commonly filled with carbonate material forming a trellis-like network. These fractures are usually marked by dark grey discolouration of the quartzites up to 2 cm on either side of the fracture which is itself rarely greater than 5 mm in width.

Plate 18: Typical fracture breccia exposed on surface. Crosscutting quartz veins are related to late D2 faulting. Locality 100 m south of A-Mine.

The fracture spacing is roughly 25 cm to 40 cm with the fracture density increasing towards the ore zone contact. The fractures thicken towards the ore zone and have the appearance of discrete, often clast-filled veins (Carbonate veins 1,2). In many areas the fractures appear to be restricted to certain beds or horizons. Figure 11 shows a quartzite which is crosscut by fractures. The fractures terminate at the fine-grained top layer of microquartzite (<5 cm) and do not continue through to the next bed. The breccias are present to a maximum depth of 70 m below the

ore bodies and occur along the entire length of the ore zone explored to date. Homolithic as well as heterolithic breccias occur although clasts are exclusively derived from the footwall lithologies.

Figure 12: Brecciation in footwall quartzite. Rotation of clasts shows that explosive boiling took place while the Mn-rich nature of the dolomite as well as the low Fe value of the sphalerite indicates these veins to be of a hydrothermal origin.

Hangingwall exposures in proximity to the Western Boundary Fault show anastomosing but preferentially orientated

veinlets. No carbonate alteration rims the fractures. They consist of muscovite and minor pyrite and are tectonic in origin.

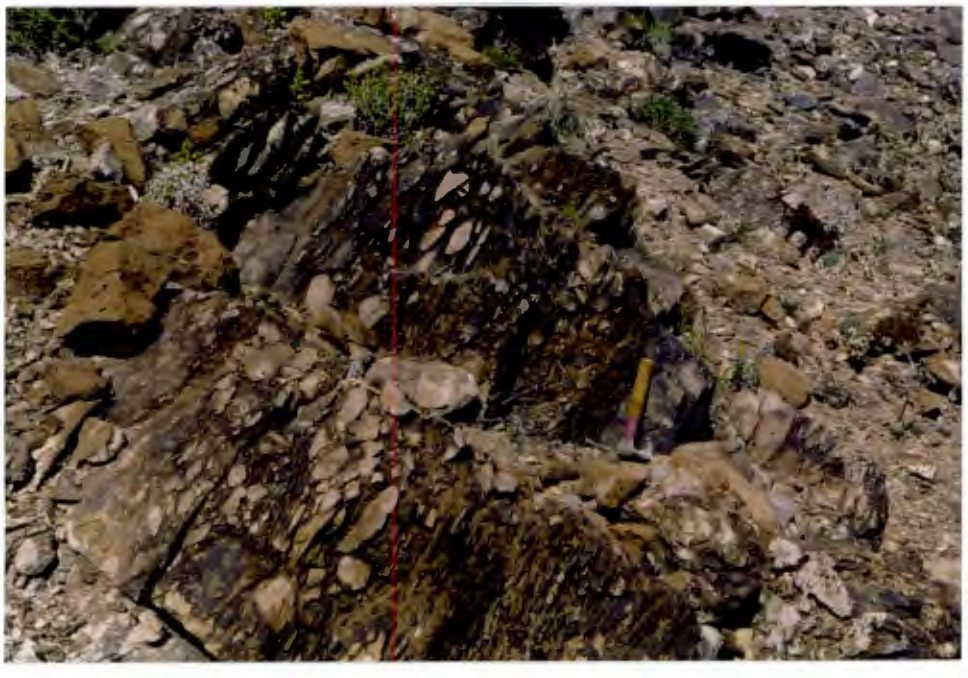

Plate 19: Typical matrix breccia exposed along contact between carbonate ore and footwall quartzites. Bedding parallel clast orientation is visible. Quartzite clasts hosted in Ba-rich carbonate matrix. Locality is MOB surface exposure.

In proximity to the ore, the rock consists of angular, generally preferentially oriented clasts of quartzite set in a mineralized carbonate matrix (Plate 19). This zone is largely continuous and varies between 0.3 and 1.0 m in thickness. This zone of matrix breccia is especially common at the contact with the carbonate ore zone as opposed to the microquartzitic lithologies. Many of the quartzite fragments are covered in a thin film of muscovite with a pronounced mineral lineation.

On surface, both breccia types have marked weathering patterns. The more common "fracture" breccia (Plates 2,18) consists of irregular, dark brown veins of carbonate material crosscutting cream-coloured silicified quartzites,

while the "matrix" breccia (Plate 19) consists of resistant quartzite clasts supported by residual, dark brown carbonatic cement. Breccias were observed occurring in quartzites interbedded with occasional dolomite horizons about 7 km east of Rosh Pinah (Plate 20). These breccias underlie the dolomite lenses and form zones about 2 m thick. They are indistinguishable from the matrix breccia of Rosh Pinah but pinch out where the breccia zone becomes a thrust contact between quartzite horizons. These zones therefore, represent fault breccias.

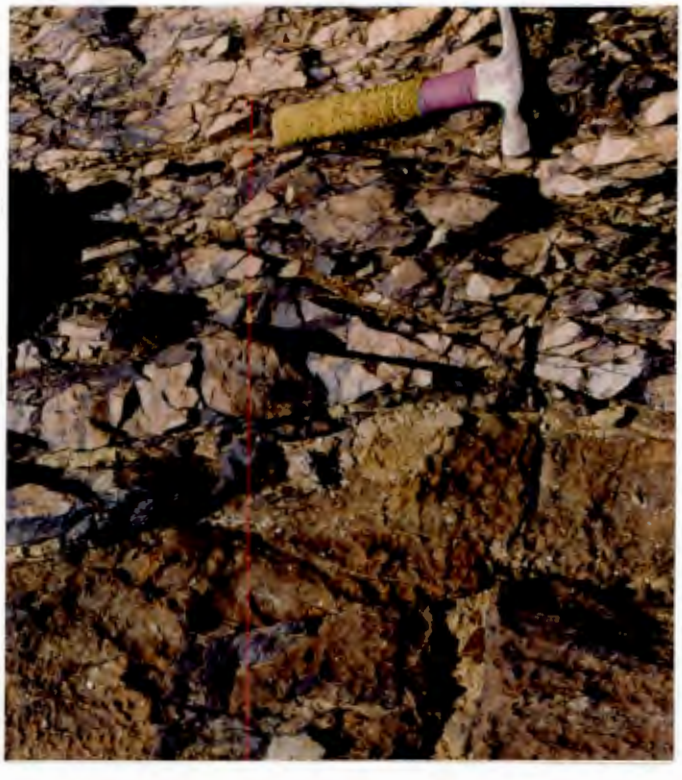

Plate 20: Thrust fault breccia produced during D1 along contact between quartzites and dolomites. Lithologies have been overturned during D2. Locality 5 km north of Rosh Pinah.

4.3 VEIN ASSEMBLAGES

Both the "matrix" as well as "fracture" breccias, although in essence being vein systems themselves are transgressed by a wide variety of later veins. Although most veins are related to structural deformation, some are part of the already described hydrothermal breccia systems. It is therefore necessary to characterize all veins with respect to their mineralogy, particularly any indicator minerals or textures which would be characteristic of a specific veining episode. Once the veins have been "fingerprinted" in this way, overprinting relationships can be recorded. This proved to be very difficult because many of the veining episodes are characterized by similar mineralogies. Another problem is the common presence of many carbonate minerals that can only be distinguished by chemically analysis.

The veins have been divided into four main types according to their major mineralogy (Table 10). These four varieties are (i) quartz veins, (ii) sulphide veins, (iii) carbonate veins and (iv) veins of meteoric origin. The various vein types within each division are arranged in a rough chronological order.

4.3.1 QUARTZ VEINS

Four generations of quartz veining were identified. They all appear to be late stage with respect to the mineralization. They fill areas of lower strain induced during D1 and D2 deformation. Many are related to faulting such as the vein arrays that occur near the Western Boundary Fault. The veins seem to be a product of lateral secretion rather than elevated high-temperature hydrothermal deposition as only localized silicification occurs associated with the quartz veins.

4.3.1.1 Type One Quartz Veins

These veins are generally sinuous with a maximum width of 2 to 3 cm. They have irregular edges and no center line i.e. deposition did not occur within a pre-existing fracture. On transgressing carbonate lithologies, these veins become carbonate-rich, the carbonate mainly calcitic in composition, implying fluid interaction with the wallrock during formation. They are usually subparallel to the S1 foliation.

4.3.1.2 Type Two Quartz Veins

Thick veins and irregular masses of medium-grained, milky quartz occur within both hangingwall and footwall lithologies. These quartz masses are up to 2 m wide and often contain coarse-grained sulphides. The sulphides consist of stretched and striated pyrite cubes up to 10 cm in diameter, dark brown chalcopyrite-rich sphalerite, granular chalcopyrite and coarsely crystalline galena. Chlorite appears to be an alteration product of stoped wallrock clasts contained within these quartz veins. Some veins are truncated by D1 faults while others transgress the same faults implying formation during D1 deformation.

4.3.1.3 Type Three Quartz Veins

These veins are rimmed by calcite and white, granular baryto-calcite. Some veins contain coarse-grained, light green baryto-calcite which commonly displays a well-developed rhombohedral habit. These veins contain chalcopyrite. They are often sigmoidal and restricted to carbonate lithologies (Fig.4). Their sense of rotation is contradictory in this diagram and it is thought that this is related to repeated flexure during the D2 event. They are mineralogically similar to type 4 carbonate veins and are regarded as being genetically related.

4.3.1.4 Type Four Quartz Veins

These common veins are barren and do not contain remobilized sulphides. They are narrow, straight edged and often occur as parallel sets. Maximum thickness is about 10 cm. They formed as a response to brittle fracture during late D2 faulting and later minor folding.

4.3.2 CARBONATE VEINS

Carbonate veins commonly crosscut the footwall, ore zone and, less commonly, the hangingwall lithologies. They represent numerous polyphase events of vein precipitation. Carbonate veins appear to have been precipitated under conditions of both high-temperature (250 - 200 ^{o}C) as well as low-temperature (<60 ^{o}C) deposition and were deposited during the formation of the ore body as well as during the deformation of the ore.

4.3.2.1 Type One Carbonate Veins

These veins make up the distinctive fracture breccia. They are composed of sulphide-bearing, carbonaceous dolomite with a high manganese content (Mn = 3.5 wt%). In Mountain Ore Body, iron and strontium are generally present in trace amounts within the dolomite although up to 5 weight percent of each has been recorded. The dolomite is fine-grained, the average grain size approximately 50 um. The veins are rarely thicker than a millimetre or so. However, in C-Mine they occur as dark grey, straight-edged veins up to 20 cm in thickness (Plate 21). The veins transgress beds of footwall quartzite and are truncated by D1 faults at the bedding plane. In thin section they contain numerous heterolithic clasts of carbonaceous dolomite in a finer grained matrix.

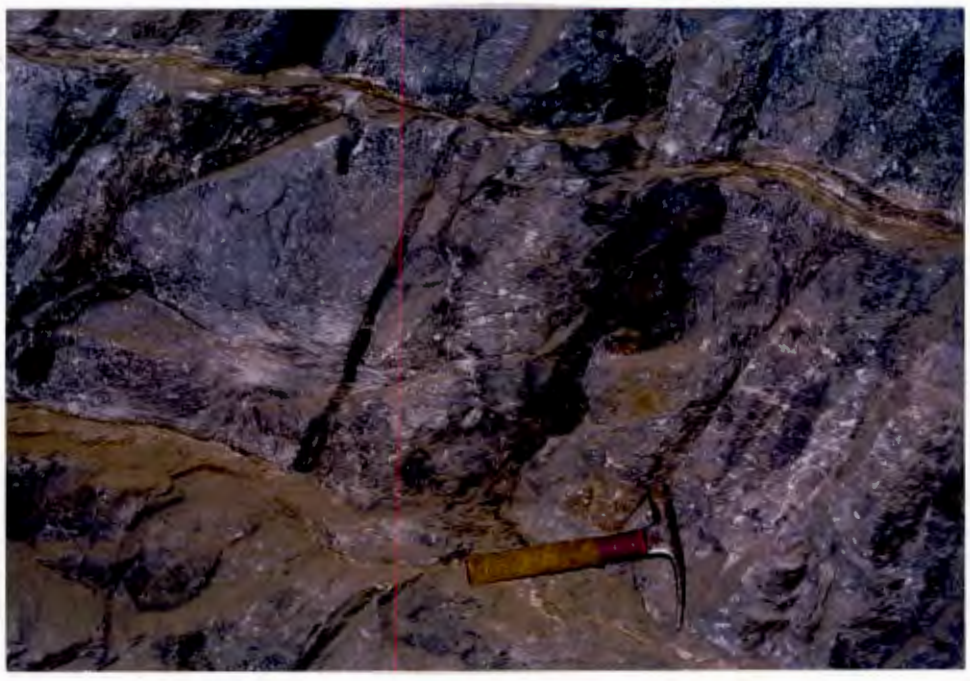

Plate 21: Carbonaceous dolomitic type 1 carbonate vein. Veins are truncated by D1 bedding-parallel faults. Locality C-Mine 410 level.

In zones of greater brecciation intensity, coarser-grained veins of similar composition but containing less carbon and less disseminated sulphides are common. These dolomite grains rarely show straight-edged boundaries and the majority are characterized by seriate contacts. Sulphides, specifically pyrite and sphalerite, occur as late stage inclusions within dolomite grains as well as along grain boundaries. There is a distinct association between the sulphides and free carbon.

Within the fine-grained lithologies these dolomite veins have a very erratic almost stylolitic appearance (Fig.12). They are interpreted as being the result of hydraulic shock. As these veins widen, surround and support clasts of wall rock, rotation of the fragments can be noticed (Fig.12).

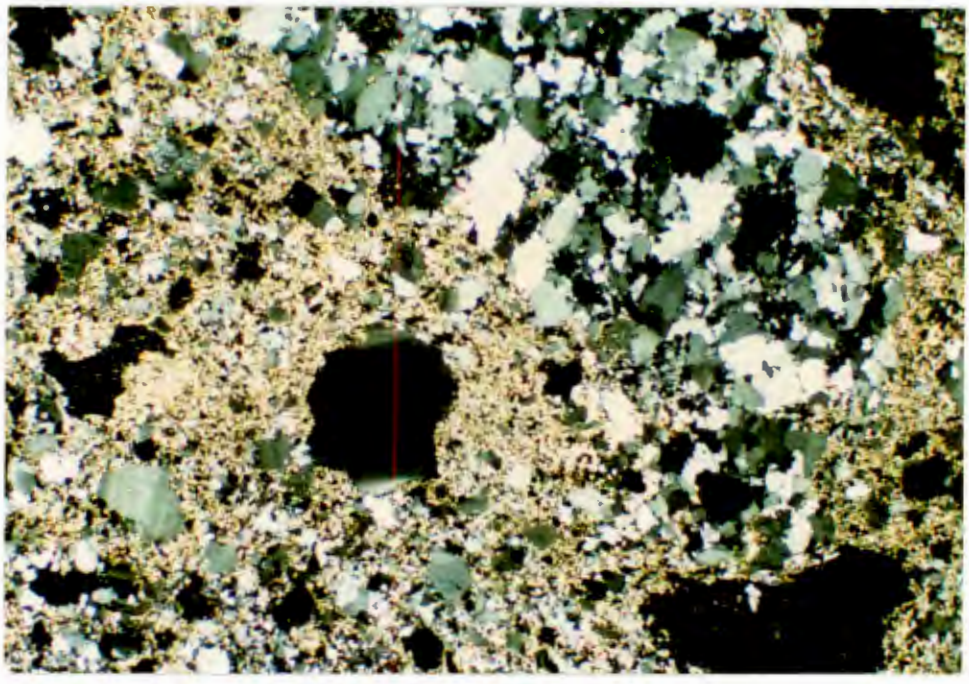

Plate 22: Brecciation of silicified footwall quartzite by hydrothermal carbonate (type 1). Disaggregation of the rock occurs preferentially along the grain boundaries. PRS 37, X.20

The sense of rotation is often contradictory which can only occur during fracture if the internal pore pressure is greater than the combined rock tensile strength and lithostatic load (Nelson & Giles, 1985). This extreme state of overpressure is produced only if the fluid is boiling.

Breccias similar in appearance to the fracture breccia (type 1 carbonate veins) but of a much later structural origin are also frequently observed. Separation of the early dolomitic fracture breccia from those related to later faulting is, however, only possible in areas where the relationship to early D1 thrusts or later faults can be observed. Figure 4 shows the development of fracture breccia below a D1 thrust fault, while mineralized footwall lithologies overlying the fault are unaffected by this brecciation. Development of the fracture breccias is also intimately related to the amount of silicification that the quartzites were subject to. In Figure 11, it can be observed that, at 14 m, there

is an abrupt end to the silicification front and with it a corresponding absence in fracture breccia.

4.3.2.2 Type Two Carbonate Vein

These veins occur in the Mountain Ore Body within 15 m of the footwall/ore zone contact and in the central area of the ore body. They reach up to 1 m in width, although most are 30 to 50 cm wide. They branch and have irregular to straight wall rock contacts (Plate 23).

Plate 23: Type 2 carbonate vein (dotted) exhibiting stoping, clast rotation and flow textures. White baryto-calcite and calcite segregations formed during differential movement during D2 while white, parallel vein set on right of plate is late stage joint filling. Locality Northern Ore Field.

The veins are a variegated white to light-grey with a greenish tinge caused by the presence of baryto-calcite. The sulphides present are chiefly pyrite, sphalerite and minor chalcopyrite and sometimes display what is interpreted as a primary flow banding, parallel to the sides of the vein. Clasts of wall rock are uncommon.

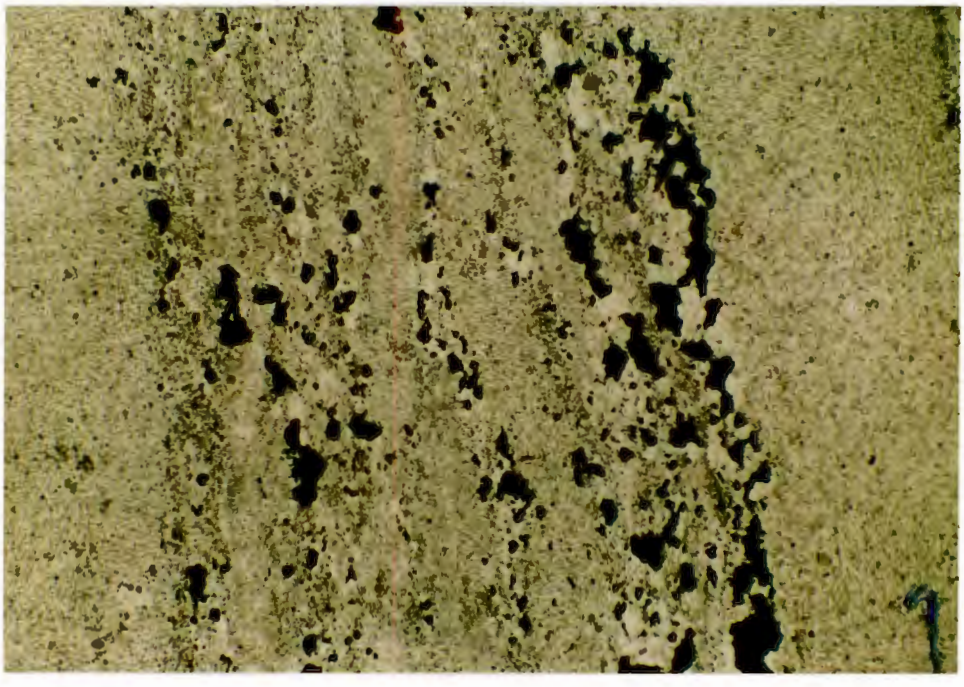

Plate 24: Hydrothermal streaming in a sample of type 2 carbonate vein. Sample orientated approximately vertically. PRS 44, X.20

One exposure [475 Cg] shows a transgressive vein containing a clast of quartzite rimmed by trails of fine to medium-grained pyrite and minor sphalerite. The clast appears to originate from the underlying quartzite bed.

4.3.2.3 Type Three Carbonate Vein

These veins occur in zones of fracture breccia below the central portions of the ore body. The veins are commonly lath-filled and rarely wider than 30 cm. They are usually relatively straight-edged with few branches, although some of the later veins are very sinuous. They vary in appearance from white, coarsely crystalline chalcopyrite-rich veins to dark grey, lath-filled veins. These veins appear identical in composition to the matrix breccia of the footwall-ore zone contact and are composed of calcite and barium carbonates. Clasts of silicic footwall quartzite are common with some veins being characterized by heterolithic

assemblages. Other veins contain only clasts derived from the immediate wallrock.

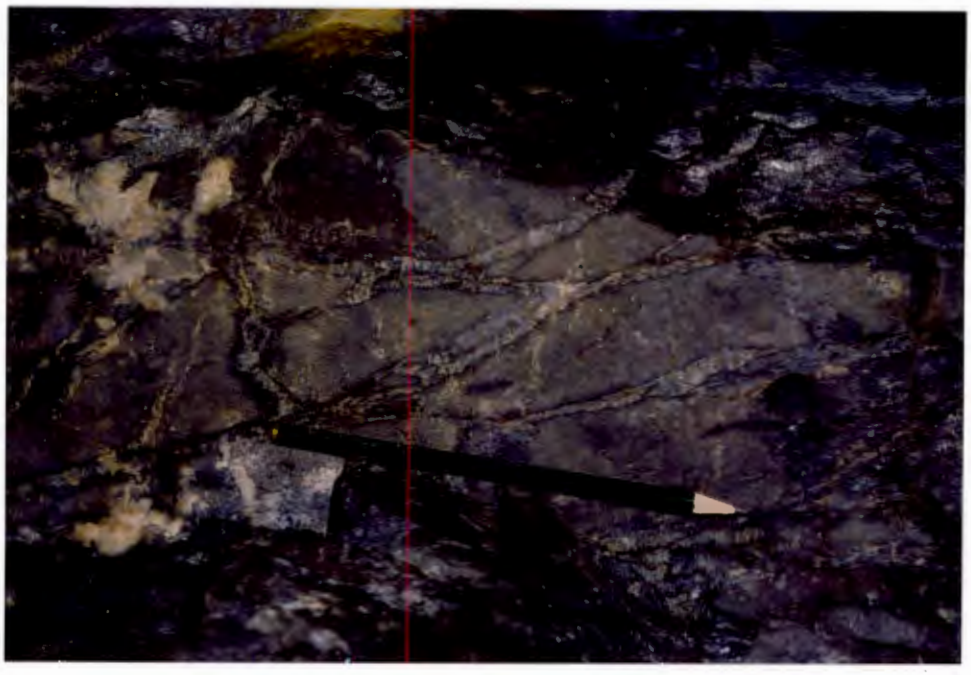

Plate 25: Type 3 carbonate vein with elongated footwall quartzite clasts produced during D1 thrust fault brecciation. Later D2-associated segregationary calcite veins overprint the breccia. Locality MOB [475De].

Some of these veins show a mineralogical zonation with sulphides, in particular light brown sphalerite, rimming quartzite clasts, which in turn are surrounded by lath-rich dolomite and then dark grey dolomite (Plate 3). Some of the veins follow pre-existing S1 foliation planes while others are deformed by D1 deformation implying that D1 continued over a protracted time interval.

Diffuse veins which occur in the lower areas of the dolomite ore (Plate 4), have a marked textural and compositional similarity to these type 3 carbonate veins. Although a complete gradation from a disaggregated collection of white spots of what is now barium carbonate to lath-filled veins can be observed, they are regarded as being related to hydrothermal activity, and hence type 2 carbonate veins, as they are deformed by the D1 fabric.

Chalcopyrite enrichment is a feature of these veins as indicated by Figure 7. Fine veins of chalcopyrite fill intergranular spaces (Plate 26) and indicate that chalcopyrite was introduced after the precipitation of the carbonates and barite, and was probably remobilized from the mineralized footwall quartzites.

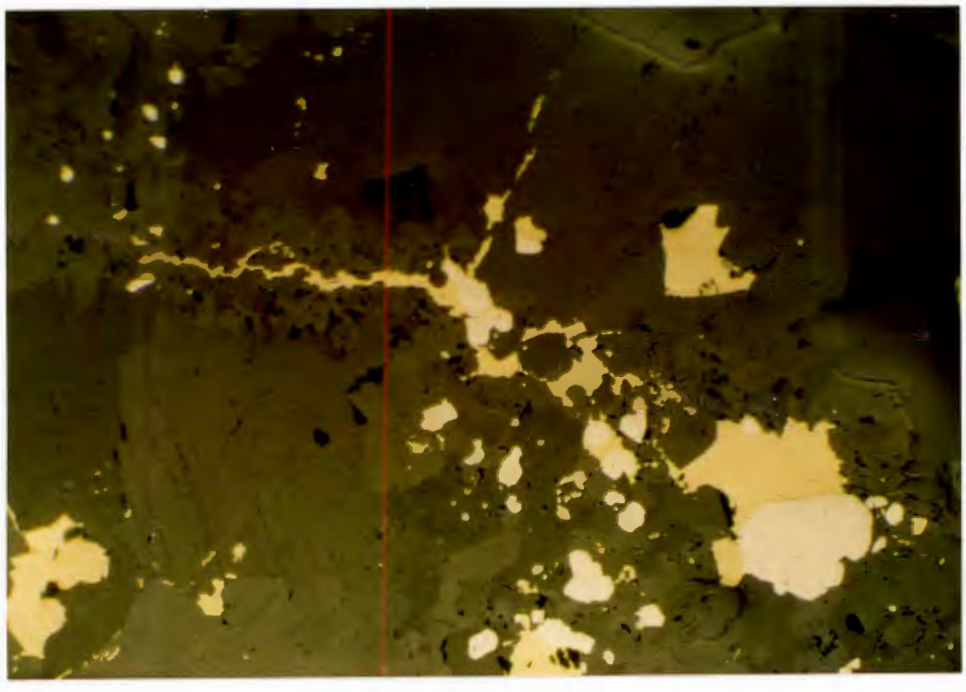

Plate 26: Chalcopyrite occurring as late stage veins in type 3 carbonate vein. PRS 45, X.40

4.3.2.4 Type Four Carbonate Vein

These veins consist of medium to coarse-grained calcite and/or norsethite and often contain associated chalcopyrite, tennantite and quartz. They usually occur in dolomitic ore and are rarely thicker than 5 cm. They vary in attitude from long and continuous to short (< 5 cm) irregular veins often grouped in linear arrays. The more continuous veins are usually parallel to the D2 foliation.

4.3.2.5 Type Five Carbonate Vein

These veins are coarse grained (>2 cm) and occur in the upper carbonate ore zone where they form straight-edged veins up to 10 cm in width. They consist of calcite and baryto-calcite and are often zoned, the baryto-calcite forming a thick rim to the vein. Many of these veins have subsequently been altered by supergene fluids and are therefore barren of sulphides.

4.3.2.6 Type Six Carbonate Vein

These are coarse-grained, monomineralic veins and segregations up to 30 cm in diameter of white calcite or ankerite. These segregations are present in both the footwall and hangingwall lithologies, specifically along bedding planes and fold closures. They are probably associated with late D2 or D3 deformation and faulting.

4.3.2.7 Type Seven Carbonate Vein

These veins are dominated by dolomite, have a maximum thickness of 15 cm and are related to late movement of the Western Boundary Fault. Remobilization of carbonate material occurred with the formation of brittle fractures in the hangingwall of the ore zone. These veins are medium grey in appearance, very fine-grained and have a polymictic texture.

4.3.3 SULPHIDE VEINS

Many of the sulphide-hosted breccias observed underground have been cited as examples of exhalative activity (Evans, 1978; van Vuuren, 1986). However, their textural concordance with D1 and D2 deformational fabrics, as well as the inclusion of clasts of already hydrothermally-altered and fractured rock show these veins to be tectonic in origin. Three types are distinguished.

4.3.3.1 Type One Sulphide Vein

These veins consist predominantly of pyrite with minor sphalerite. They are narrow (<1 mm) and are oriented parallel to S1 surfaces.

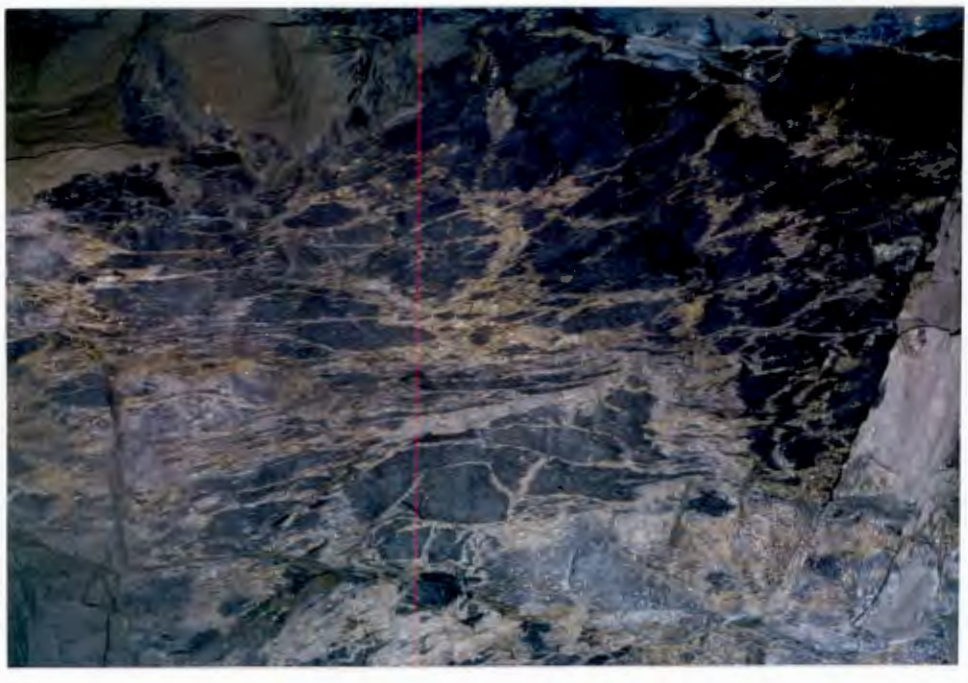

Plate 27: Pyritic, D1 crackle breccia developed in microquartzite. Breccia clasts are oriented into S0 parallel foliation direction. Locality MOB [470Bh].

The microquartzite lithologies show this vividly with "feathering" of the sulphides subparallel to bedding occurring within the rock (Plate 27). Remobilization of sulphides during D1 resulted in these veins.

4.3.3.2 Type Two Sulphide Vein

These veins are coarser-grained (3 - 4 mm) than type 1 sulphide veins. They transgress the footwall as well as the ore zone lithologies. The honey-coloured sphalerite and pyrite veins display classical evidence of "durgbewegung" (Plate 28) which is indicative of tectonic injection of semi-plastic sulphides.

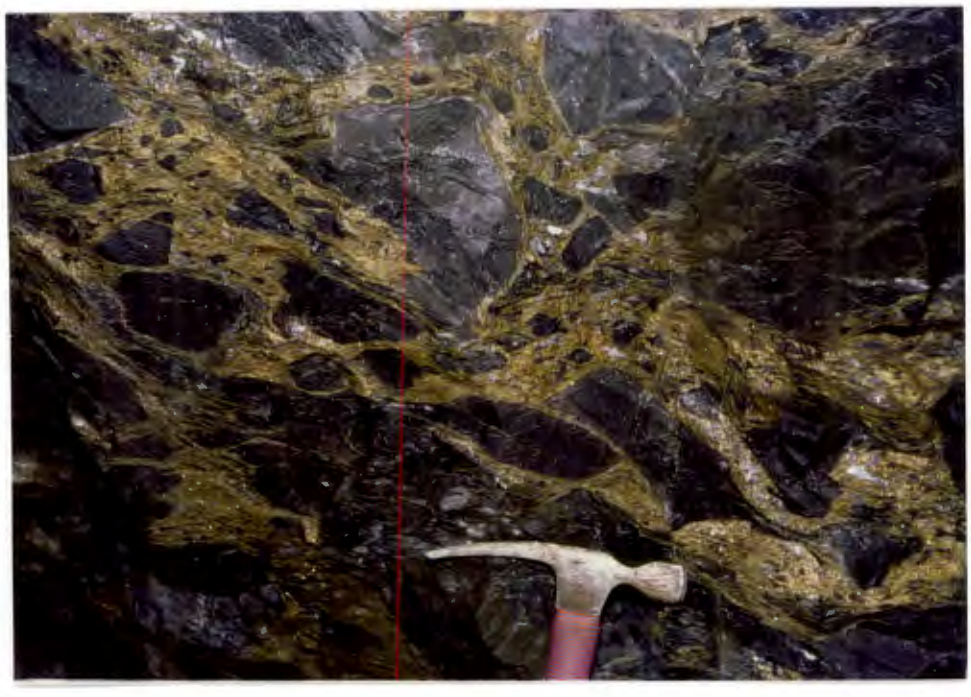

Plate 28: Pyrite and sphalerite "durgbewegung" in footwall quartzites. Evidence of type 1 carbonate veining (arrowed) can be observed in some of the clasts. Clast composition is heterolthic and little structural orientation is noticed. Locality MOB [470Bg].

The concordance of these veins with D2 structures observed in C-Mine (Fig.10i) as well as the Mountain Ore Body, would indicate their formation occurred during D2 deformation.

4.3.3.3 Type Three Sulphide Veins

These irregular, coarse-grained pyrite-dominated veins occur within the hangingwall in the vicinity of the Western Boundary Fault. They are also associated with minor, late-stage related faults. The subhedral pyrite grains (Plate 7) are angular and hosted in a carbonate matrix. Chalcopyrite replaces pyrite in a cruciform habit. Veins are normally irregular and anastomosing, except where they are associated with late D2 faulting. Here they appear as narrow, straight-edged veins often parallel to type 4 quartz veins (Plate 30).

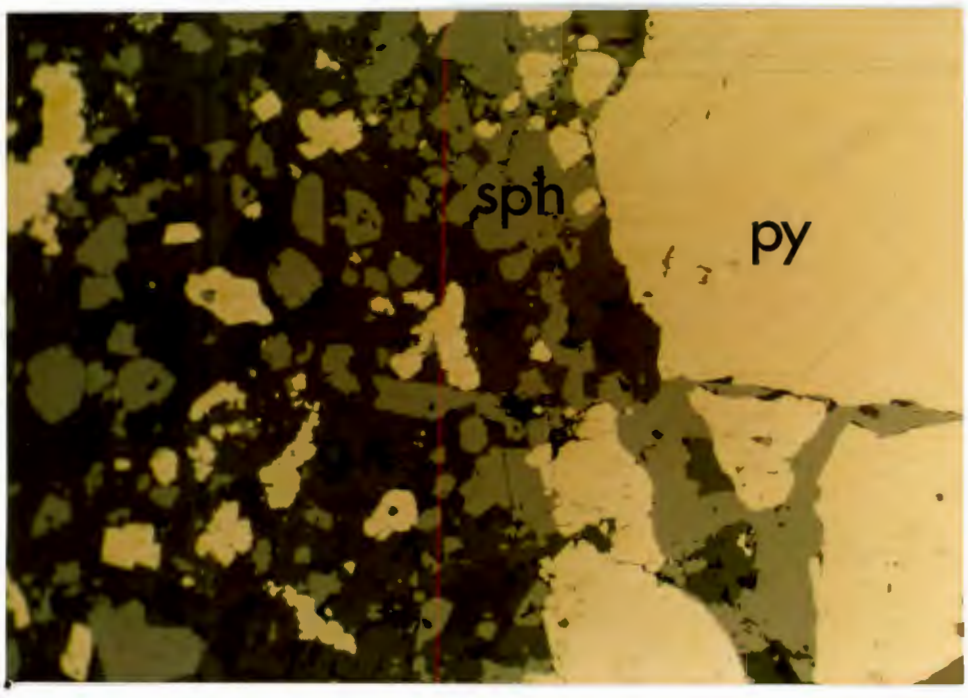

Plate 29: Texture of sulphide matrix in zone of "durgbewegung". Pyrite (py), sphalerite (sph) and gangue (gn). PRS 41, X.40

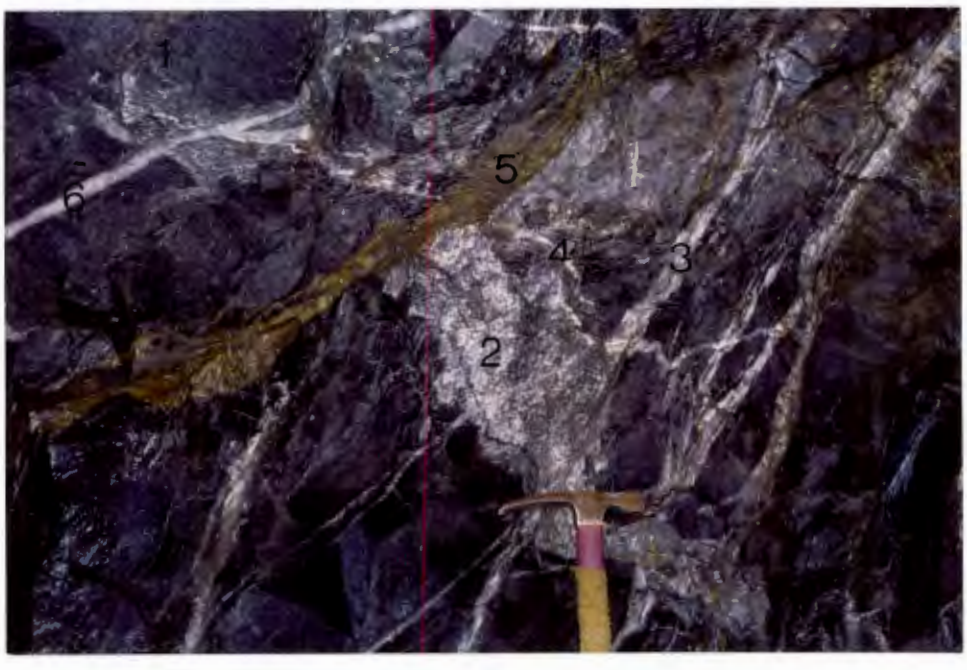

Plate 30: Multiple vein assemblage in footwall quartzites. Bedding is roughly horizontal while type 1 carbonate veins and spots are present. Veins are identified as follows: 1. Irregular type 3 carbonate (D1 in age), 2. Type 4 carbonate vein (early D2 in age), 3. irregular quartz + baryto-calcite vein (D2), 4. type 3 sulphide vein (late D2) and 5. type 4 quartz vein. Locality MOB [470Ch].

Table 10: Classification of vein types and their mineral assemblages observed in Mountain Ore Body.

QUARTZ VEINS	APPEARANCE	DISTRIBUTION	MAJOR MINERALOGY (in decreasing abundance)
Type 1 D1	Sinuous to straight, irregular edges. Become carbonate-rich when crossing carbonate lithologies	Crossing all lithotypes in the footwall	Quartz, baryto-calcite, chalcopyrite, calcite
Type 2 D1	Irregular masses of milky quartz up to 2m across	Quartzite lithologies, both hanging and footwall	Quartz, Fe-rich sphalerite, chalcopyrite, galena, pyrite, chlorite
Type 3 D2	Sigmoidal veins occurring as tension gashes. Carbonate rims to these veins	In carbonate veins in footwall	Quartz, baryto-calcite, chalcopyrite
Type 4 Late Faulting	Straight-edged, narrow, parallel sets often related to nearby fault	Hangingwall, footwall, ore zone	Quartz, calcite (rare)

CARBONATE VEINS	APPEARANCE	DISTRIBUTION	MAJOR MINERALOGY (in decreasing abundance)
Type 1 Exhalative	Fine-grained, dark grey and transgressive to SO. Rarely wider than 10cm and becoming increasingly "ptygmatic" with decrease in width	Mainly highly silicified footwall quartzites as well as lower ore zone microquartzite	Dolomite, pyrite, sphalerite, chalcopyrite, organic carbon
Type 2 Exhalative	Medium to coarse grained white, light green or cream, exhibiting "flow-banding" and included wall rock clasts. Veins are irregular and apophysis	Footwall and extended into ore zone lithologies. Commonly in centre of ore body	Calcite, baryto-calcite barite, quartz, kaolinite, chalcopyrite, sphalerite, tennantite, celsion
Type 3 D1	Light grey to cream, medium grained with abundant chalcopyrite and sphalerite. Groundmass often filled with taths of barium carbonate	Footwall quartzites and microquartzite	Dolomite, norsethite, baryto-calcite, calcite, sphalerite, chalcopyrite, pyrite
Type 4 D2	Coarse-grained, white veins < 5cm in thickness	Carbonate ore, rarely in footwall	Calcite, norsethite, tennantite, quartz
Type 5 D2	Coarse-grained, white to greenish, often zoned	Upper carbonate ore	calcite, baryto-calcite
Type 6 D3	Coarse-grained white, monomineralic with no associated sulphides	In both hanging and footwall in structural traps along bedding planes	calcite, ankerite
Type 7 Late Faulting	Fine-grained medium grey with included fine-grained wall rock clasts	Associated with western boundary fault	Dolomite, calcite, pyrite

SULPHIDE VEINS	APPEARANCE	DISTRIBUTION	MAJOR MINERALOGY (in decreasing abundance)
Type 1 D1	Fine-grained, sinuous to angular network of pyrite-rich veins	Microquartzite, fine-grained footwall quartzites	Pyrite, sphalerite, chalcopyrite
Type 2 D2	Medium to coarse-grained, amber-yellow, breccia matrix filling. ("Durgbewegung")	Hetero- and homolithic footwall quartzite breccias. Associated with early SO parallel faults	Pyrite, sphalerite, chalcopyrite, galena (tr)
Type 3 Late Faulting	Coarse-grained, 5 - 10cm thick, foliation parallel veins	Footwall near ore zone contact, certain areas within ore zone, hangingwall quartzites in proximity to faults	pyrite, chalcopyrite, dolomite, muscovite, minor sphalerite
METEORIC VEINS			
Type 1	White coarse-grained, open space filling along structural discontinuities such as joints, shear zones and cleavage planes	In carbonate lithologies of ore zone and footwall quartzites where extensive supergene alteration has occurred	Barite, galena, calcite, marcacite, ankerite
Type 2	"Porous", deeply weathered material reflecting alteration of pre-existing veins	Footwall carbonate veins	Baryto-calcite, gypsum, baryte, quartz, calcite, kaolinite, hemimorphite, native-Cu

4.3.4 METEORIC VEINS

These veins are normally associated with the weathered portion of the ore zone (Ch. 3.2.6). Their paragenesis is undisputed and they are mineralogically complex. They are not classified on mineralogical grounds in this study.

Two major vein settings are present. The more common are coarse-grained, mainly baritic and/or calcitic segregationary veins following planes of structural discontinuity within both the weathered ore zone and footwall quartzites. These veins are up to 30 cm in width. The presence of marcasite is diagnostic in their identification.

The second set is best developed in the deeply weathered zones of the ore body such as the lower central zones and those areas associated with faulting. Supergene alteration of pre-existing footwall veins has occurred resulting in leaching and complete mineral reconstitution.

5. DISCUSSION

5.1 ENVIRONMENT OF DEPOSITION

The presence of highly alkaline, rhyolitic lavas associated with thick sequences of rapidly deposited volcanoclastic and immature, basement-derived sedimentary material suggests that the Gariep sediments were laid down within a rift-related basin (De Villiers & Söhnge, 1959; Martin, 1965; Kröner, 1974). This common association is recorded in the African Rift system (Reading, 1986), as well as ancient analogues such as the Damaran Group (Miller, 1983).

The Rosh Pinah formation appears to represent deposition within a subsidiary, fault-bounded, second-order basin within the Gariep Basin itself. The absence of listric faults in the immediate basement to the east, indicates that rifting occurred towards the west and that the Rosh Pinah basin was being controlled by vertical graben or half-graben faulting. Topographically higher basement is therefore expected to the west which would support the contention that the Hilda formation was deposited under shallow water conditions.

The presence of occasional mass-debris flows within the massive turbiditic beds attests to the presence of active rifting occurring during the deposition of Rosh Pinah sediments. Flat-pebble conglomerates as well as rare lenses of boulder conglomerates occur. The turbiditic beds were presumably triggered by earthquake activity as discussed by Walker (1975) or as observed in the Laingsburg formation of the Karoo (A. Fuller, pers comm.). Deposition appears to have been particularly active as few of the beds possess a fine-grained, suspension-derived, upper argillic portion. The presence of glass shards within the argillites indicates an important volcanic component of these rocks. This suggests that the argillites were also relatively rapidly deposited. Deposition of turbidites need not be under deep-

water off-shelf conditions. For example, the first record of turbidite deposition was in Lake Geneva below a water depth of 180 m (Forel, 1885). As the inferred maximum dimensions of the Rosh Pinah basin are 25 km by 10 km (Edwards, 1984) this may indicate a maximum water depth of approximately 200 m in the Rosh Pinah basin.

Much of the geologic evidence indicates fairly shallow water deposition. The ubiquitous presence of carbonate, either dolomite or calcite, in the sediments, as well as lenses of massive dolomite in the sequence indicate deposition under shallow-water conditions - the carbonate lenses being deposited during periods of diminished clastic input. A thin, 5 cm thick layer of dark grey, concretionary spheroids up to 0.5 cm in diameter occurs as a capping overlying a feldspathic quartzite bed (PRS 98). These prove, under the microscope, to be oolites which form only under conditions of wave action. They were presumably transported to this site and therefore indicate a proximity to the palaeo-shoreline. Basic, submarine extrusives occurring within the sequence are vesiculated rather than pillowed which is also indicative of shallow water conditions. Taking these points into consideration a maximum depth of synsedimentary sulphide deposition is postulated to be no greater than 150 to 200 m.

The predominance of laminated rather than ripple-bedded argillites as well as the absence of any reworking of the sediments indicates stagnant, stillwater conditions. Anaerobic conditions certainly prevailed as indicated by the highly carbonaceous nature of the argillites.

SEDEX as well as VMS deposits are a common feature of basin development as witnessed by the almost exclusive association of these deposits within rift environments (Gustafson & Williams, 1981). These deposits were divided by Plimer (1986) into two groups on the grounds of their association with either aborted rifting of thick sedimentary piles or successful rifting which has developed into a mature basin or ocean. Although many loose generalizations are used to

differentiate the two end members, SEDEX deposits associated with failed-rifts (aulacogens) are characterized by low metamorphic grades and hypersaline, shale-carbonate sequences with the non-sulphide minerals of the deposit being identical to those of the surrounding sediments. The mature-rift deposits are characterized by deep water (?), turbidite-metavolcanic sequences with distinct upward and outward metal zonation from Cu to Zn to Pb to Mn. These features indicate that Rosh Pinah formed during the early development of a mature rift.

Deposition of the sulphides occurred during a period of quiescence which is indicated by the fine-grained lithologies of the ore zone. Although intercalated quartzite beds do occur (Van Vuuren, 1988) they are rare and sometimes appear to represent thrust slices of footwall quartzite which have been faulted into the ore-body. Deposition of the sulphides was rapid as indicated by the variability of the ore-zone lithologies as well as the occurrence of soft-sediment features (Plate 4) indicative of slumping (Mills, 1983). As the ore zone follows approximately 1000 m of turbiditic quartzite deposition, and is continuous along the same stratigraphic horizon into argillite and sometimes carbonate lenses, it implies that a major change in tectonic activity occurred at this time. It would appear that the mineralization was associated with this event. Resumption of active tectonism terminated the deposition of the ore lithologies and was probably associated with a cessation in hydrothermal activity.

Examples of hangingwall silicification in the A-Mine area as well as hangingwall brecciation have been cited in the past as examples of continued exhalative activity (Van Vuuren, 1986; De Kock, 1987). This study regards these as post-lithification features associated with fault movement along the hangingwall contact. Areas of intense carbonate alteration above C-Mine as well as the horizon of "immediate" hangingwall carbonate have been regarded as a result of continued exhalative activity (De Kock, 1987; C.J.

Hodgson, pers comm.). The absence of appreciable mineralization argues against this. The carbonate enrichment could therefore be a diagenetic feature as is the Ba-enrichment in the hangingwall sediments. This type of diagenetic enrichment is supported by observations at Jason in Canada (Smee & Bailes, 1986) and Moyvoughly in Ireland (Kucha, 1988). It is important to note that if the carbonate lithologies represent times of slow sediment input, they should also be enriched with respect to metals relative to the regional background recorded in the quartzites.

A significant feature of the hangingwall sediments is the common presence of pyrrhotite as the dominant iron sulphide present. It occurs as irregular, flame-like grains which form up to 2% by volume of the rock. The rapidly deposited turbidites would not be able to support anaerobic conditions as did the argillite horizons and hence, if minor exhalative activity was continuing, there would be a deficiency in reduced sulphur and pyrrhotite would form. Finlow-Bates and Large (1978) suggested that the relative stability of pyrrhotite and pyrite deposition is a factor of water depth. A sudden deepening of the basin would result in pyrrhotite deposition, and the resumption of turbidite deposition. Renewed movement on the inward dipping, boundary faults could therefore result in the closing off of the hydrothermal conduits resulting in negligible mineralization being associated with the hangingwall carbonate lenses.

5.2 SOURCE AND COMPOSITION OF ORE FLUIDS

The traditional model for the formation of SEDEX deposits involves the progressive warming up of connate water in the sedimentary pile (Russel et al., 1981). Ultra-reactive fluids, produced through geothermal heating of seawater, basinal brines or fluids derived from the dewatering of evaporitic lithologies, progressively leach metals contained within the sediments. The metal cations combine, and are

transported, as chloride ion complexes (Lydon, 1983). On encountering a relatively low pressure pathway such as a fault, a change in lithology or permeability, the fluid is channelled towards the surface (Sibson et al., 1975) where the metals are deposited as sulphides at the site of ore formation. A thick (8000 m for a Zn-Pb deposit) sedimentary pile, an elevated geothermal gradient or an external source of ore fluids all enhance the generation of high temperature, hydrothermal cells.

Hypersaline fluids derived from the dewatering of evaporites have been suggested as a source of chloride complexes for metal leaching in the Mount Isa (Neudert & Russel, 1981) as well as McArthur River areas (Lambert, 1981) of Australia. Evaporites are a rock type often recorded within rift sequences but which are absent in the Rosh Pinah environment. The absence of these sediments in the Rosh Pinah area, however, indicates that ore forming fluids, if derived from the released pore fluids were similar to normal sea water.

Although there is evidence that many sulphide deposits represent the sulphidization of pre-existing metal compounds below the sediment-water interface, there is enough compelling evidence to suggest that direct hydrothermal precipitation was an important process of sulphide formation. The observation of hydrothermal vents such as Atlantis II in the Red Sea (Degens & Ross, 1969) and the Salton Sea (McKibben & Elders, 1985), indicate that cooling, H_2S-bearing fluids, can precipitate metal sulphides. The predominance of sulphate lithologies and the absence of sulphur-depleted minerals, such as pyrrhotite, in the Mountain Ore Body, suggests that sulphur was in abundant supply in the ore-forming fluid. Mixing of seawater with the hydrothermal, saline, metal-bearing solutions occurred during thermal boiling and precipitated sulphate minerals as well as appreciable dolomite.

The majority of the sulphides occurring at Rosh Pinah are regarded as being the result of direct hydrothermal precipitation for the following reasons:

i) The presence of framboidal pyrite, sphalerite and galena, is indicative of precipitation as a result of sudden temperature decrease or quenching (Lydon, 1983).

ii) The extremely fine-grained nature (<10 μm) of type 1 pyrite as well as microquartzite-hosted sphalerite (both regarded as pre-metamorphic), indicates sulphide precipitation during exhalative activity (Lydon,1983). Identical sulphide textures are recorded at McArthur River (Lambert, 1981) and the Pb-Zn rich facies of Mount Isa (Perkins, 1984) and a similar origin is interpreted.

The textures and chemical data presented indicate that the characteristic lath-shaped barium carbonates occurring within the deposit are of replacement origin. The lath-shaped minerals which have been replaced reflect therefore the original ore solution composition. A rare inclusion of rhodocrosite intergrown with barite was observed in the baritic, northern portion of the ore body (Plate 5). These barite grains are distinctly lathlike, the habit typical of diagenetic barite (Deer et al., 1966). Diagenetic barite documented in the Karoo Sequence (Reimer, 1978) consisted of radiating clusters of thin, spindly laths. At Red Dog, Alaska, replacement of diagenetic barite laths by sulphides is recorded (Lange et al., 1985). Similar occurrences are noted by Vogt and Stumpfl (1987) at Abra, Western Australia, with a characteristic lath-like habit. Anhydrite was also present in large amounts at Abra.

It is proposed that the barium carbonate laths in the Rosh Pinah sequence represent replaced barite and perhaps anhydrite grains, which grew during ore diagenesis. Veins related to D1 structural deformation (type 3 carbonate veins) also contain replaced laths, indicating that replacement of the laths occurred after D1 deformation.

The metal zonation pattern presented in Fig. 7d. is more suggestive of a volcanogenic origin than a SEDEX deposit. This is supported by the similarity of the gangue and sulphide mineral zonation and stratigraphy to that of the Kuroko ores (Sato, 1977), as well the plot of total metal percentages. The proximity of the Spitzkop volcanic centers, i.e., less than 10 km to the north (Edwards, 1984), to the site of ore deposition as well as the relatively thin sediment thickness (<1000 m) of the Rosh Pinah formation could indicate that volcanogenic-derived hydrothermal solutions were involved in the genesis of the Rosh Pinah deposit and not the sediment-derived fluids that are commonly inferred (Russel et al., 1981).

A rare Ti-Cl-silicate (baotite) occurs in footwall quartzites of the A-Mine, and is regarded as a primary hydrothermal mineral (ISCOR internal report) possibly indicating a granitic or substantially evolved acid magmatic source for some of the hydrothermal components.

The occurrence of incompatible elements such as Sn associated with the ignimbrite-hosted Neves Corvo deposit in the Iberian Cu-Fe belt (F.J.Sawkins, pers comm.) as well as significant boron and Sn-mineralization at Sullivan in British Columbia (Hamilton et al., 1983), indicate that deep-seated intrusions may be more important in the formation of volcanogenic, as well as SEDEX deposits, than has been previously understood.

An important feature in supporting a syngenetic hydrothermal source rather than precipitation of Mississippi Valley Type epigenetic fluids is the total absence of fluorite in the ore. Fluorite is a notable component of Mississippi Valley Type deposits as are associated hydrocarbons.

5.3 DISCUSSION OF STRUCTURAL OBSERVATIONS

The penetrative north-north-west trending mineral lineation of the area and symmetric to asymmetric folds, that vary in style from open to tight and show south-westerly overturning in the vicinity of the mine, were recognised by McMillan (1968) and suggested to be D1 in age. The plunge of these folds seldom exceeds 40° and is commonly horizontal. An axial planar "S1" fabric is developed subparallel to the lithological strike, and an "L1" lineation is defined by "extreme elongation of boulders and incipient mineral (pyrophyllite?) growth" (McMillan, 1968; p.123). These observations were not invalidated by subsequent work in the area (Page & Watson, 1976; Kindl, 1979).

Although McMillan (1968) correlates this fabric with the D1 event, his thin-section analysis shows that this strain-slip cleavage is in some cases produced by a second stage deformation of a pre-existing bedding-parallel fabric.

Edwards (1984) correlated the regional fabric with the formation of the extensive northwest trending folds of the Rosh Pinah hills and Spitzkop mountains. The folds of the Spitzkop area are recognised by an interlimb angle of greater than 40° which is tighter than at Rosh Pinah. These folds are generally recumbent towards the southwest.

However, it was only recently that the presence of an earlier deformation phase was substantiated (Davies & Coward, 1982). They suggested that extensive layer-parallel slip accompanied by the development of a S0-parallel fabric had occurred prior to the formation of the major folds in the area. Much of this interpretation of the Rosh Pinah area, was obtained from work at the nearby Scorpion prospect as well as from structural relationships of the coastal assemblage in the vicinity of Chameis Bay. This work has been strongly supported by the study of Von Veh (1988), who concluded that a major deformation event, consisting of large scale thrusting, preceded the regional folding event.

Two tectonostratigraphic terrains are identified within which extensive horizontal displacement occurred. These terrains are synonymous with the mio- and eugeosynclinal assemblages defined by Krõner (1974). The Marmora terrane lies to the west, while the shallow water Port Nolloth terrane unconformably overlies the basement to the east. They are separated by the Schakalsberg thrust fault. Von Veh (1988) suggests that the "docking" of the oceanic suite of volcanic and deep water sediments of the Marmora terrain, caused the development of a foreland-propagating imbricate fan. This resulted in the development of an extensive duplex system in the south (Richtersveld area) and the related D2 fabric elements.

It appears, however, that the effects of D1 deformation were far greater in the north, and that the Richtersveld was largely unaffected by the D1 event. From the data recorded in this study, it appears that the first stage of deformation was initial thrusting directed towards the south-east that was overprinted by later north-north-west oriented folds. This relationship occurs in the Anninaub area approximately 30 km north west of Rosh Pinah (Siegfried, 1986) and at the nearby Scorpion prospect (AAC, 1983).

The bulk of the strain resulting from D1 and D2 tectonism is accomodated as bedding parallel shear in the quartzite lithologies of the Rosh Pinah formation. This is because of the extremely large competency contrast between the massive quartzite beds and the discrete argillaceous bedding partings. The ubiquitous presence of carbonate material along these bedding-parallel shear zones may be the result of fluid migration that accompanies thrusting (Hubbert & Rubey, 1959). The presence of carbonate material also facilitates ductile flow at shallow depths (Chapple, 1978). The appearence of many S0-parallel breccias, brecciated beds and distinct clast orientation indicates that extensive brittle fracture brecciation occurred during D1.

The characteristic S2, sigmoidal cleavage (Fig. 11, Plate 12,13), developed as an axial planar cleavage to the D2 asymmetric compressional folds. The main controls on the development of this cleavage are layer-parallel slip accompanying compressional folding (Chapple & Spang, 1974) and significant, sinistral strike-slip shear. The shear fabric θ′ is rotated parallel to bulk shear as it approaches the shear zone itself while the angle of 0′ increases away from the shear zone together with a corresponding decrease in intensity until it is indistinguishable from the undeformed host rock (Lister & Williams, 1980). The shear zone controlling the development of these structures at Rosh Pinah is the bedding plane. During D2 folding, the quartzites would have acted as a stacked series of parallel shear zones separated by homogeneous interlayers. A conjugate (fracture?) cleavage (Platt, 1984) is observed at Rosh Pinah and follows the θ′ fabric along discrete surfaces. Similar structures have been documented in thrusted quartzites of the Witwatersrand Supergroup (Roering & Smit, 1987) and in anastomosing shear zones within granite gneiss of the Maggia nappe core zone (Simpson, 1983).

5.4 FORMATION OF THE FOOTWALL BRECCIA

A genetic model for the formation of the footwall breccia must account for the following observations:

i) Fracture textures show that brecciation occurred exclusively under conditions of brittle fracture

ii) Many of the vein assemblages described consist of secondary minerals, commonly pseudomorphing pre-existing sulphate minerals

iii) Brecciation increases in intensity towards the ore zone contact as well as the thickest parts of the ore bodies.

iv) Many of the breccias are only mineralized in the matrix.

As demonstrated in section 4.1.1 the hydrothermal silicification of the footwall sediments occurred prior to the deposition of the dolomitic and baritic ore zone lithologies. The silicification resulted in the formation of an impermeable cap rock of variable thickness. This layer would result in the trapping of continued, incoming hydrothermal solutions. Similar observations have been made at the Amulet deposits of Canada, (Gibson, 1979, in Franklin et al., 1981) where self-sealing of the feeder system by silica preceded the main ore-forming event.

Self-sealing produced by a decrease in silica solubility appears to be the most common situation. At the Johnson River volcanogenic massive sulphide deposit (Steefel, 1987) however, the development of an impermeable anhydrite layer occurred. This resulted in the containing and insulation of later fluids and the deposition of sphalerite, silica and barite. At Rosh Pinah, the trapped fluids could have developed into short lived, small scale, Hele-Shaw type hydrothermal cells (Solomon et al., 1987) which would have leached already deposited metals from the underlying sediments. The presence of the spotted footwall quartzite

approximately 20 to 40 m below the ore zone contact, is possible evidence that the fluids and the cap rock interacted during the development of the hydrothermal cells. Due to increased temperature and volatile inflow the contained fluids reached a condition of overpressure, and thereby caused fracturing at the sea floor. Evidence of type 1 and 2 carbonate veins extends to a depth of 50 m to 60 m below the ore zone contact although with very little mineralization at depth.

The appearance of laths in breccia veins regarded as being the result of D1 brecciation (Type 3 carbonate vein) and which represent replaced sulphates, indicates that the carbonate replacement episode occurred late in the overall history of the deposit. Deposition of mineralized dolomite and laths of barite therefore occurred during bedding-parallel faulting during D1. The matrix breccia which forms a 1 m thick zone along the contact is a result of this D1 movement along the footwall contact. The competency contrast between the brittle, silicified footwall and the carbonate and sulphide lithologies resulted in extensive brecciation and remobilization of carbonates, sulphates and sulphides of the ore zone into the resulting fractures to produce type 3 carbonate veins. Crosscutting vein relationships suggest this to be a continuous yet episodic event. It appears likely that folding during D2 also resulted in deposition of veins of a similar composition and textural character. The majority of sulphide veining also appears to have occurred during this event. It is envisaged that replacement occurred late in the D2 event, when faulting, associated with large amounts of CO_2-rich fluids expelled from decarbonation reactions at depth, flushed through the system and replaced many of the sulphates of the ore deposit. This is supported by the drop in isotopic signatures recorded.

6 CONCLUSIONS

The evidence presented in this study proves that the majority of the sulphides present in the Rosh Pinah massive sulphide deposit were formed during the deposition of the sedimentary hostrocks. The deposit can therefore be considered as a classic example of sulphide deposition resulting from syngenetic hydrothermal activity. The reasons put forward as evidence of syngenetic deposition are as follows;

i. The ore zone is stratiform and can be followed for at least 1400 m.

ii. The ore zone lithologies are lenticular, pinch out as do sedimentary horizons and are concordant with the bedding in the hostrock quartzites.

iii. Sedimentary structures such as soft sediment deformation, graded bedding, rip-up clasts, etc. are displayed by sulphide as well as gangue minerals.

iv. There is a vertical as well as lateral change in metal zonation following a stratigraphic pattern.

v. Relict framboidal as well as colloform sulphide textures are present.

vi. Clasts of ore zone lithotypes are present in the immediate hangingwall quartzites.

vii. The footwall beneath the ore bodies is hydrothermally altered.

viii. Textural and structural studies within the ore zone show that the sulphides were folded and metamorphosed along with the enclosing rocks and are therefore pretectonic.

It is proposed that the rocks of the ore zone reflect mixed heritages and that the bulk is of a detrital or seawater chemical source. The sulphides, barite and the majority of

silica of the lower microquartzitic lithologies comprises the hydrothermal component.

Three main compositional cycles of hydrothermal activity appear to have taken place. Initial mineralization was associated with hydrothermal alteration involving extensive areas of silica deposition. This event was restricted to the footwall feldspathic quartzites and lower microquartzite lenses and was associated with appreciable copper precipitation in the form of chalcopyrite. Deposition occurred as a result of decreased silica solubility during cooling. The extensive silicification had the important consequence of forming an impermeable caprock below which subsequent hydrothermal solutions were trapped.

As a result of this hydrothermal entrapment a higher temperature system formed, eventually boiled adiabatically and brecciated the footwall and lower ore zone lithologies by its passage to the seafloor. The type 1 carbonate veins were precipitated during this event. Much of the ore body was formed at this stage with mineralized dolomite muds being deposited. The common occurrence of similar but unmineralized dolomite lenses in the sequence supports the contention that the majority of the dolomite is in fact of seawater origin. The hydrothermal component therefore, consists of sulphide mineralization as well as Ba and Mn which combined with the dolomite.

The final hydrothermal event involved the introduction of Ba-Cu-Ag enriched fluids subsequent to the formation of the dolomite ore. The result of this introduction was the formation of rare, Ba-rich veins (type 2 carbonate veins) and the lenses of massive barite ore. It appears that the migration of these fluids through the semi-unconsolidated dolomite mud resulted in areas of Ba-enrichment. During cooling and early diagenesis, barite laths crystallized in these areas forming the characteristic, sulphide-rimmed laths observed in the dolomite ore. Hydrothermal activity appears to have terminated with the resumption of turbidite deposition.

Although instability caused by sedimentation in a rapidly subsiding basin has been regarded as important in the formation of the structural features observed in the area (Kroner, 1974; Page & Watson, 1976; Burns, 1978), it is considered that slumps, listric faults and soft-sediment folds are a relatively minor component of the structural history.

The initial D1 event produced the regional foliation and related elements by the augmentation of the pre-existing S0 fabric. This deformation progressively increased in amplitude and intensity, merging into the D2 event. The two phases are only distinguishable in areas of obvious overprinting.

D1 deformation was controlled by compressive layer-parallel slip which resulted in the formation of S0-parallel thrust faults, a penetrative bedding-parallel foliation and the initiation of a pronounced mineral and stretching lineation. This mineral lineation defines a thrust transport direction from the north-west.

As D1 merged into D2 in the Rosh Pinah area, sinistral strike-slip deformation became dominant. This produced a steep, north dipping lineation characterized by extreme clast elongation.

The outward propagation of lateral thrusts (Daly, 1988) to the east, resulted in compressive back-folding in the proximity to the basement contact. The sigmoidal cleavage observed in the ore body as well as surrounding areas developed as a response to this deformation. This foliation is therefore D2 in origin and is coaxial to the regional D2 folds. D2 deformation culminated in the shearing out of the synclinal axes of the D2 folds by high-angle reverse faults. Brittle-regime, thin-skinned thrusting and faulting of this kind involves periodic stick and slip (Chapple, 1978) so that these faults continued to act as planes of movement. Reversal of initial movement has occurred along the faults east of the mine..

The existence of minor fold structures parallel to the D2 regional folds but postdating them, indicates that compressive tectonism continued. Their vergence shows that they were possibly produced by gravitationally controlled folding as a result of basement uplift in the east. The D3 folds produced in this event could have produced the Mitre Peak syncline 20 km to the south of Rosh Pinah (McMillan, 1968) as well as deformed outliers of the Nama. The doubly plunging nature of some anticlines, such as the Mountain Ore Body structure, may have resulted from later crossfolding of the regional D2 folds, although this could be a feature of the D2 folds themselves.

The majority of the veins recorded, except the syngenetic, hydrothermal type 1 and type 2 carbonate veins are of a structural origin. This is proved by the relationship between the ore lithologies and the vein compositions themselves. Type 3 carbonate veins were formed as a consequence of D1 deformation producing an extensive brecciated area into which components of the ore zone were remobilized and deposited. The majority of the thicker carbonate veins observable in the footwall were formed at this stage. The deposition of hydrothermal silica in the footwall forming areas of extreme competency, is crucial for the development of the carbonate-hosted Rosh Pinah breccia. Much of the footwall mineralization of the Rosh Pinah deposit therefore reflects Mississippi Valley Type overprinting of a classic SEDEX deposit.

Replacement of the hydrothermal as well as D1 deposited sulphates occurred during late D1 or D2 deformation and was a result of decarbonation reactions associated with metamorphism at this stage.

7 ACKNOWLEDGEMENTS

I wish firstly to thank Dr. John Moore, my thesis supervisor, for his supportive comments. His experienced interpretations of both underground and surface exposures, was a great help in the days spent mapping underground at Rosh Pinah.

My thanks go also to Dr. Stu Smith who introduced me to the tubes and vacuums of the carbonate isotope line. The departments of Geology and Mineralogy as well as Geochemistry are thanked for the necessary back-up and logistical support as well as entertaining and informative discussions.

Lastly I wish to thank the staff of the Rosh Pinah geology office, as well as Dr. Hans Luthy of ISCOR, for drill hole data and their contributions in understanding this very complex deposit.

Part of the funding for this project was made available through a grant from the Foundation for Research and Development.

8 REFERENCES

Anglo American Company (1983) Excursion guide to the Skorpion massive sulphide deposit. 12 pp.

Allsopp H.L., Kostlin E.O., Welke H.J., Burger A.J., Kroner A. and Blignault H.J. (1979) Rb-Sr and U-Pb geochronology of late Precambrian - early Palaeozoic igneous activity in the Richtersveld (South Africa) and southern South West Africa. Trans. Geol. Soc. S. Afr., 82: 185-204

Barnes H.L. (ed.) (1979) Geochemistry of hydrothermal ore deposits. Second edition, Wiley, New York.

Blignault H.J. (1977) Structural-metamorphic imprint on part of the Namaqua Mobile Belt in South West Africa. Precambrian Res. Unit Univ. Cape Town Bull., No.23

Blount D.N. and Moore C.H. (1969) Depositional and non-depositional carbonate breccias, Chiantla quadrangle, Guatemala. Geol. Soc. America Bull., 80: 429-442

Boyer S.E. and Elliott D. (1982) Thrust systems. Bull. Am. Assoc. Pet. Geol., 66: 1196-1230

Brathwaite R.L. (1974) The geology and origin of the Rosebery ore deposit, Tasmania. Econ. Geol., 69: 1086-1101

Burns A. (1978) Geological account of the Rosh Pinah area. Unpub. report, geology and exploration department, ISCOR, 14pp.

Butler R.W.H. (1982) The terminology of structures in thrust belts. J. Struc. Geol., 4: 239-245

Carne R.C. and Cathro R.J. (1982) Sedimentary exhalative (sedex) zinc-lead-silver deposits, northern Canadian Cordillera. CIM Bulletin, 75: 66-78

Chapple W.M. (1978) The mechanics of thin-skinned fold-and-thrust belts. Geol. Soc. America Bull., 89: 1189-1198

Chapple W.M. and Spang J.H. (1974) Significance of layer-parallel slip during folding of layered sedimentary rocks. Geol. Soc. of Am., 85: 1523-1534

Chauhan D.S. (1984) Sedimentary pyrite from Pb-Zn deposits of the Zawar and Rajpura-Dariba regions and its bearing on the genesis of base metal sulphides., in Wauschkuhn et al. (eds.) Syngenesis and epigenesis in the formation of mineral deposits, Springer-Verlag, Berlin, pp. 36-42

Davies C.J. and Coward M.P. (1982) The structural evolution of the Gariep arc in southern Namibia (South-West Africa). Precambrian Res., 17: 137-197

Daly M.C. (1988) Crustal shear-zones in central Africa: a kinematic approach to Proterozoic tectonics. Episodes, 11: 5-11

De Kock N.J. (1987) Die veranderinge van die wandgesteentes in die omgewing van die ertsliggame van Rosh Pinah. Unpub. MSc. thesis, University Pretoria, 155 pp.

De Villiers J. and Sohnge P.G. (1959) The geology of the Richtersveld. S. Afr. Geol. Surv. Mem., No. 48

Deer W.A., Howie R.A. and Zussman J. (1966) An introduction to the rock forming minerals. Longman, London, 528 pp.

Degens E.T. and Ross D.A. (eds.) (1969) Hot brines and recent heavy metal deposits in the Red Sea. Springer-Verlag, New York, 600 pp.

Duchac K.C. and Hanor J.S. (1987) Origin and timing of the metasomatic silicification of an early archaean komatiite sequence, Barberton mountainland, South Africa. Precam. Res., 37: 125-146

Edwards J.G. (1984) On the western portion of the Rosh Pinah concession (excluding the Trekpoort basin). ISCOR Interim report (1982-1984), 23 pp.

Engelder J.T. (1974) Cataclasis and the generation of fault gouge. Geol. Soc. Am. Bull., 85: 1515-1522.

Etheridge M.A. and Wilkie J.C. (1979) Grainsize reduction, grain boundary sliding and the flow strength of mylonites. Tectonophysics, 58: 159-178

Evans A.M. (1987) An introduction to ore geology. Geoscience texts, Blackwell Scientific Publications, Oxford, 358 pp.

Fehn U. (1986) The evolution of low-temperature convection cells near spreading centers: a mechanism for the formation of the Galapagos mounds and similar manganese deposits. Econ. Geol., 81: 1396-1407

Finlow-Bates T. (1979) Cyclicity in the lead-zinc-silver-bearing sediments at Mount Isa mine, Queensland, Australia, and rates of sedimentation. Econ. Geol., 74: 1408-1419

Finlow-Bates T. and Large D.E. (1978) Water depth as a major control on the formation of submarine exhalative ore deposits. Geol. Jb., D30: 27-39

Forel F.A. (1885) Les ravins sous-lacustres des fleuves glaciores. Compt. Rend., 101: 725-728

Franklin J.M., Lydon J.W. and Sangster D.F. (1981) Volcanic-associated massive sulphide deposits. Econ. Geol., 75TH. ANNIV. VOL., 485-627

Fuchtbauer H. and Richter D.K. (1981) Internal breccias near early geosynclinal platform margins. (abstr.) AAPG Bulletin 65: 928

Gardner H.D. and Hutcheon I. (1985) Geochemistry, mineralogy and geology of the Jason Pb-Zn deposits, Macmillan Pass, Yukon, Canada. Econ. Geol., 80: 1257-1276

Green G.R., Solomon M. and Walshe J.L. (1981) The formation of the volcanic-hosted massive sulphide ore deposit at Rosebery, Tasmania. Econ. Geol., 76: 304-338

Greenman L. (1966) The geology of area 2515C Luderitz, South West Africa. Unpubl. M.Sc. thesis, University of Cape Town

Gulson B.L., Perkins W.G. and Mizon K.J. (1983) Lead isotope studies bearing on the genesis of copper orebodies at Mount Isa, Queensland. Econ. Geol., 78: 1466-1504

Gustafson L.B. and Williams N. (1981) Sediment-hosted strataform deposits of copper, lead and zinc. Econ. Geol. 75TH. ANNIV. VOL., 139-178

Hamilton J.M., Delaney G.D., Hauser R.L. and Ransom P.W. (1983) Geology of the SulliVan deposit, Kimberley, B.C., Canada., in Sangster D.F. (ed.) Short course in sediment-hosted stratiform deposits, Min. Assoc. Can., 8: 31-84

Hannak W.W. (1981) Genesis of the Rammelsberg ore deposit near Goslar/upper Harz, Federal Republic of Germany., in Wolf K.H. (ed.) Handbook of strata-form and stratiform ore deposits, Vol.9, Elsevier Scientific Publishing Company, Amsterdam, pp. 551-642

Harrel J. (1984) A visual comparator for degree of sorting in thin and plane sections. J. Sed. Petr., 54: 646-650

Hartnady C.J.H. (1978) The structural geology of the Naukluft nappe complex and its relationship to the Damaran orogenic belt, SWA/Namibia. Unpubl. Ph.D. thesis, Univ. Cape town, South Africa, pp.

Hartnady C.J.H., Newton A.R. and Theron J.N. (1974) The stratigraphy and structure of the Malmesbury Group in the southwestern Cape. Precambrian Res. Unit Univ. Cape Town Bull 15: 193-213

Hartnady C.J.H., Joubert P. and Stowe C.W. (1985) Proterozoic crustal evolution in southwestern Africa. Episodes, 8: 236-244

Heyl A.V.(1974) Isotopic evidence for the origin of Mississippi Valley-type mineral deposits: a review. Econ. Geol., 69: 992-1006

Hodgson C.J. (1989) The structure of shear-related, vein-type gold deposits: a review. Ore Geol. Rev., 4: 231-273

Hoefs J. (1980) Stable isotope geochemistry. Springer-Verlag, Berlin, 208pp.

Hoy T. (1982) Stratigraphic and structural setting of stratabound lead-zinc deposits in southeastern British Columbia. CIM. Bull., 75: 114-134.

Hubbert M.K. and Rubey W.W. (1959) Role of fluid pressure in mechanics of overthrust faulting. Bull. Geol. Soc. Am., 70: 115-166

Jambor J.L., (1979) Mineralogical evaluation of Proximal-distal features in New Brunswick massive-sulphide deposits. Can. Mineral., 17: 649-664.

Kindl S. (1979) Reconnaissance geological map of the Rosh Pinah and northern Richtersveld areas, 1:50 000, ISCOR geology and exploration dept.

Krause F.F. and Oldersha A.E. (1979) Submarine carbonate breccia beds - depositional model for 2-layer sediment gravity flows from the Sekwi Formation (lower Cambrian)

Mackenzie mountains, northwest territories, Canada. Can. J. Earth Sc., 16: 189-199

Krebbs W. (1981) The geology of the Meggen ore deposit., in Wolf K.H. (ed.) Handbook of strata-bound and stratiform ore deposits, Vol. 9, Elsevier Scientific Publishing Company, Amsterdam, pp. 509-550

Kroner A. (1974) Late Precambrian formations in the western Richtersveld. Trans. roy. Soc. S. Afr., 41: 375-433

Kucha H. (1988) Zn-Pb sulphides as rim cements, filling cements and replacements of carbonate sediments, Moyvoughly, Ireland - a product of two convective cells. Trans. Instn. Min. Metall. (Sect. B: Appl. earth sci.), 97: B64-76

Kucha N. and Wieczorek A. (1984) Sulphide-carbonate relationships in the NaVan (Tara) Zn-Pb deposit, Ireland. Mineral. Deposita, 19: 208-216

Lambert I.B. (1981) The McArthur River zinc-lead-silver deposit: features, metallogenesis and comparisons with some other stratiform ores., in Wolf (ed.) Handbook of strata-bound and stratiform ore deposits, Vol. 6, Elsevier Scientific Publishing Company, Amsterdam, pp. 535-585

Lange I.M., Nokleberg W.J., Plahuta J.T., Krouse H.R. and Doe B.R. (1985) The geologic setting, petrology and geochemistry of stratiform sphalerite-galena-barite deposits, Red Dog Creek and Drenchwater Creek areas, northwestern Brooks Range, Alaska. Econ. Geol., 80: 1896-1926

Large D.E. (1981) Sediment-hosted submarine exhalative lead-zinc deposits. A review of their geological characteristics and genesis., in Wolf K.H. (Ed.), Handbook of strata-bound and stratiform ore deposits, vol. 9: 469-507

Large D.E. (1983) Sediment-hosted massive sulphide lead-zinc deposits: an empirical model., in Sangster D.F. (ed.) Short course in sediment-hosted stratiform lead-zinc deposits, MAC, 8: 1-30

Lash G.G. (1984) Density-modified grain flow deposits from an early palaeozoic passive margin. J. Sed. Petr., 54: 557-562

Lister G.S. and Williams P.F. (1979) Fabric development in shear zones: theoretical controls and observed phenomena. J. Struc. Geol., 1:#4 283-297

Lovering T.S. (1969) The origin of hydrothermal and low temperature dolomite. Econ. Geol., 64: 743-754

Lovering T.S. (1972) Jasperoid in the United States - it's characteristics, origin and economic significance. Geol. Surv. U. S. Prof. Paper, 710, 164pp.

Lydon J.W. (1983) Chemical parameters controlling the origin and deposition of sediment-hosted strataform lead-zinc deposits., in Sangster D.F. (ed.) Short course in sediment-hosted stratiform lead-zinc deposits. Min. Assoc. Can., 8: 175-250

McClay K.R. (1983) Deformation of stratiform lead-zinc deposits., in Sangster D.F. (ed.) Short course in sediment-hosted stratiform lead-zinc deposits. Min. Assoc. Can., 8: 283-309

MacIntyre D.G. (1982) Geologic setting of recently discovered stratiform barite-sulphide deposits in northeast British Columbia. CIM. Bull., 75: 99-113

McKay W.J. and Hazeldene R.K. (1987) Woodlawn Zn-Pb-Cu sulphide deposit, New South Wales, Australia: An interpretation of ore formation from field observations and metal zonation. Econ. Geol., 82: 141-164

McKibben M.A. and Elders W.A. (1985) Fe-Zn-Cu-Pb mineralization in the Salton Sea geothermal system, Imperial Valley, California. Econ. Geol., 80: 539-559

McLeod G. (1977) Further notes on the geology and it's significance to the genesis of the Rosh Pinah Zn-Pb sulphide deposit. ISCOR internal report, 19 pp.

McMillan M.D. (1968) The geology of the Witputs - Sendelingsdrif area. Bull. Precambrian Res. Unit, Univ. Cape Town, 4: 177 pp.

Maiden K.J., Chimamba L.R. and Smalley T.J. (1986) Cuspate ore-wall rock interfaces, piercement structures and the localization of some sulphide ores in deformed sulphide deposits. Econ. Geol., 81: 1464-1472

Mallio W. and Gheith M. (1972) Textural and chemical evidence bearing on sulphide-silicate reactions in metasediments. Mineral. Deposita, 7: 13-17

Martin H. (1965) The Precambrian geology of South West Africa and Namaqualand. Cape Town: Precambrian Res. Unit Univ. Cape Town

Martin H. and Porada H. (1977) The intracratonic branch of the Damara orogen in South West Africa. 1. Discussion of geodynamic models. Precambr. Res., 5: 311-338

Mathias B.V. and Clark G.J. (1975) Mount Isa Cu and Ag-Pb-Zn orebodies - Isa and Hilton mines, In Knight C.L., ed., Economic Geology of Australia and Papua New Guinea, I. Metals: Aust. Inst. Min. Metal. Mon. 5: 351-372

Matthews P.E. (1988) Breccia sheets and dykes: evidence of hydraulic fracture in Palaeozoic Natal Group sandstones near Durban, Natal. Extended abstracts, 22nd Earth Science Congress Geol. Soc. S. Afr., 838 pp.

Miller R.McG. (ed) (1983) Evolution of the Damaran orogen of South West Africa/Namibia. Geol. Soc. S. Afr. Spec. Publ., No.11

Mills P.C. (1983) Genesis and diagnostic value of soft-sediment deformation structures - A review. Sediment. Geol., 35: 83-104

Mrose M.E., Chao E.T., Fahey J.J., Milton C. (1961) Norsethite $BaMg(CO_3)_2$ - a new mineral from the Green River Formation, Wyoming. Am. Miner., 46: 420-429

Nelson C.E. and Giles D.L. (1985) Hydrothermal eruption mechanisms and hot spring gold deposits. Econ. Geol., 80: 1633-1639

Neudert M.K. and RussellR.E. (1981) Shallow water and hypersaline features from the mid-Protorozoic Mount Isa sequence. Nature, 293: 284-286

Obee H.K. and White S.H. (1986) Microstructural and fabric heterogeneities in fault rocks associated with a fundamental fault. Phil. Trans. R. Soc. Lond., A317: 99-109

Ohle E.L. (1985) Breccias in Mississippi Valley-Type deposits. Econ. Geol., 80: 1736-1752

Page D.C. and Watson M.D. (1976) The Pb-Zn deposit of Rosh Pinah mine, South West Africa. Econ. Geol., 71: 306-327

Paris I., Stanistreet I.G. and Hughes M.J. (1985) Cherts of the Barberton greenstone belt interpreted as products of submarine hydrothermal activity. Jour. Geol., 97: 111-129

Perkins W.G. (1984) Mount Isa silica-dolomite and copper orebodies: the result of a syntectonic hydrothermal alteration system. Econ. Geol., 79: 601-637

Pinkney D.M. and Rye R.O. (1972) Variations of O^{18}/O^{16}, C^{13}/C^{12}, texture and mineralogy in altered limestone in the Hill mine, Cave-in-Rock district, Illinois. Econ. Geol., 67: 1-18

Platt J.P. (1984) Secondary cleavages in ductile shear zones. J. Struc. Geol., 6: 439-442

Plimer I.R. (1986) Sediment-hosted exhalative deposits - products of contrasting ensialic rifting. Trans. Geol. Soc. S. Afr., 89: 57-73

Ramdohr P. (1969) The ore minerals and their intergrowths. Pergamon Press, Oxford

Ramsay J.G. (1980) Shear zone geometry: a review. J. Struc. Geol., 2: 83-99

Reading H.G. (1986) African Rift tectonics and sedimentation: an introduction. in Frostick L.E., Rensaut R.W., Reid I. and Tiercelin J.-J. (eds.) Sedimentation in the African rifts. Geological Society special publ., 25: 382 pp.

Reid D.L. (1979a) Age relationships within the Mid-Proterozoic Vioolsdrif batholith, lower Orange River region. Trans. Geol. Soc. S. Afr., 82: 305-311

Reid D.L. (1979b) The late Precambrian Gannakouriep mafic dyke swarm, lower Orange River region. Geol. Soc. S. Afr. 18th. Congr. Abstracts, 1: 282-285

Reimer T.O. (1978) Detrital barite in the Karoo Supergroup of southern Africa. Mineral. Deposita, 13: 235-244

Ritter U. (1976) Preliminary report on the geology of the north-eastern Richtersveld. Precambrian Res. Unit Univ. Cape Town Ann. Rept., 13: 42-48

Robertson A.H. and Woodcock N.H. (1986) The role of the Kyrenia range lineament, Cyprus, in the geological evolution of the eastern Mediterranean area. Phil. Trans. R. Soc. Lond., A317: 141-177

Roedder E. (1984) Fluid inclusions., in Reviews in Mineralogy, Miner. Soc. Am., Vol. 12

Roering C. and Smit C.A. (1987) Bedding-parallel shear, thrusting and quartz vein formation in Witwatersrand quartzites. J. Struc. Geol., 9: 419-427

Rogers A.W. (1915) The geology of part of Namaqualand. Trans. Geol. Soc. S. Afr., 18: 72-101

RussellM.J., Solomon M. and Walshe J.L. (1981) The genesis of sediment-hosted, exhalative zinc + lead deposits. Mineral. Deposita, 16: 113-127

Rye R.O. and Ohmoto H. (1974) Sulphur and carbon isotopes and ore genesis: a review. Econ. Geol., 69: 826-842

Sato T. (1972) Behaviors of ore-forming solutions in seawater. Mining Geology (Japan), 22: 31-42

Sato T. (1977) Kuroko deposits: their geology, geochemistry and origin. in Volcanic processes in ore genesis: Lond. Inst. Mining and Metallurgy, 153-161

Sawkins F.J. (1969) Chemical brecciation, an unrecognised mechanism for breccia formation? Econ. Geol., 64: 613-617

Schidlowski M., Eichman R. and Junge C.E. (1975) Precambrian sedimentary carbonates: carbon and oxygen isotope geochemistry and implications for the terrestrial oxygen budget. Precambrian Res., 2: 1-69

Scott S.D. and Barnes H.L. (1971) Sphalerite geothemometry and geobarometry. Econ. Geol., 66: 653-669

Sibson R.H., Moore J.M. and Rankin A.H. (1975) Seismic pumping - a hydrothermal fluid transport mechanism. J. Geol. Soc. Lond., 131: 653-659

Siegfried P.R. (1986) The geology of Anninaub Prospect, southern Namibia. Unpubl. BSc(Hons) thesis, Univ. of Cape Town, 70 pp.

Siegfried P.R. and Tilbrook J. (1985) Preliminary study of metal zonation patterns and palaeogeographic reconstruction of the Rosh Pinah ore body and some exploration implications. ISCOR internal report, 16 pp.

Sillitoe R.H. (1985) Ore-related breccias in volcanoplutonic arcs. Econ. Geol., 80: 1467-1514

Simpson C. (1983,a) Strain and shape-fabric variations associated with ductile shear zones. J. Struc. Geol., 5: 61-72

Simpson C. (1983,b) Displacement and strain patterns from naturally occurring shear zone terminations. J. Struc. Geol., 5: 497-506

Smee B.W. and Bailes R.J. (1986) The use of lithogeochemical patterns in wall rock as a guide to exploration drilling at the Jason lead-zinc-silver-barium deposit, Yukon Territory. In: C.E. Nichols (Editor), Exploration for ore deposits of the North American Cordillera. J. Geochem. Explor., 25: 217-230

Solomon M., Walshe J.L. and Eastoe C.J. (1987) Experiments on convection and their relevance to the genesis of massive sulphide deposits. Australian J. of Earth Sci., 34: 311-323

South African Committee for Stratigraphy (SACS) (1980) Stratigraphy of South Africa. Part I. Lithostratigraphy of the Republic of South Africa, South West Africa/Namibia, and

the Republics of Bophuthatswana, Transkei and Venda. S. Afr. Geol. Surv. Handbook No.8

Speer J.A. (1983) Crystal chemistry and phase relations of orthorhombic carbonates. in Reeder R.J. (ed.) Carbonates: Mineralogy and chemistry. Reviews in Min., 11: 145-190

Steefel C.I. (1987) The Johnson River prospect, Alaska: Gold-rich sea-floor mineralization from the Jurassic. Econ. Geol., 82: 894-914

Sundias N. (1966) Carbonates in manganese ores at Langban. Ark. Miner. Geol., 5: 279-285

Swager C.P. (1985) Syndeformational carbonate-replacement model for the copper mineralization at Mount Isa, northwest Queensland: a microstructural study. Econ. Geol., 80: 107-125

Swart R. (1986) A note on the occurrence of scapolite in the northern zone of the Damaran orogen. Communs. Geol. Surv. SWA/Namibia, 2: 61-62

Tankard A.J., Jackson M.P.A., Eriksson K.A., Hobday D.K., Hunter D.R. and Minter W.E.L. (1982) Crustal evolution of southern Africa - 3.8 Billion years of earth history. Springer-Verlag, Berlin, 523 pp.

Taylor S. and Andrew C.J. (1978) Silvermines orebodies, county Tipperary, Ireland. Trans. Instn Min. Metall. (Sect. B: Appl. earth sci.), 87: B111-124

Thorman C.H. and Nahass S. (1979) Reconnaissance geologic study of the Vazante zinc district, Minas Gerais, Brazil. Geol. Surv. U. S. Prof. Paper, 1126-I

Tucker M.E. (1981) Sedimentary petrology: an introduction. Blackwell, Oxford, 252pp.

Valley J.W. and O'Neil J.R. (1981) $^{13}C/^{12}C$ exchange between calcite and graphite: a possible thermometer in Grenville marbles. Geochim. Cosmochim. Acta, 45: 411-419

Van Vuuren C.J.J. (1986) Regional setting and structure of the Rosh Pinah zinc-lead deposit, South West Africa/Namibia. In Anhaeusser C.R. and Maske S. (eds) Mineral deposits of southern Africa. Vols. I & II, Geol. Soc. S. Afr., Johannesburg

Vogt J.H. and Stumpfl E.F. (1987) Abra: a strata-bound Pb-Cu-Ba mineralization in the Bangemall Basin, Western Australia. Econ. Geol., 82: 805-825

Vokes F.M. (1976) Caledonian massive sulphides in Scandanavia. A comprehensive review., in Wolf K.H. (Ed.), Handbook of strata-bound and stratiform ore deposits, Vol. 6: 79-127

Von Veh M.W. (1988) The stratigraphy and structural evolution of the late Proterozoic Gariep Belt in the Sendelingsdrif - Annisfontein area, northwestern Cape Province., Unpubl. Ph.D. thesis, Univ. Cape Town, 121 pp.

Vorob'yev Y.I., Konev A.A., Afonia G.G., Sapozhnikov A.N., Malyshonok Y.V., Paradina L.F. and Lapides I.L. (1985) New carbonate varieties of the $BaCO_3/SrCO_3$ isomorphous series. Transactions (Doklady) of the U.S.S.R. academy of sciences: earth science sections, 163-167

Walker R.G. (1975) Generalized facies models for resedimented conglomerates of turbiditic association. Geol. Soc. Amer. Bull., 86: 737-748

Walker R.G. (1976) Facies models 2: Turbidites and associated coarse clastic deposits. Geoscience Canada, 3: 25-36

Warne S. St. J. (1962) A quick field or laboratory staining scheme for the differentiation of the major carbonate minerals. Jour. of Sed. Petr., 32: 29-38

Watson M.D. (1980) The geology, mineralogy and origin of the Zn-Pb-Cu deposit at Rosh Pinah, South West Africa. Unpublished Ph.d thesis, Univ. Pretoria, 250 pp.

White D.E. (1981) Active geothermal systems and hydrothermal ore deposits. Econ. Geol., 75TH. ANNIV. Vol., 392-423

White S.H., Bretan P.G. and Rutter E.H. (1986) Fault-zone reactivation: kinematics and mechanisms. Phil. Trans. R. Soc. Lond., A317: 81-97

Whitehead R.E. (1973) Environment of stratiform sulphide deposition; Variation in Mn:Fe ratio in host rocks at Heath Steele Mine, New Brunswick, Canada. Mineral. Deposita, 8: 148-160

Williams P.F. (1984) Multiply deformed terrains - problems of correlation. J. Struc. Geol., 6: 269-280

Winn R.D. and Bailes R.J. (1987) Stratiform lead-zinc sulphides, mudflows, turbidites: Devonian sedimentation along a submarine fault scarp of extensional origin, Jason deposit, Yukon Territory, Canada. Bull. Geol. Soc. of Amer. Bulletin, 98: 528-539.

Woodcock N.H. and Fischer M. (1986) Strike-slip duplexes. J. Struc. Geol., 8: 725-735

MAP 1 A

MOB 490 LEVEL

Lithological Map

LEGEND

- Hangingwall Feldspathic Quartzite
- B — Baritic Ore
- Carbonate Ore
- Microquartzite Ore
- Massive Sulphide Ore
- Brecciated Footwall Quartzite
- Footwall Feldspathic Quartzite
- Lithological Contact
- Fault
- Tunnel Outline

0 20 40

m

STRUCTURE

- Bedding
- S2 Cleavage
- Shears
- S2 Lineation
- S1 Lineation

B D E

a b c d e f g h i j

230m 210m 150m 120m 90m 60m 0m

Limit of breccia

WESTERN BOUNDARY FAULT

EASTERN BOUNARY FAULT